SIMULTANEOUS OSCILLATIONS

AT TWO UNRELATED FREQUENCIES

THE GENERATION OF SIMULTANEOUS OSCILLATIONS AT UNRELATED FREQUENCIES USING A SINGLE NON-LINEAR ELEMENT

by

N. B. JONES, B. Sc.

A Thesis

Submitted to the Faculty of Graduate Studies

in Partial Fulfilment of the Requirements

For the Degree

Master of Engineering

McMaster University

May 1965

MASTER OF ENGINEERING (1965) McMASTER UNIVERSITY
(Electrical Hamilton, Ontario

TITLE: The Generation of Simultaneous Oscillations at Unrelated Frequencies Using a Single Non-linear Element

AUTHOR: N. B. Jones, B.Sc. (Manchester University)

SUPERVISOR: Dr. A. S. Gladwin, Chairman
Department of Electrical Engineering

NUMBER OF PAGES: x, 108

SCOPE AND CONTENTS:

This thesis is principally concerned with the conditions under which a feedback oscillator with a single non-linear element can support two component waves. These component waves are required to have unrelated frequencies.

A theory is produced to predict the oscillation frequencies and amplitudes and examine their stability. The conclusions reached in this thesis are then compared with those reached by previous workers in the same field.

The concluding parts of the thesis contain an examination of the possible approximations which can be made in order to represent various non-linear elements mathematically and also a demonstration of a system for examining frequency relationships without recourse to direct numerical measurement.

ACKNOWLEDGMENTS

The author wishes to express appreciation for the valuable criticism and ideas received from Dr. A. S. Gladwin, who was the supervisor of the research which is presented in this thesis, and to Dr. R. A. Woodrow for his interest and support.

The author also wishes to acknowledge the generous financial support of the thesis project by the Defence Research Board, under grant No. 5503-09.

TABLE OF CONTENTS

LIST OF ILLUSTRATIONS

LIST OF SYMBOLS

a	Parameter of non-linear element
A	$\frac{C_1 a_1 W_{10} + C_2 a_2 W_{20}}{(C_1 + C_2)^{1/2} (C_1 W_{10}^2 + C_2 W_{20}^2)^{1/2}}$
A_1	Amplitude of component at frequency W_1
A_2	Amplitude of component at frequency W_2
A_d	Amplitude of component at frequency $(W_1 - W_2)$
a_1	Damping factor of circuit tuned to W_{10}
a_2	Damping factor of circuit tuned to W_{20}
b	Parameter of non-linear element
$b_0, b_1, b_2..$	Fourier coefficients in the expansion of $\mathrm{Exp}(b A_2 \cos W_2 t)$
$c_0, c_1, c_2..$	Fourier coefficients in the expansion of $\mathrm{Exp}(bA_d \cos(W_1 - W_2)t))$
C	$\frac{C_1 C_2}{C_1 + C_2}$
C_g	Grid capacitance
C_1	capacitance of equivalent parallel circuit tuned to W_{10}
C_2	Capacitance of equivalent parallel circuit tuned to W_{20}
D	Total direct voltage at the input to the non-linear element
DW_{10}	Bandwidth of circuit tuned to W_{10}
DW_{20}	Bandwidth of circuit tuned to W_{20}
d_1	Amplitude of the disturbance at frequency W_1
d_2	Amplitude of the disturbance at frequency W_2
$d_0(t), d_1(t), ...$	Fourier coefficients in the expansion of $\mathrm{Exp}(be^{s_1 t} \cos W_1 t)$
$e_0, e_1, ...$	Fourier coefficients in the expansion of $\mathrm{Exp}(bA_1 \cos W_1 t)$
i_a	Anode current

K	Equivalent linear gain to both main components when $A_1 = A_2$
K_1	Equivalent linear gain to component at frequency W_1
K_2	Equivalent linear gain to component at frequency W_2
K_3	Equivalent linear gain to component at frequency W_3
k_1	Equivalent linear gain to the transient at frequency W_1
k_2	Equivalent linear gain to the transient at frequency W_2
L_1	Inductance of equivalent parallel circuit tuned to W_{10}
L_2	Inductance of equivalent parallel circuit tuned to W_{20}
$p(=s+jW)$	Laplace complex variable
p_1	$s_1 + jW_1$
p_2	$s_2 + jW_2$
R_g	Grid leak resistance
R_1	Resistance of equivalent parallel circuit tuned to W_{10}
R_2	Resistance of equivalent parallel circuit tuned to W_{20}
s	Real part of p
s_1	Real part of p_1
s_2	Real part of p_2
t	Time from arbitrary origin (seconds)
VB	External direct voltage input to the non-linearity
v_g	Grid voltage
w	Imaginary part of p
W_1	The higher oscillating frequency (radians per second)
W_2	The lower oscillating frequency (radians per second)
W_3	The zero phase shift frequency which lies between W_1 and W_2
W_{10}	$= 1/(l_1 C_1)^{1/2}$

W_{20} $= 1/(L_2C_2)^{1/2}$

$$W_0 = \frac{(C_1W_{10}^2 + C_2W_{20}^2)^{1/2}}{(C_1 + C_2)^{1/2}}$$

$Z(p)$ $Z_1(p) + Z_2(p)$

$Z_1(p)$ The operational impedence of the circuit tuned to W_{10}

$Z_2(p)$ The operational impedence of the circuit tuned to W_{20}

Note; parameters which are followed by primes (e.g. C_1') refer to the equivalent parameter in the approximate circuit.

SECTION 1

INTRODUCTION

If a normal, single frequency sine wave oscillator has a natural frequency of W_1 then it will, in the practical case, also contain in its output some, or all, of the harmonics of W_1. These harmonics are usually unwanted, since they only represent distortion of the wave form, and to minimise this, the linear part of the oscillator is normally arranged to have a frequency response which strongly attenuates the harmonics. There is no reason, however, why the circuit should not be arranged to select one of the harmonics to suffer less attenuation than the others so that this harmonic is of considerable size when compared with the fundamental. The presence of this second signal will naturally affect the reaction of the non-linear element to the fundamental, but its very existence depends on the presence of the fundamental component, and so any change in the amplitude of this will result in a change, in the same sense, in the amplitude of the harmonic component. In this way the existence of a double frequency oscillator of this type can be intuitively appreciated.

Consider, on the other hand, the case in which two sine waves with a more complicated relationship between the frequencies, or with completely unrelated frequencies, are applied to a non-linear element. The output will consist of harmonics of both, together with all cross-modulation products, as well as the two fundamental frequencies. If these two fundamental components were filtered out, amplified, and

used to supply the input to the non-linear element, the system could conceivably continue to oscillate in the same mode, without any external assistance. It is not possible to make any generalised statements at this time, since with all normal non-linear elements, a disturbance of one amplitude will not necessarily result in a change of the other in the same sense, and will in fact, usually have the opposite effect. If the two frequencies are related by $mf_1=nf_2$, where m and n are integers, then with most non-linear elements there will be some cross-modulation terms in the output which are of the same frequency as the fundamentals, so in this case, the existence of one oscillation can, to some extent, help to support the other. When the frequencies are not related, there is no exchange of energy from one component to the other, and the possibility of the stable existence of the two components depends entirely on the form of the non-linear element, unless some special contrivance is used.

Several attempts have been made in the past to make an examination of the conditions under which two unrelated components could exist stably together in the same oscillator. One obvious method, which will be mentioned here, but not discussed in detail, is to separate the two components and apply each to a different amplitude limiting device. This can be done either by using the same negative resistance, which can then be assumed linear, as in references (1) and (2) or by using two non-linear negative resistances (Reference 3), one for each component. This latter case is essentially equivalent to having two oscillators with part of the linear circuit in common. In the former case, the energy supplying element, and the amplitude limiting elements

are separate, but again the only parts of the circuits of the two components which are common, are approximately linear. In neither case is it necessary for the performance of the oscillator that the common part of the circuitry should be anything but linear.

Another system which can be used to maintain two unrelated frequency components with a single non-linear element is to use, as the energy supplying element, a valve which has its bias voltage moving up and down at the difference frequency. (Reference (4) and (5)). This can be considered as another method of coupling the components.

These last two methods are considered in more detail in section (8).

The third alternative, which presents a far more complicated picture, is that in which the same non-linear element is used to limit the amplitudes of both components and where no extra coupling is introduced. That is, the two components have a non-linear element in common, and hence one component amplitude can affect the other. This paper will be concerned with an oscillator of this type, of which it is also true that one component does not supply any energy to the other; that is, the two frequencies are incommensurable. It will be shown that the oscillator can be self-starting under these conditions, and that the two frequency mode, once established, is stable.

The non-linear element used here is a 6BA6 remote cut off pentode, for which arrangements have been made to ensure that the characteristic curve can be represented to within $\pm$ 3% by an exponential. The reason for the choice is purely mathematical, since this type of oscillation has also been produced by the author, and by Disman and

Edson (Reference 6) using a 6AK5 sharp cut off pentode, which is best approximated by a three-halves power law. However, the use of a three-halves power law curve produces mathematical expressions which are very difficult, if not impossible to solve analytically. Double integrations are involved, which also prove difficult to compute numerically, due to the discontinuity in the characteristic at the cut-off point. The actual form of the non-linear element will be discussed in Section (3) and Appendix (I), but an important point to be made here is that the amplitude limitation is achieved by employing automatic bias of the class C type, and not by a saturation phenomenon.

The type of analysis used in this paper is to replace the non-linear element by two equivalent linear elements, each acted upon by one component only. These equivalent linear elements will have transfer properties which are independent of frequency since the frequencies are incommensurable, but will depend on both component amplitudes. In order to apply the approximation of the equivalent linear gains, it is necessary to assume that the input to the non-linear element contains only a limited number of component sine waves; in this case, two. This condition is fulfilled by arranging that the linear part of the circuit attenuates all harmonics and modulation products to such an extent that they are negligible at the grid of the pentode The difference frequency component is the largest of the neglected components and its effect is discussed in some detail in section (7).

The two component waves existing in this oscillator have comparable frequencies and amplitudes, and so it is not simply sufficient to regard one as modifying the shape of the non-linear element, upon which

the other acts. The equivalent linear gains are in fact expressed as functions of the two amplitudes, which can then be predicted from the Barkhausen oscillating conditions, as can the frequencies. It will be explained, however, that due to the nature of the equivalent gain functions, the predicted amplitudes are only close approximations to those observed experimentally when these amplitudes are very nearly equal. With this in mind, certain predicted amplitudes and frequencies will be presented alongside the corresponding experimental ones, and it will be seen that the agreement is reasonably close.

The conditions under which the two oscillations can exist stably are presented in the form of restrictions on the circuit parameters, and one example of a stable situation is calculated to demonstrate that it does in fact conform to these restrictions. Another criterion is established to give the conditions under which both the oscillations can start to build up from the noise inherent in the circuit.

Appendix III of this report will be concerned with a description of a system for testing the periodicity of the wave at the input of the non-linear element, and the possibility of the component waves synchronixing completely, or pulling in and out of synchronism, is discussed in connection with the effect on the practical results.

SECTION 2

THE "EQUIVALENT LINEAR GAIN" CONCEPT

(2.1) Introduction

The method employed in the analysis of non-linear systems depends to a large extent upon the requirements of the specific problem, and upon the convenience of solution, because it is seldom easy to solve, directly, the non-linear differential equations involved. The equations, in fact, cannot always be formulated. One method devised to give a solution in these circumstances, is that in which the non-linear element is approximated by a series of straight lines. A set of linear differential equations corresponding to each line is solved, using the starting conditions resulting from the final conditions of the previous section. This method can be applied to any degree of accuracy required, simply by increasing the number of straight line segments, although the labour involved increases in proportion. This type of method is of great use in the analysis of relaxation oscillators for example, or in fact, of any system in which the wave form is markedly non-sinusoidal.

This so called "piece wise linear approximation" has many disadvantages. These include its complexity and the fact that, even with the same non-linearity, each specific case must be examined individually. It is fortunate, therefore, that there are alternatives to this, which

can be applied with considerable accuracy, if certain conditions are fulfilled. If for example, the wave form at the input of the non-linear element could be approximated by the sum of a small number of sine waves, it would be possible to approximate the non-linear element to an equal number of linear elements, each of which was acted upon by one component, and whose slopes were functions of the amplitudes of all the components. This is the method of the "equivalent linear gains" or "describing functions", and is the one used here (References 7, 8 and 9). These equivalent linear gains are in no way related to the linear segments referred to above and they are in fact a fixed number of abstract linear circuit elements which are considered to replace completely the non-linear element for the purpose of analysis. The piece-wise approximation is simply a representation of the non-linear element by an arbitrary number of consecutive straight line segments.

When the equivalent linear gains technique is used to approximate the non-linear elements in a feedback loop, the assumption that there is a limited number of frequency components at the input is equivalent to saying that all the harmonics of each component, and all the cross modulation products produced at the output of the non-linearity are attenuated before they return to the input. In the present case there are two main components whose frequencies are defined by the condition that the loop phase shift should be zero. Typical gain and phase characteristics for the feedback circuit are shown in figures (1) and (2) from which it can be seen that the two zero phase shift frequencies f_1 and f_2; which will later be shown to be the two stable oscillating frequencies, suffer much less attenuation than do other frequencies somewhat removed from them.

A typical frequency spectrum at the input is given if figure (3), and does, in fact, show that all components other than f_1 and f_2 represent at the most 5% of the fundamentals, and so the approximation that there are only two input frequencies is a reasonable one.

(2.2) Definitions of the Equivalent Linear Gain

There are several definitions of the equivalent gains in use, all of which are equivalent, and the one actually used depends on which is most convenient for the particular problem. In the case of the two input equivalent gain functions, two of the alternative definitions are given as follows:

1) Each equivalent linear gain is the ratio of the amplitude at one fundamental frequency at the output, to the amplitude of the same component at the input. The output component amplitude is calculated by Fourier analysis of the output wave form, which is itself either expressed analytically or constructed graphically from the non-linear element.

2) The equivalent linear gains are defined as those gains which, when each is acted upon by one component, produce outputs whose sum has a minimum mean-square difference with the output of the non-linear element. (Reference 10).

The equivalence of these two definitions can be proved, but it is not necessary to do this for the present purposes. In the analysis of the system involved here, however, the equivalent linear gain will be calculated in both ways, and so the equality can be verified in this case (Appendix II)

FIG. 1

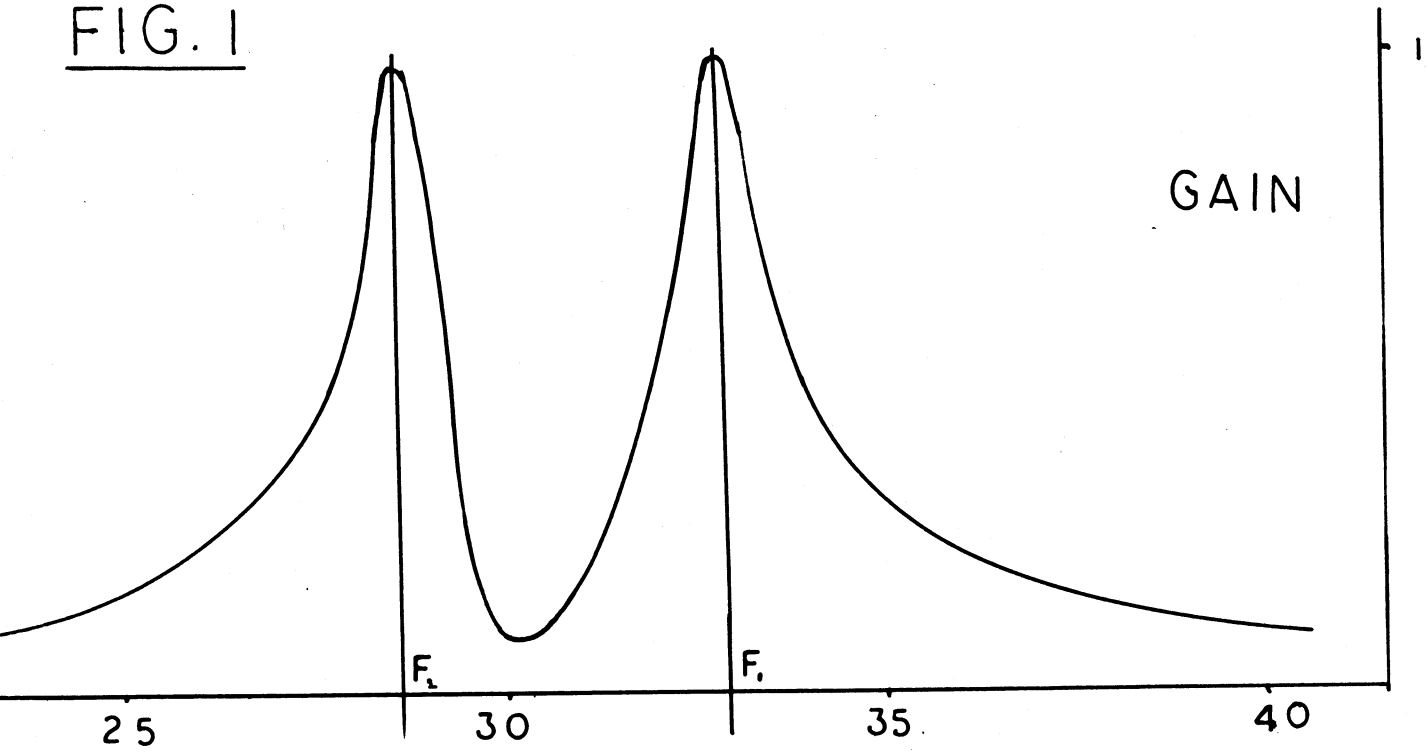
GAIN
1
F2
F1
25
30
35
40
FREQUENCY Kc./s.

FIG. 2

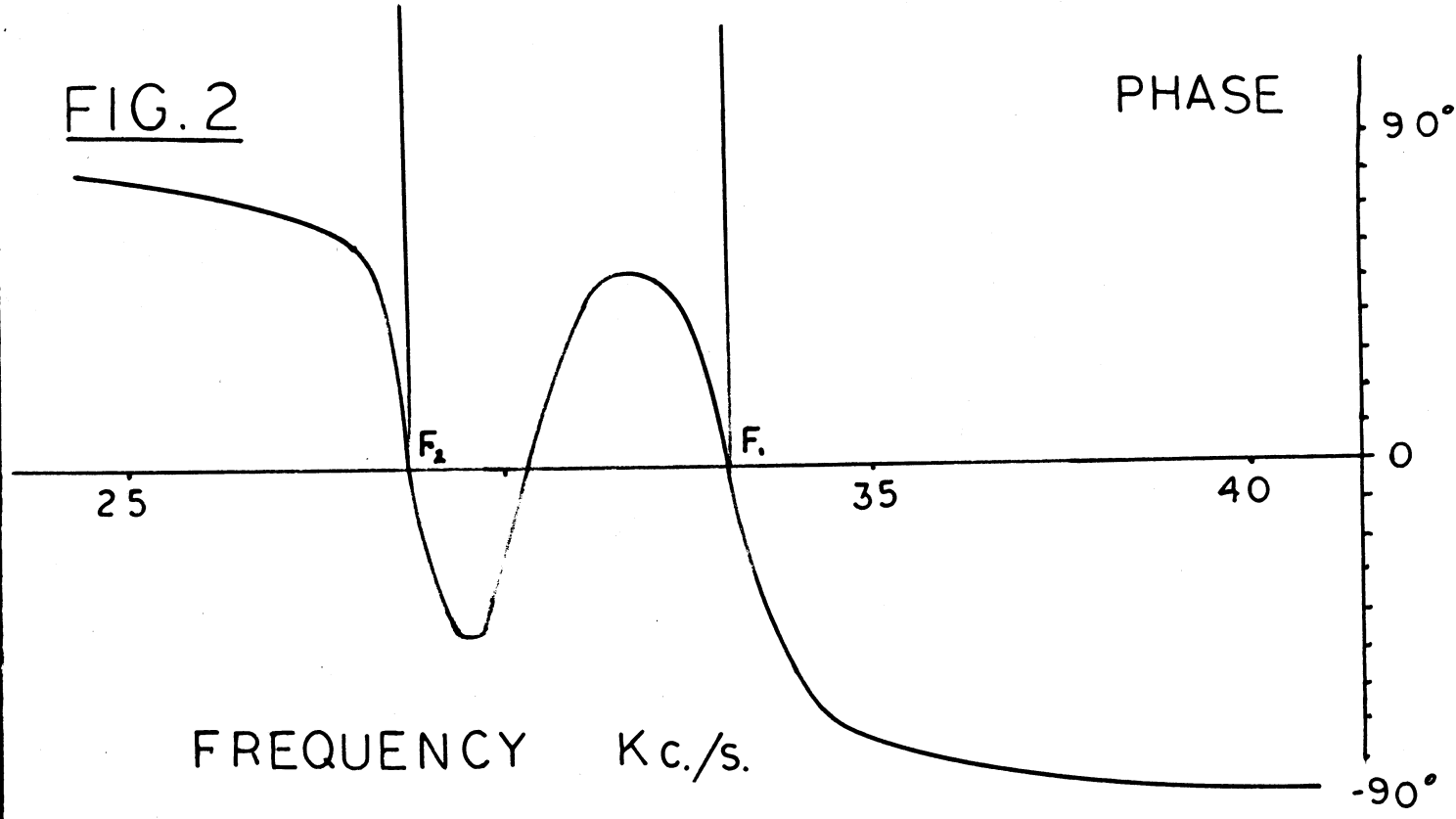
PHASE
90°
0
-90°
F2
F1
25
35
40
FREQUENCY Kc./s.

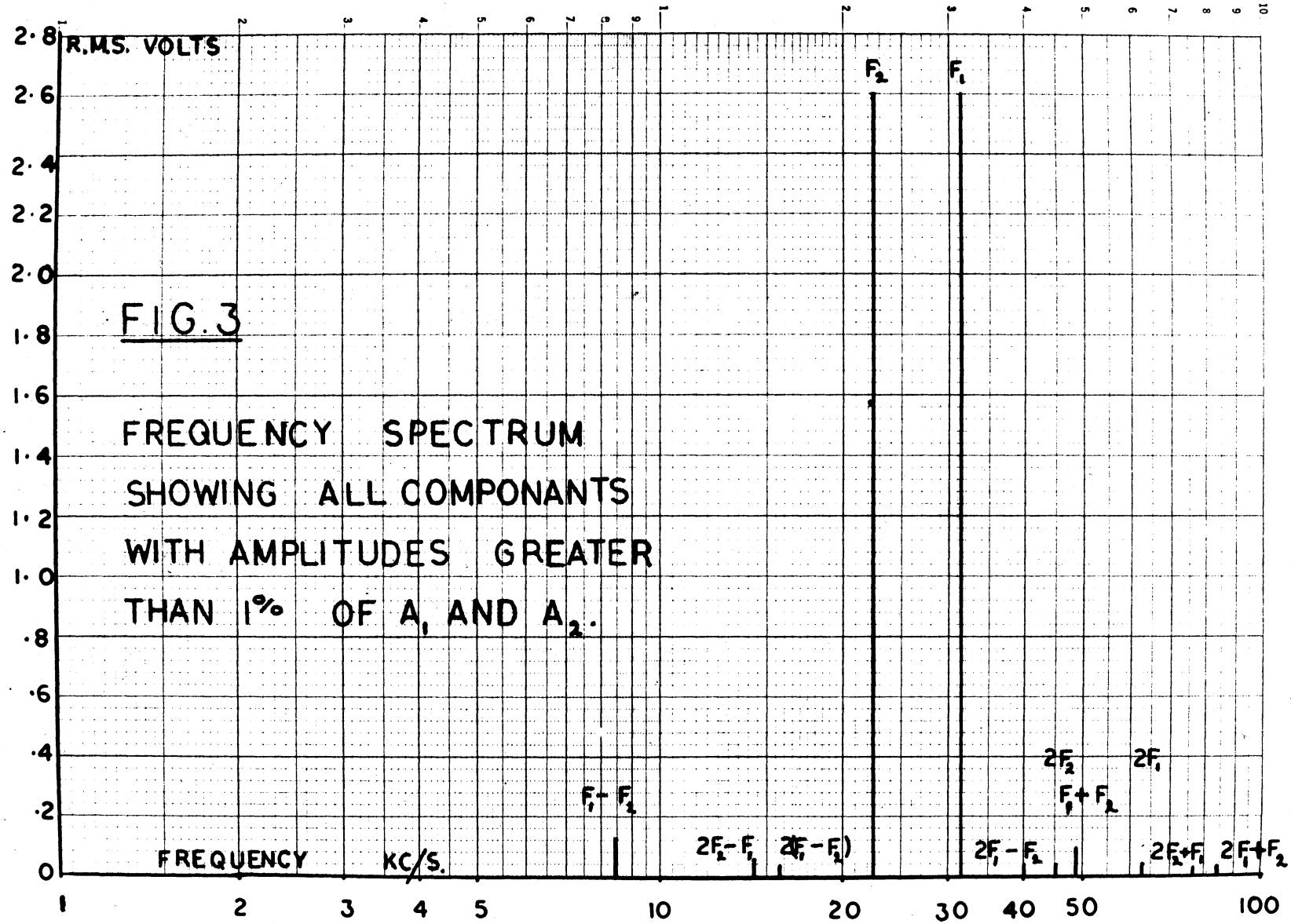
R.M.S. VOLTS
2·8
2·6
2·4
2·2
2·0
1·8
1·6
1·4
1·2
1·0
·8
·6
·4
·2
0
FIG.3
FREQUENCY SPECTRUM
SHOWING ALL COMPONANTS
WITH AMPLITUDES GREATER
THAN 1% OF A1 AND A2.
F2
F1
F1+F2
2F2-F1
2F1-F2
2F2
F1+F2
2F1
2F2+F1
2F1+F2
FREQUENCY KC/S.
1
2
3
4
5
10
20
30
40
50
100

(2.3) Possible Sources of Error

When using this equivalent linear gain technique, it is of great importance to account for any phase shifts introduced by the non-linear element, since, in an oscillator, these can affect the possible natural frequencies. Such phase changes, suffered by components passing through a non-linear element, can be produced by one of two mechanisms. They could be caused by the non-linear element being something other than single valued, or by there being some relationship between the frequencies of two or more of the input components. The first of these does not affect the present problem, because the non-linear element is entirely resistive at the frequencies involved. The second type of phase shifting is also assumed to be non-existent for the purposes of the analysis, since the harmonics of each component have been presumed to be of negligible amplitude at the grid, and the two main components themselves are arranged to have incommensurable frequencies.

The degree of approximation made by neglecting the harmonics, can easily be seen by reference to the previously given input frequency spectrum (figure 3). However, the relationship between the two main frequencies is difficult to estimate, and hence the degree of approximation is not known. Nevertheless, even if there were a relationship of the type of $mf_1 = nf_2$, a method is available to ensure that m and n are large, (appendix III), in which case the strength of the m^{th} and $(m-1)^{th}$ harmonics of f_1 and the n^{th} and $(n-1)^{th}$ harmonics of f_2 can be taken to be so small that any extra components at frequencies f_1 or f_2 produced by their reactions together can be entirely neglected.

SECTION 3

THE CHOICE OF NON-LINEAR ELEMENT

(3.1) Power Series Representation

It has been shown theoretically by previous investigators (References (1), (11), (12)) that the form of the non-linear element is the critical factor controlling the possible existence of an oscillation mode containing two unrelated frequencies. It has been concluded from these references, that if the characteristics were approximated by a power series, then the following statements can be made. First of all, it is not possible to obtain unrelated double frequency oscillations at all if the approximation includes terms only up to the third power: secondly, it is possible to obtain these oscillations when up to the fifth power terms are included. However, in this latter case, the system will not be self-starting at the two frequencies, and in fact the oscillations will have to be initiated from some external source. For these reasons, the non-linear characteristic to be used must be considered either, as a power series containing powers at least to the seventh, or alternatively, as some shape which cannot be closely approximated by a power series with a reasonably small number of terms. It will be shown in the appendices that the second alternative can result in a close approximation, which is also easy to handle mathematically.

(3.2) Functional Representation

It is evident that, practically, there is only a small number of non-linear negative resistance shapes available without building special circuits. These are included in the transfer characteristics of tunnel diodes, transistors, tubes and similar amplifiers. In the appendix on curve-fitting, various mathematical formulae are compared with the grid voltage anode current curves of several pentode tubes. From this it can be seen that, while a three halves power law curve is a good approximation to the characteristic of a sharp cut off pentode, like that of a 6AK5, a single exponential curve is not. Unfortunately, a three halves power law curve is much more difficult to handle mathematically than is the exponential.

Appendix I, however, does show also that an exponential curve can be used as a fairly good approximation to the characteristic of a remote cut off pentode such as a 6BA6. Moreover, the accuracy of the fit can be greatly increased by arranging for the grid voltage to be restricted to that region of the figure (4) which is approximately a straight line. This part of the curve, regarded as straight, can be extended without loss of accuracy, by decreasing the anode current values at low grid voltages and is simply achieved by causing a decrease in the instantaneous screen voltage as the grid voltage approaches zero. By feeding the screen from the supply voltage via a resistance, but without using a decoupling condenser, the desired negative feedback will be effected, since as the anode current rises, the screen current will rise and reduce the screen voltage, upon which the anode current is strongly dependent.

FIG.4 6BA6 REMOTE CUT OFF PENTODE

ANODE VOLTAGE 330

SCREEN VOLTAGE 100

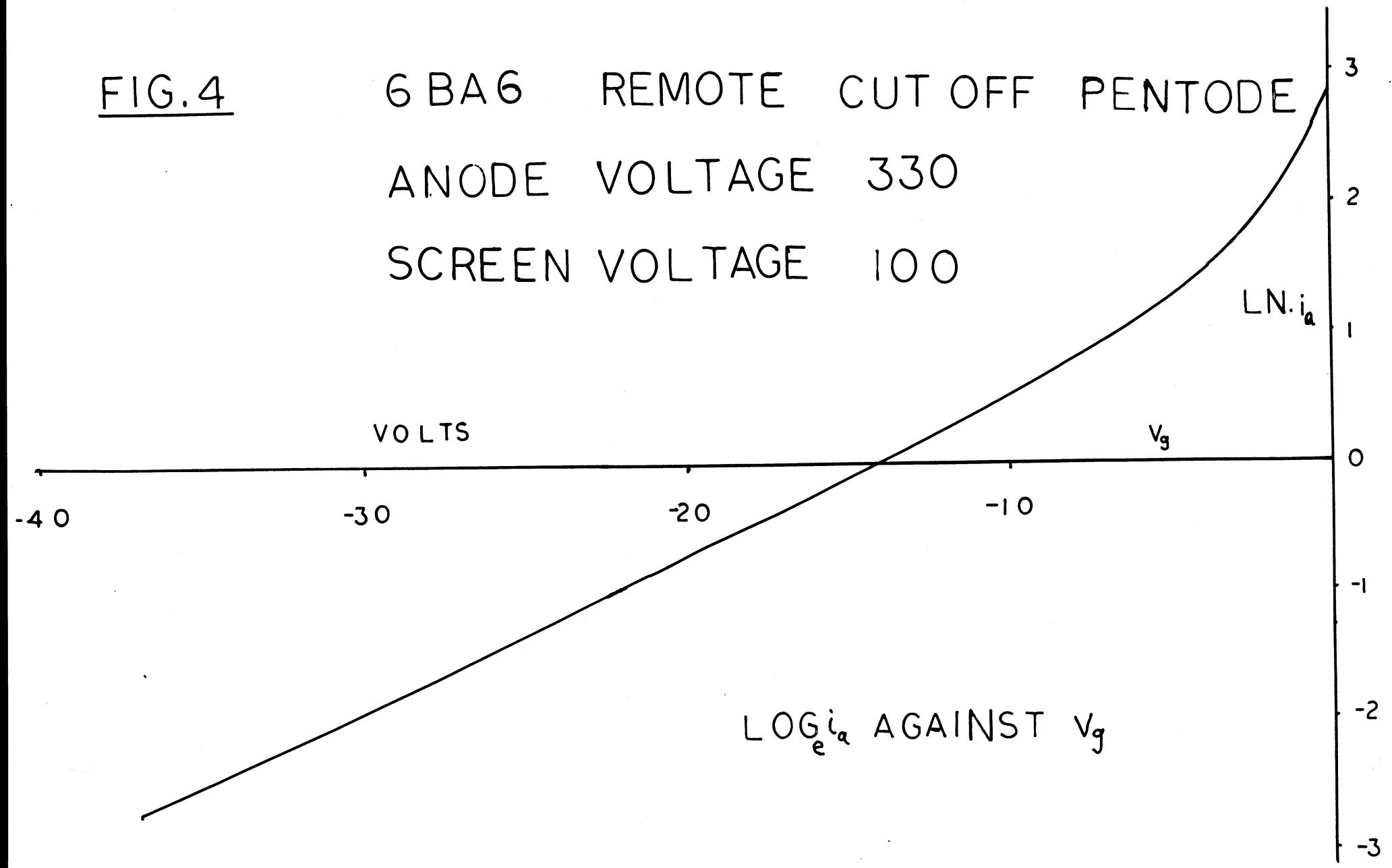

FIG. 5

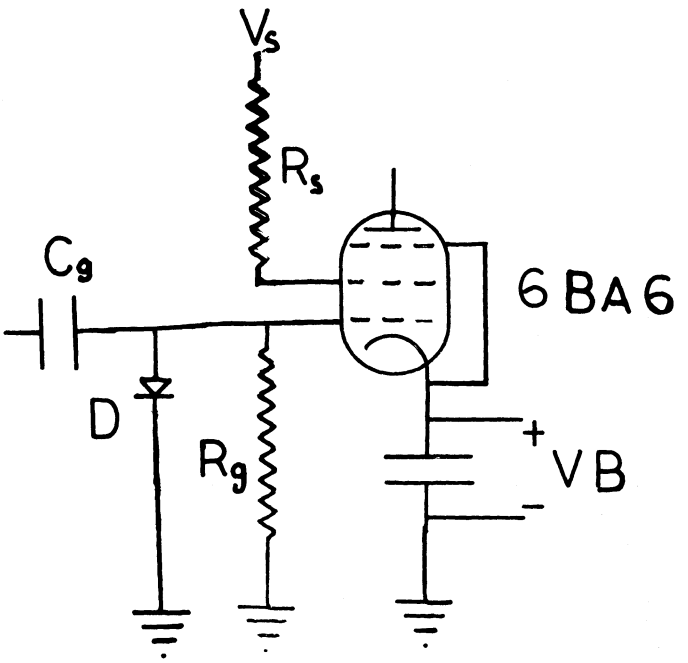

THE NON-LINEAR ELEMENT AND BIASING ARRANGEMENTS

FIG. 6

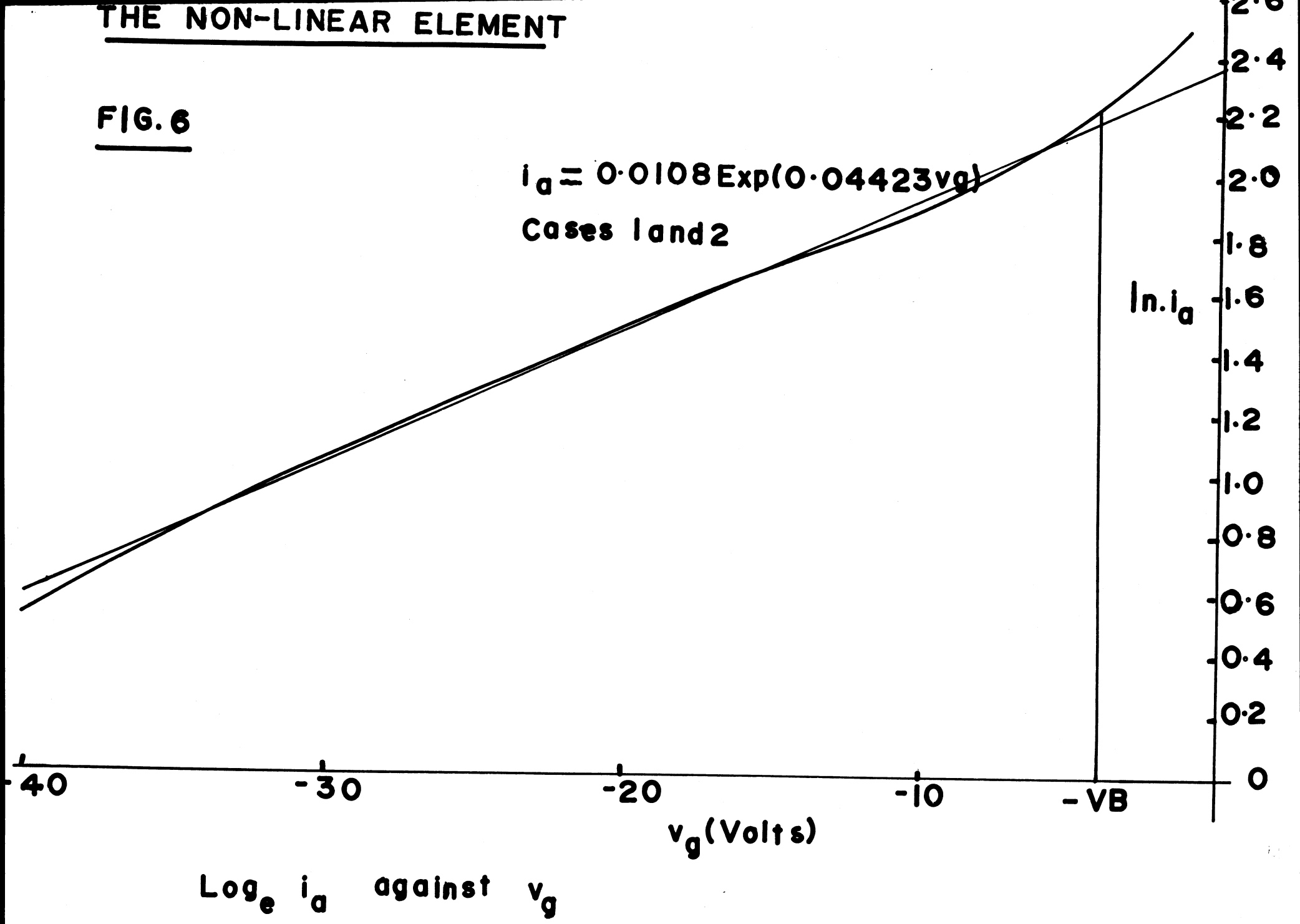

$\mathrm{Log}_e\ i_a$ against v_g

The non-linear element finally decided upon, therefore, is as shown in figure (5), which has as a typical characteristic, in terms of log i_a against v_g, that shown in figure (6), where i_a is the anode current, and v_g is the grid-cathode voltage. It can be seen that it is to within (±3%) a straight line within a range of v_g from -4volts to about -37 volts, and so is, to this degree of accuracy, a single exponential curve. The restriction on the highest obtainable grid-cathode voltage is enforced by injection of the direct voltage VB in the cathode lead; and the limiting action of the non-linearity is obtained from the diode rectifier D, in conjunction with R_g and C_g, producing an additional bias which is dependent on the size of the two component amplitudes.

Section (7) of this paper shows that the double frequency mode of oscillation can occur even with the component at the difference frequency at the grid being quite strong, but that if it were made too large one main component would suddenly die out. Moreover, it is also an experimental fact that the mode exists quite stably when the difference frequency component is negligibly small. If the difference frequency component at the input is neglected, therefore, that is to say, the time constant R_gC_g is made large in comparison with $I/(W_1-W_2)$, the equivalent linear gain of the non-linearity can be expressed as:

$$K_1 = \frac{2aI_1(bA_1)I_0(bA_2)\mathrm{Exp}(-b(A_1+A_2+VB))}{A_1} \quad ,$$

$$K_2 = \frac{2aI_0(bA_1)I_1(bA_2)\mathrm{Exp}(-b(A_1+A_2+VB))}{A_2} \quad ,$$

where A_1 and A_2 are the amplitudes of the two components, and the exponential approximation to the characteristic is $i_a=a\mathrm{Exp}(bv_g)$. $I_0(x)$ is

the zero order modified Bessel function and $I_1(x)$ is the first order modified Bessel function. K_1 is the equivalent linear gain to the component of frequency f_1 and amplitude A_1 and is in units of amperes per volt, since a is in amperes and A_1 in volts. K_2 is the corresponding gain to the other component. These expressions are established in appendix (II).

SECTION 4

THE FREQUENCY AND AMPLITUDE EQUATIONS

(4.1) The Feedback Loop and Block Diagram

The linear portion of the circuit, the feedback loop, consists basically of two parallel tuned circuits in series and a linear amplifier which is used as a phase inverter and is shown in figure (7); B is negative and v_a is the anode voltage resulting from the flow of the anode current i_a through the two tuned circuits whose combined inpedance is Z(p). The complete loop can now be represented by the block diagram of figure (8), where K is the equivalent linear gain of the non-linearity to the particular component being considered. In figure (9) G(p)= -BZ(p) and includes the phase inversion produced by the fact that an increase in the anode current will cause the anode voltage to change by an amount $i_a Z(p)$ in the opposite sense.

(4.2) The Oscillation Conditions

The impedance $\mathbf{Z}(p)$ is calculated from the two tuned circuit by considering the L's as pure inductances, and the R's as including all the losses in each corresponding circuit. Let $Z_1(p)$ be the impedance of C_1 in parallel with R_1 and L_1:

$$\text{therefore } \frac{1}{Z_1(p)} = \frac{1}{R_1} + \frac{1}{pL_1} + pc_1$$

$$= \frac{p^2 L_1 R_1 C_1 + pL_1 + R_1}{pL_1 R_1}$$

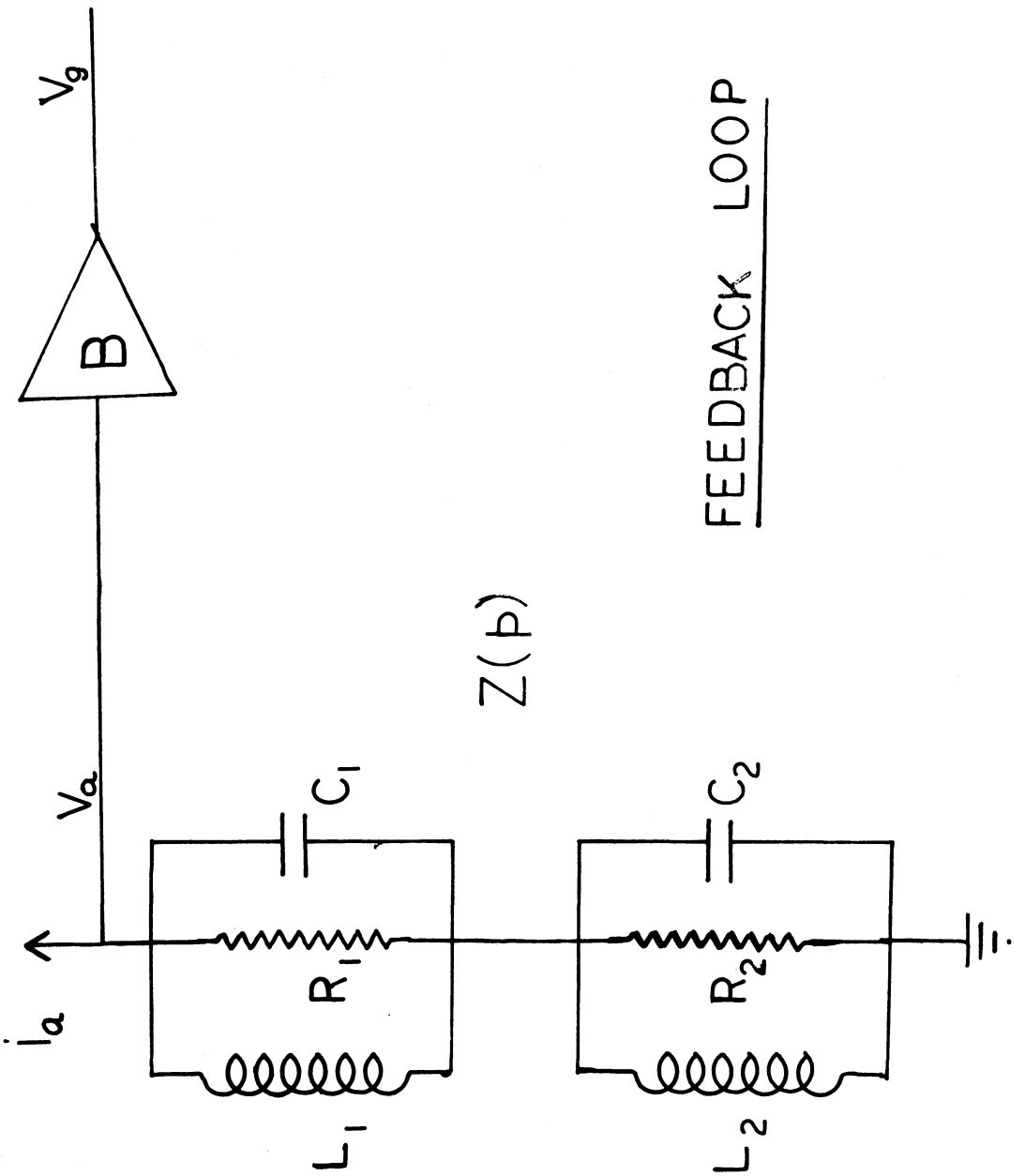

FIG. 7

THE BLOCK DIAGRAM

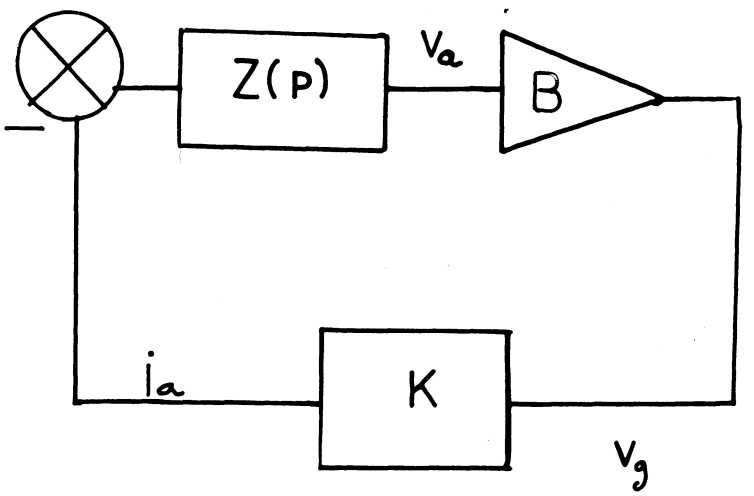

FIG. 8

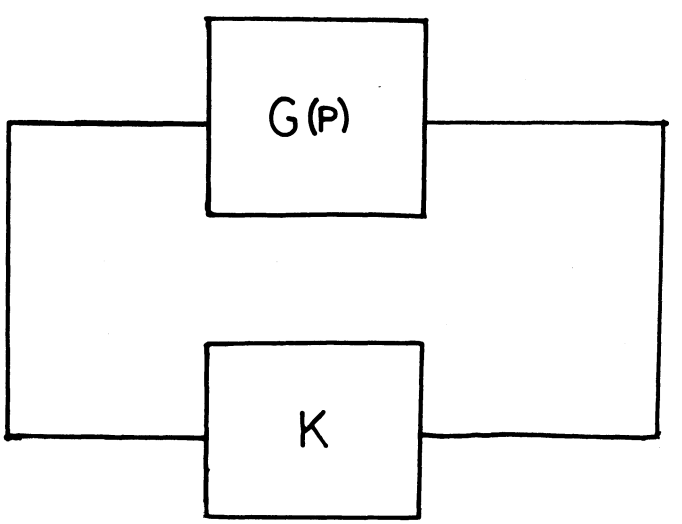

FIG. 9

$$\text{therefore } Z_1(p) = \frac{p}{C_1(p^2 + p/R_1C_1 + 1/L_1C_1)}$$

$$= \frac{p}{C_1(p^2 + p/R_1C_1 + 1/L_1C_1)(p^2 + 2a_1W_{10}p + W_{10}^2)} \quad (1)$$

$$\text{where } W_{10}^2 = \frac{1}{L_1C_1} \quad (2)$$

$$\text{and } a_1 = \frac{(L_1C_1)^{1/2}}{2R_1C_1} \quad (3)$$

$$\text{Similarly } Z_2(p) = \frac{p}{C_2(p^2 + 2a_2W_{20}p + W_{20}^2)} \quad (4)$$

$$\text{where } W_{20}^2 = \frac{1}{L_2C_2} \quad (5)$$

$$\text{and } a_2 = \frac{(L_2C_2)^{1/2}}{2R_2C_2} \quad (6)$$

But $Z(p) = Z_1(p) + Z_2(p)$

$$\text{therfore } Z(p) = p\left[\frac{1}{C_1(p^2 + 2a_1W_{10}p + W_{10}^2)} + \frac{1}{C_2(p^2 + 2a_2W_{20}p + W_{20}^2)}\right]$$

$$= \frac{p\left[(C_1 + C_2)p^2 + 2(C_2a_2W_{20} + C_1a_1W_{10})p + C_1W_{10}^2 + C_2W_{20}^2\right]}{C_1C_2(p^2 + 2a_1W_{10}p + W_{10}^2)(p^2 + 2a_2W_{20}p + W_{20}^2)}$$

$$= \frac{p(p^2 + 2ApW_0 + W_0^2)}{C(p^2 + 2a_1W_{10}p + W_{10}^2)(p^2 + 2a_2W_{20}p + W_{20}^2)} \quad (7)$$

$$\text{where } C = \frac{C_1C_2}{(C_1 + C_2)} \quad (8)$$

$$A = \frac{(C_1 a_1 W_{10} + C_2 a_2 W_{20})}{(C_1 + C_2)^{1/2}(C_1 W_{10}^2 + C_2 W_{20}^2)^{1/2}} \qquad (9)$$

$$W_0^2 = \frac{(C_1 W_{10}^2 + C_2 W_{20}^2)}{(C_1 + C_2)} \qquad (10)$$

In the above expression p is the Laplace complex variable s + jw, and the frequency response of the feedback loop is G(jw). The oscillating conditions can now be expressed implicitly, by writing down the requirements that, at each frequency, the signal amplitude and phase should be unchanged by passing completely round the loop;

that is $G(jW_1)K_1 = 1$ (11)

and $G(jW_2)K_2 = 1$ (12)

This represents four equations resulting from the phase and amplitude conditions applied to both components and they can be obtained by separating the real and imaginary parts of the above two equations.

(4.3) The Frequency Equation

The frequency equations can be reduced to one, since the condition that the imaginary part of G(jw) = 0 contains all possible zero phase shift frequencies. Hence the frequency equation is

$$\mathrm{Im.}\frac{(p)}{C}\ \frac{(p^2 + 2ApW_0 + W_0^2)}{(p^2 + 2a_1W_{10}p + W_{10}^2)(p^2 + 2a_2W_{20}p + W_{20}^2)} \Bigg|_{p=jw} = 0$$

i.e. $$\mathrm{Re.}\frac{(W_0^2 - w^2 + 2jAwW_0)}{(W_{10}^2 - W^2 + 2ja_1W_{10}w)(W_{20}^2 - w^2 + 2ja_2W_{20}w)} = 0$$

therefore $$\mathrm{Re.}\ (W_0^2 - w^2 + 2jAW_0w)(W_{10}^2 - w^2 - 2ja_1W_{10}w)(W_{20}^2 - w^2 - 2ja_2W_{20}w) = 0$$

$$\text{i.e. } (W_0^2 - w^2)(W_{10}^2 - w^2)(W_{20}^2 - w^2) + (W_0^2 - w^2)(-4a_1W_{10}w^2W_{20}a_2)$$

$$+ (W_{10}^2 - w^2)(4Aa_2W_0W_{20}w^2) + (W_{20}^2 - w^2)(4Aa_1W_0W_{10}w^2) = 0$$

which is a cubic equation in w^2.

$$\text{Let } w^2 = V,\ W_0^2 = V_0,\ W_{10}^2 = V_1 \text{ and } W_{20}^2 = V_2 \tag{13}$$

$$\text{therefore } V^3 - (V_0 + V_1 + V_2 + 4(a_1a_2W_{10}W_{20} - a_2AW_{20}W_0 - Aa_1W_0W_{10}))V^2$$

$$+ (V_1V_2 + V_2V_0 + V_0V_1 + 4(a_1a_2W_{10}W_{20}V_0 - a_2AW_{20}W_0V_1 - Aa_1W_0W_{10}V_2))V$$

$$- V_1V_2V_0 = 0 \tag{14}$$

$$\text{Let } -(V_0 + V_1 + V_2 + 4(a_1a_2W_{10}W_{20} - a_2AW_{20}W_0 - Aa_1W_0W_{10})) = B_2 \tag{15}$$

$$\text{Let } (V_1V_2 + V_2V_0 + V_0V_1 + 4(a_1a_2W_{10}W_{20}V_0 - a_2AW_{20}W_0V_1 - Aa_2W_0W_{10}V_2')) = B_1 \tag{16}$$

$$\text{and } -V_1V_2V_0 = B_0 \tag{17}$$

$$\text{Therefore } V^3 + B_2V^2 + B_1V + B_0 = 0 \tag{18}$$

is the frequency equation, whose roots will be the square of the angular frequencies at which the phase shift is zero.

The coefficients B_0, B_1 and B_2 could be calculated from the values of A, a_1, a_2, W_0, W_{10}, and W_{20} given by the relationships (2), (3), (5), (6), (9), and (10); that is, directly from the values of the circuit parameters. But it is more convenient and accurate to measure the response curves of the two tuned circuits separately in order to measure W_{10}, W_{20}, R_1, R_2, DW_{10} and DW_{20} and then use the realtionships:

$$a_1 = \frac{DW_{10}}{2W_{10}} \tag{19}$$

$$a_2 = \frac{DW_{20}}{2W_{20}} \tag{20}$$

$$C_1 = \frac{1}{2W_{10}R_1a_1} \tag{21}$$

$$C_2 = \frac{1}{2W_{20}R_2a_2} \tag{22}$$

$$W_0 = \frac{(C_1V_1 + C_2V_2)^{1/2}}{(C_1 + C_2)} \tag{23}$$

$$A = \frac{(a_1W_{10}C_1 + a_2W_{20}C_2)}{W_0(C_1 + C_2)} \tag{24}$$

in which DW_{10} is the bandwidth of the circuit tuned to W_{10} and $R_1 = Z_1(jW_{10})$, and corresponding definitions hold for DW_{20} and R_2.

Having obtained the values of the coefficients in the frequency equation (18) it can be solved as follows:

if x is defined as $x = \frac{(3B_1 - B_2^2)}{3}$

and y as $y = \frac{(2B_2^3 - 9B_2B_1 + 27B_0)}{27}$

let $\phi = \text{arc. cos.} \frac{-1/2\ y}{(-x^3/27)^{1/2}}$ (Reference (13))

then the roots of equation (18) are given by:

$$V = 2(-x/3)^{1/2} \cos(\phi/3) \tag{25}$$

$$V = 2(-x/3)^{1/2} \cos(\phi/3 + 2\pi/3) \tag{26}$$

$$V = 2(-x/3)^{1/2} \cos(\phi/3 + 4\pi/3) \tag{27}$$

From these the zero phase shift frequencies can be obtained in cycles per second by taking the square roots and dividing by 2π. Let these frequencies be, in descending order of magnitude, f_1, f_3, and f_2. It

will be shown in section (6) that the frequencies f_1 and f_2 are in fact very close to the actual oscillating frequencies obtained. The frequency f_3, which is between f_1 and f_2 represents an unstable oscillating condition which does not exist in practice.

(4.4) The Amplitude Equations

Once the oscillating frequencies have been predicted, it is then possible to solve the amplitude equations. The amplitude equations are given by the real parts of equation (11) and (12) and are:

$$\text{Re.}\ \frac{-B(jW_1)(W_0^2 - W_1 + 2jW_1AW_0)}{C(W_{10}^2 - W_1^2 + 2ja_1W_{10}W_1)(W_{20}^2 - W_1^2 + 2ja_2W_{20}W_1)} = \frac{1}{K_1} \qquad (28)$$

$$\text{and Re.}\ \frac{-B(jW_2)(W_0^2 - W_2^2 + 2jW_2AW_0)}{C(W_{10}^2 - W_2^2 + 2ja_1W_{10}W_2)(W_{20}^2 - W_2^2 + 2ja_2W_{20}W_2)} = \frac{1}{K_2} \qquad (29)$$

But the formulation of these two equations can be made very much easier by noting that, at W_1 and W_2, the imaginary part of $G(jw) = 0$ from the definition of the frequency equation. Hence equations (28) and (29) can be rewritten as:

$$\left|G(jW_1)\right| = \frac{1}{K_1}$$

$$\text{and} \quad \left|G(jW_2)\right| = \frac{1}{K_2}$$

since $|G|$ = Re. (G) when Im.(G) = 0 and Re. (G) is greater than zero since B is negative. Consequently the amplitude equations are:

$$\frac{-B(W_1)((V_0 - W_1^2)^2 + 4W_1^2A^2V_0)^{1/2}}{C((V_1 - W_1^2)^2 + 4W_1^2a_1^2V_1)^{1/2}((V_2 - W_2^2)^2 + 4W_2^2a_2V_2)^{1/2}} = \frac{1}{K_1} \qquad (30)$$

$$\text{and} \quad \frac{-B(W_2)((V_0 - W_2^2)^2 + 4W_2^2A^2V_0)^{1/2}}{C((V_1 - W_2^2)^2 + 4W_2^2a_1^2V_1)^{1/2}((V_2 - W_2^2)^2 + 4W_2^2a_2V_2)^{1/2}} = \frac{1}{K_2} \qquad (31)$$

The left hand sides of equations (30) and (31) can be evaluated using the previously found values of V_0, A, V_1, a_1, V_2 and a_2 together with equation (8).

The right hand sides are functions of the two amplitudes, such as:

$$\frac{A_1}{2I_0(bA_2)I_1(bA_1)aExp(-b(A_1 + A_2 + VB))}$$

and so equations (30) and (31) are not amenable to direct analytic solutions.

The solutions are simply obtained in the special case in which $A_1 = A_2$ since a graph of the function

$$\frac{A_1}{2I_0(bA_1)I_1(bA_1)aExp(-b(2A_1 + VB))}$$

can be drawn as a function of $A_1(=A_2)$ and the intersection with the line representing Re. $(G(jW_1))$ will give the amplitudes of the components (figure 10). This can be done since one would expect Re. $(G(jW_1))$ = Re. $(G(jW_2))$. The values of $\left|G(jW_1)\right|$ and $\left|G(jW_2)\right|$ evaluated from the roots of the frequency equations are in fact very nearly equal under these circumstances. Some results obtained by taking the average value $\left|G(jW_1)\right|$ and $\left|G(jW_2)\right|$ are presented in section (6) and it will be seen that they agree with the experimentally obtained amplitudes to within about 10%.

The case of unequal amplitudes could, theoretically, be solved by constructing a complete set of curves of

$\frac{A_1}{2I_0(bA_2)I_1(bA_2)aExp(-b(A_1 + A_2 + VB))}$ against A_1 with various values

of A_2 and another set for

$$\frac{A_2}{2I_0(bA_1)I_1(bA_2)aExp(-b(A_1 + A_2 + VB))}$$ against A_2 with various values of A_1. The line representing $|G(jW_1)|$ is super-imposed on the first set and that representing $|G(jW_2)|$ on the second. This procedure can be simplified, however, by noting that $K_1(A_1, A_2) = K_2(A_2, A_1)$, that is, K_1 becomes K_2 if A_1 and A_2 are interchanged. This means that only one diagram needs to be used with the two lines representing $|G(jW_1)|$ and $|G(jW_2)|$ super-imposed on it, as in figure (II).

Once this figure is constructed, it is a simple matter to obtain pairs of values for A_1 and A_2 which satisfy the equation $|G(jW_1)|$ equals $1/K_1$ and another set of pairs which satisfy $|G(jW_2)|$ equals $1/K_2$. This is done by writing down the coordinates of the points where the $|G(jW_1)|$ line crosses the 1/K lines and then renaming the A_1 axis the A_2 axis, regarding the A_2 increments as A_1 increments and reading off another set of coordinates from the intersection of the $|G(jW_2)|$ line with the 1/K lines.

At this stage there will be two lists of values for A_1 and A_2 each of which satisfies one of the equations (30) or (31). Theoretically, therefore, it would be expected that by drawing a graph of A_1 against A_2 from these values, the point of intersection would give the oscillation amplitudes, since this would be the only pair of values which would satisfy both equations simultaneously.

One example, attempted in this manner, did not reveal any results since the two lines on the A_1 vs. A_2 graph did not intersect (see figure (12)). But the conditions of the experiment did, in actual fact

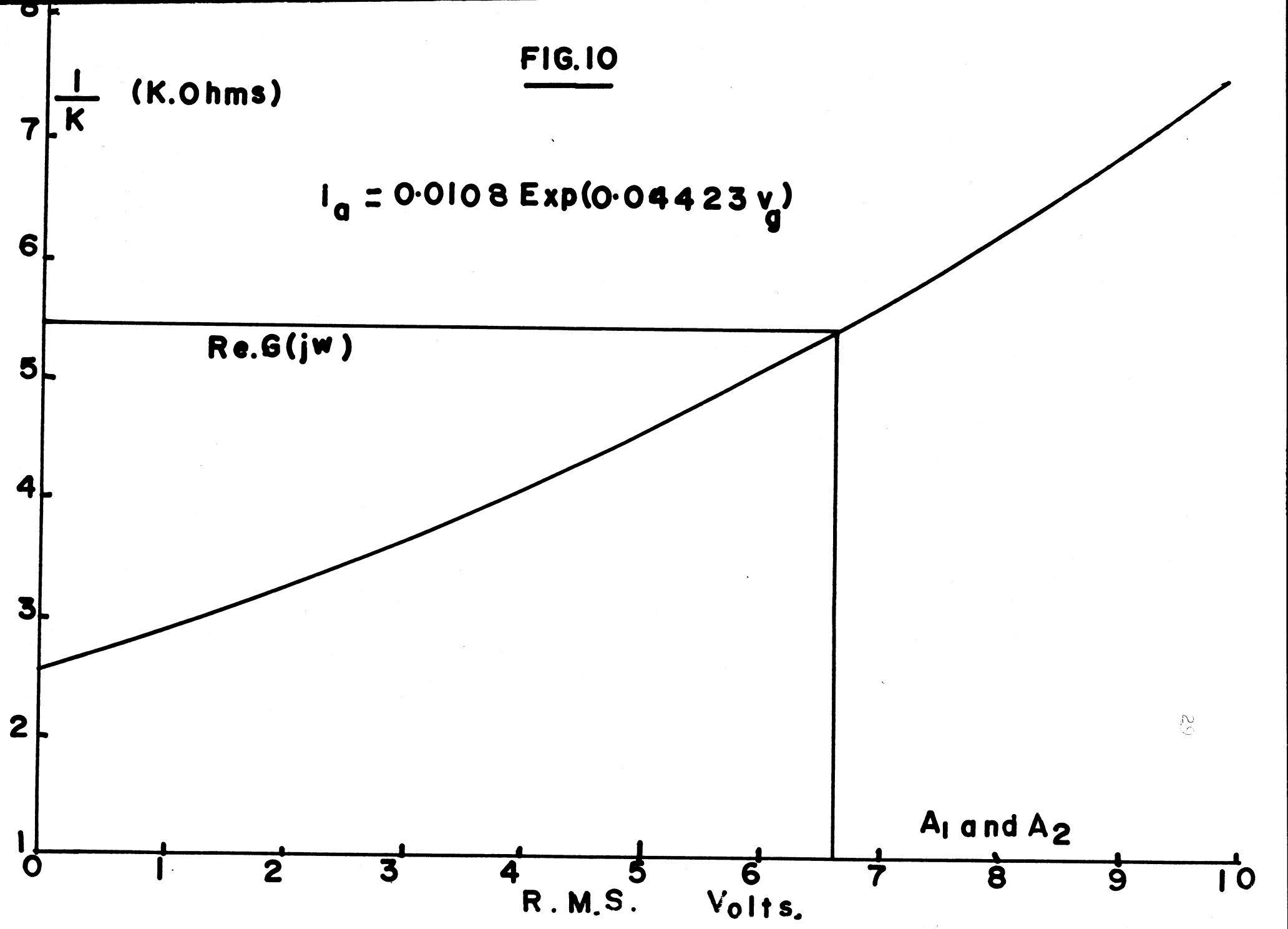
FIG. 10
1/K (K.Ohms)
$I_a = 0.0108 \, Exp(0.04423 \, v_g)$
Re.G(jw)
A1 and A2
R.M.S. Volts.
0
1
2
3
4
5
6
7
8
9
10

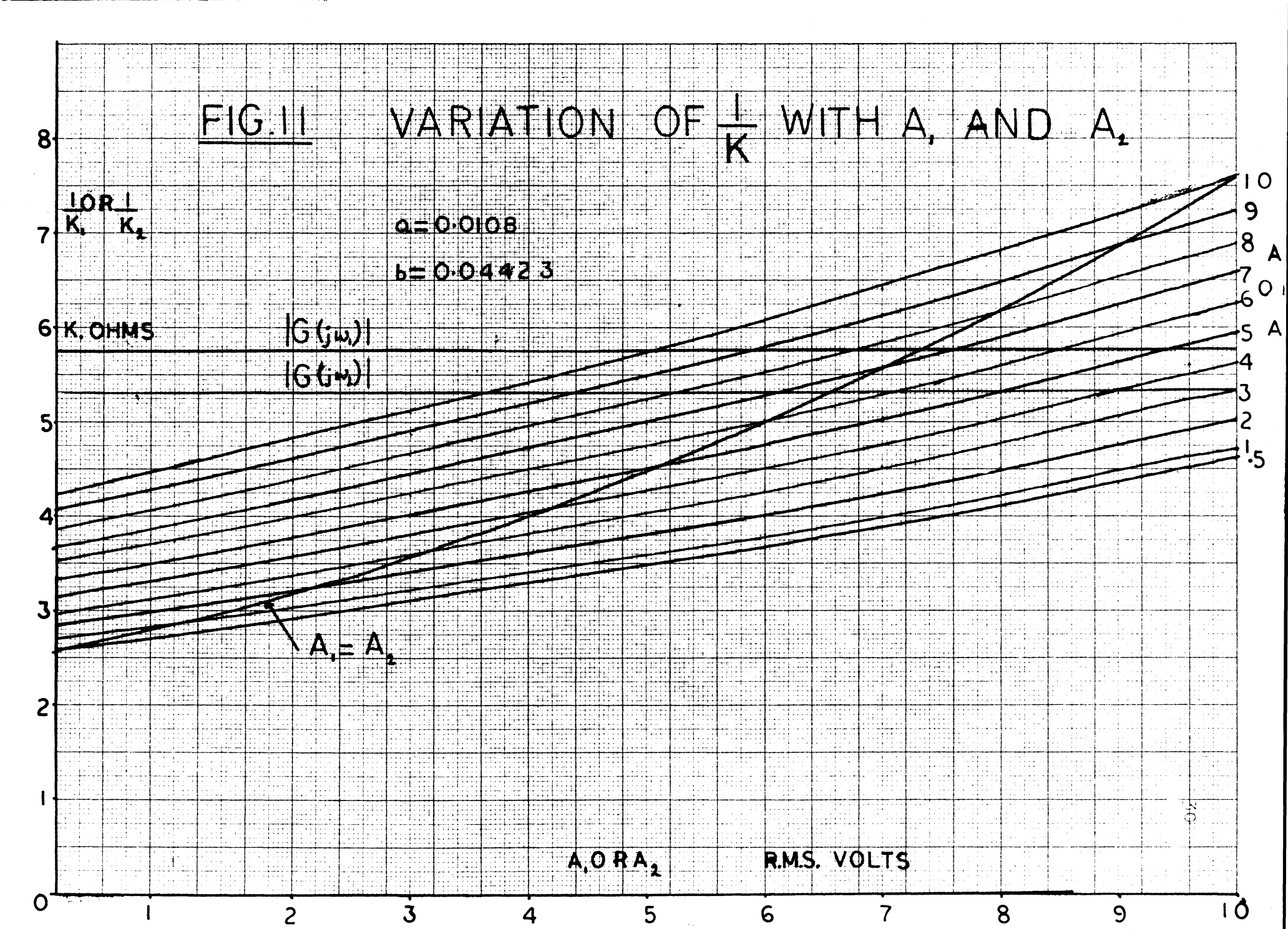
FIG. 11 VARIATION OF 1/K WITH A1 AND A2
1/K1 OR 1/K2
K. OHMS
a = 0·0108
b = 0·04423
|G(jω1)|
|G(jω2)|
A1 = A2
A1 OR A2
R.M.S. VOLTS
10
9
8
7
6
5
4
3
2
1·5
A
0
A
0
1
2
3
4
5
6
7
8
9
10

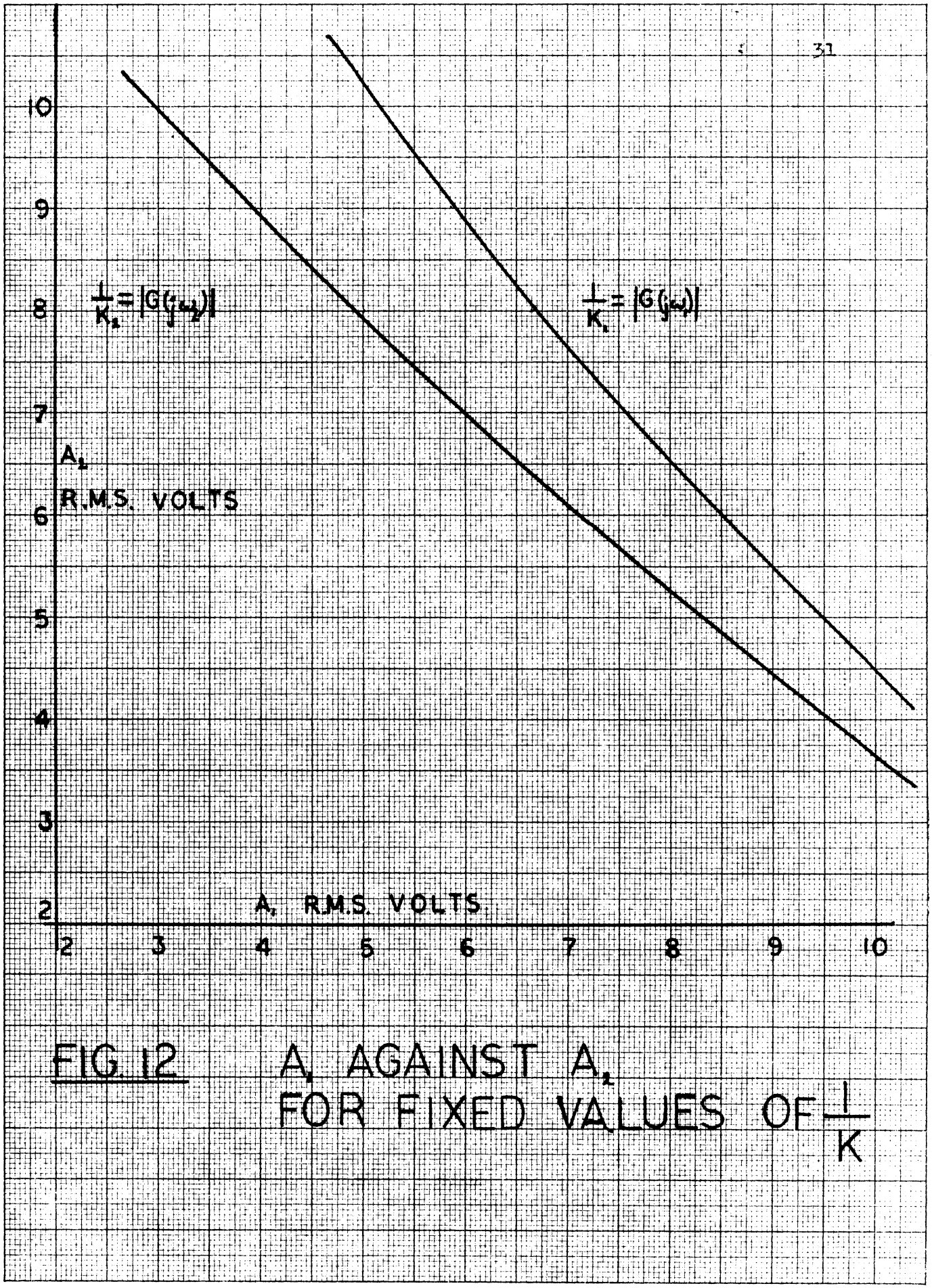

FIG. 12 A_2 AGAINST A_1 FOR FIXED VALUES OF $\frac{1}{K}$

produce real non-zero values for the amplitudes.

The inaccuracies involved in this method are so large that it can be of no practical use without greatly refining the measuring techniques, and the approximation of the non-linear element, but it is of interest theoretically, because it demonstrates the sources of error in the analysis. These errors are discussed in more detail in section (7), but for the moment it is sufficient to say that solution of the amplitude equations is here restricted to the case where the two amplitudes are equal, since this can be done with much greater accuracy than when they are not equal.

(4.5) Alternative Methods

There is an alternative method of predicting the oscillation frequencies and amplitudes. This is to take a complete frequency response curve as in figures (1) and (2) and treat each maximum as if it were produced by a single tuned circuit. The oscillating frequencies are accurately given by the zero phase shift frequencies f_1 and f_2 and agree closely with those calculated in the manner previously shown. The amplitudes are given by choosing the directly measured values of $|G(jw)|$ at these frequencies; the fact that this does not improve the accuracy of the predicted amplitudes suggests that the main source of error is in the treatment of the non-linear element.

One further alternative is to simplify the expression for $G(jw)$ by assuming at frequency f_1 the other tuned circuit is almost entirely capacitive and that at f_2 the first tuned circuit is almost entirely inductive. The individual frequency response curves can be used to

give the sizes of $|Z_1(jW_2)|$ and $|Z_2(jW_1)|$ or else they could be calculated, but in both cases, the effect of one on the zero phase shift frequency of the other can be estimated to give f_1 and f_2. The effect of one tuned circuit on the height of the other peak can also be estimated in this way in order to give, directly, values for $|G(jW_1)|$ and $|G(jW_2)|$. Again, however, the final estimation of the amplitudes is, as before, graphical solutions of $|G(jW_1)| = 1/K_1$ and $|G(jW_2)| = 1/K_2$.

(4.6) Summary

To summarise this section, therefore, the possible oscillating angular frequencies are given by the square root of the solutions of $V^3 + B_2V^2 + B_1V + B_0 = 0$, and the amplitudes (A) of the oscillations can best be found by a graphical solution of $|G(jw)| = 1/K(A)$, where $w = W_1$ or W_2 and K is equal to $\frac{2aI_0(bA)I_1(bA)Exp(-b(2A + VB))}{A}$ and is restricted to the case of equal amplitudes. $|G(jw)|$ is the average value of $|G(jW_1)|$ and $|G(jW_2)|$ calculated directly from the solution of the frequency equation.

SECTION 5

THE STABILITY AND STARTING ABILITY OF THE OSCILLATIONS

(5.1) Possible Oscillatory Modes

The previous section described a system for obtaining theoretical values for the oscillation frequencies and amplitudes: in this, it was assumed that the system oscillated in a mode containing both the frequencies f_1 and f_2, and only these two frequencies. Equation (18), however, does have six real solutions for w , three positive and three negative, where each of the negative roots is equal in magnitude to the corresponding positive root. The negative roots are of no concern in the present case, because they have no significance in reality. It is required, however, to establish which of the three positive roots represents stable oscillating components, and whether two or more of these components can exist together permanently in a single mode. In particular, it is necessary to show that the mode considered, containing f_1 and f_2, and only f_1 and f_2 components, is stable and can exist in practice, as it was assumed in the previous section.

There are seven possible oscillation modes containing finite frequency components. The first to be considered is the one of interest here, and stability criteria will be set up to show that this mode can in fact be stable in the presence of the disturbances inherently present in the system. Next it will be shown that either of the two modes containing only one of the components f_1 and f_2, can under certain

circumstances, be the only stable mode. The remaining four modes contain components with a frequency given by the third root of the equation (18). Some indication will be given for the physical reasons why these modes cannot, in practice, exist.

Finally it will be shown that if a particular mode is capable of stable existence, then it is also capable of starting from circuit noise without external assistance.

(5.2) The Stability of the Double Frequency Mode

Consider first, therefore, the stability of the mode containing components at frequencies f_1 and f_2. If it is assumed that the oscillations are existing in the state suggested in section (4), and the oscillations are disturbed from this state, the stability can be investigated by observing the reaction of the circuit to that disturbance. If this disturbance dies away as time goes on, then it can be assumed that the oscillations can persist without departing appreciably from the conditions assumed: that is, the oscillating frequencies and amplitudes are stable.

If the disturbance produces transients at the grid, which are exponentially changing increments in the steady state amplitudes, then the grid signal can be expressed as;

$$A_1\cos W_1 t + A_2\cos W_2 t + d_1 \mathrm{Exp}(s_1 t)\cos W_1 t + d_2 \mathrm{Exp}(s_2 t)\cos W_2 t - (A_1 + A_2) - VB \qquad (32)$$

It is assumed that the transients have been in existence for such a short time that the d.c. level $A_1 + A_2 + VB$ has not had time to change. (The grid time constant has already been postulated to be large.)

The anode cureent would now be given by;

$$i_a = aExp((A_1 cosW_1 t + A_2 cosW_2 t + d_1 Exp(s_1 t) cosW_1 t + d_2 Exp(s_2 t) cosW_2 t - (A_1 + A_2 + VB)b \quad (33)$$

$$= aExp(-(A_1 + A_2 + VB)b) Exp(bA_1 cosW_1 t) Exp(bA_2 cosW_2 t) Exp(bd_1 Exp(s_1 t) cosW_1 t) Exp(bd_2 Exp(s_2 t) cosW_2 t)$$

$$= aExp(-(A_1 + A_2 + VB)b)(e_0 + e_1 cosW_1 t + ...) (b_0 + b_1 cosW_2 t + ...) (c_0(t) + c_1(t) cosW_1 t + ...) (d_0(t) + d_1(t) cosW_2 t + ...) \quad (34)$$

where the terms not written down contain the higher harmonics of W_1 and W_2.

$$e_0 = I_0(bA_1) \quad (35)$$

$$e_1 = 2I_1(bA_1) \quad (36)$$

$$b_0 = I_0(bA_2) \quad (37)$$

$$b_1 = 2I_1(bA_2) \quad (38)$$

$$c_0(t) = I_0(bd_1 Exp(s_1 t)) = I + 1/4\ b^2 d_1^2 Exp(2s_1 t) + ... \quad (39)$$

$$c_1(t) = 2I_1(bd_1 Exp(s_1 t)) = bd_1 Exp(s_1 t) + 1/8.b^3 d_1^3 Exp(3s_1 t) + ... \quad (40)$$

$$d_0(t) = I_0(bd_2 Exp(s_2 t)) = I + 1/4\ b^2 d_1^2\ Exp(2s_2 t) + ... \quad (41)$$

$$d_1(t) = 2I_1(bd_2 Exp(s_2 t)) = bd_2 Exp(s_2 t) + 1/8.b^3 d_2^3 Exp(3s_2 t) + ... \quad (42)$$

where the terms not written down contain powers of d_1 or d_2 greater than the third.

In the case of the harmonics of W_1 and W_2 it has already been decided that these terms can be neglected because of the attenuating

action of the feedback loop. The terms in the expansions of $c_0(t)$, $c_1(t)$, $d_0(t)$, and $d_1(t)$, can all be neglected except for the first, not only beaause the coefficients decrease as the term order increases, but also because it can be assumed that d_1 and d_2 are small disturbances, and so their squares and higher powers can be neglected. It should be noted that the number b is less than unity.

The component of the anode current at frequency W_1 can now be written down as;

$$aExp(-(A_1 + A_2 + VB)b)(e_1b_0\cos W_1t + e_0b_0c_1(t)\cos W_1t)$$

of which

$$aExp(-(A_1 + A_2 + VB)b)e_0b_0c_1(t)\cos W_1t$$

is the transient portion. This is very nearly equal to

$$aExp(-(A_1 + A_2 + VB)b)I_0(bA_1)I_0(bA_2)bd_1Exp(s_1t)\cos W_1t$$

Let this equal

$$k_1d_1Exp(s_1t)\cos W_1t$$

There will be a similar current transient at angular frequency W_2, which can, in the same way, be written as,

$$k_2d_2Exp(s_2t)\cos W_2t,$$

where

$$k_2 = aExp(-(A_1 + A_2 + VB)b)I_0(bA_1)I_0(bA_2)$$

It is now necessary to calculate the response of the linear part of the circuit to the waves $k_1d_1Exp(s_1t)\cos W_1t$ and $k_2d_2Exp(s_2t)\cos W_2t$ and equate these to the original transients $d_1Exp(s_1t)\cos W_1t$ and $d_2Exp(s_2t)\cos W_2t$.

The response of G(p) to a wave such as VExp(pt) is VExp(pt)G(p) and so the response to $k_1d_1Exp(s_1t)\cos W_1t$ is $Re.(k_1d_1Exp(pt)G(p))$, with

$p = s_1 + jW_1$.

At this point we use the assumption, already implied, that the transients are exponentially varying components at the oscillating frequencies, and that these frequencies are unaffected by the presence of the transients. In other words, the imaginary part of $G(s_1 + jW_1)$ is taken to be zero like the imaginary part of $G(jW_1)$.

This assumption, that the transients are at the oscillating frequencies, amounts to regarding the gain characteristic of figure (1) as having even symetry around f_1 and f_2 and the phase characteristic of figure (2) as having odd symetry around f_1 and f_2. In the practical case, since the Q's of the tuned circuits are high, this approximation is fairly close to the real situation provided the disturbances are not too large.

The transfer function $G(p)$ to each particular frequency can now be approximated by those of single equivalent turned circuits. They are

$$G_1(p) = \frac{-BP}{C_1'(p^2 + 2a_1'W_{10}'p + W_{10}'^2)} \quad \text{for } p = s_1 + jW_1 = p_1$$

$$G_2(p) = \frac{-BP}{C_2'(p^2 + 2a_2'W_{20}'p + W_{20}'^2)} \quad \text{for } p = s_2 + jW_2 = p_2$$

With this in mind $G_1(s_1 + jW_1)$ and $G_2(s_2 + jW_2)$ can be taken as real and the closed loop equations for the transients are now

$k_1d_1G_1(s_1 + jW_1)\text{Re.Exp}((s_1 + jW_1)t) = d_1\text{Re. Exp}((s_1 + jW_1)t)$ and

$k_2d_2G_2(s_2 + jW_2)\text{Re.Exp}((s_2 + jW_2)t) = d_2\text{ Re.Exp}((s_2 + jW_2)t)$

that is $k_1G_1(s_1 + jW_1) = 1$ (43)

and $k_2G_2(s_2 + jW_2) = 1$ (44)

or writing $p_1 = (s_1 + jW_1)$ and $p_2 = (s_2 + jW_2)$ (45)

and $k_1G_1(p_1) = 1$ (46)

Taking (45) as an example, the conditions of stability can now be established. These conditions result from the restrictions on the circuit parameters, which are required to ensure that the roots of equation (45) all have negative real parts. That is, all possible values of s_1 are less than zero, and so the transient will eventually die out. Equation (45) is;

$$\frac{-k_1 B p_1}{C_1'(p_1^2 + 2p_1 a_1' W_{10}' + W_{10}'^2)} = 1$$

That is $- k_1 B p_1 = C_1' (p_1^2 + 2a_1' W_{10}' p_1 + W_{10}'^2)$

$$p_1^2 + (2a_1' W_{10}' + \frac{k_1 B}{C_1'}) p_1 + W_{10}'^2 = 0$$

from which $p_1 = -(a_1' W_{10}' + \frac{k_1 B}{2C_1'}) \pm j(W_{10}'^2 - (a_1' W_{10}' + \frac{k_1 B}{2C_1'})$ (47)

$$= s_1 + jW_1$$

Therefore $s_1 = -(a_1' W_{10}' + \frac{k_1 B}{2C_1'})$

The stability criterion can now be set down as the requirement that $a_1' W_{10}' + \frac{k_1 B}{2C_1'}$ should be positive. That is a_1' should be greater than $\frac{-k_1 B}{2C_1' W_{10}'}$ and so the stability criterion reduces to a limit on the minimum amount of damping which can be used. This is as would be expected, since with no damping at all there would be no losses and no mechanism by which the transient could loose energy. The gain of the non-linear element would then cause the amplitude of the disturbance to increase.

The conditions of stable oscillation in the double frequency mode, are thus dependent on a compromise being found between conflicting criteria. Firstly, that the damping factors should be low enough to ensure that the linear circuit behaves as an efficient filter to remove the unwanted components and also so that the symetry approximations can be made, and secondly the damping factors should not be so low as to enable any transients in the amplitudes to increase with time.

A similar condition results from equation (44), and the two become identical when the amplitudes of the steady state oscillations are equal.

In section (6), one of the practical examples, which is known to be stable, and has typical circuit parameters, is tested against these conditions and they are shown to be satisfied.

It is sufficient for the present purposes to show that it is possible to satisfy the prescribed conditions of stability of the double frequency mode with real circuit parameters. This is done as already stated, in the converse manner of showing that a real set of parameters can satisfy the conditions; consequently, it has now been shown that the amplitudes and the frequencies of the oscillations can be predicted and that they can also be stable.

The complete treatment of the stability problem which concerns this mode can only be effected by considering the complete transfer function for $Z(p)$ as given in equation (7) and would entail consideration of phase shifts produced by the transients. These phase shifts could be neglected and the stability conditions established using Routh's criteria (Reference 14). However, this is equivalent to the symetry conditions

already assumed and so the simplified transfer function entails no further approximation.

(5.3) The Starting Ability of the Double Frequency Mode

The conditions that the double frequency mode is self-starting from the circuit noise can be set down by stating that the loop gain to the two frequencies at zero amplitude should be greater than zero. That is,

$G(jW_1)\ abExp(VB)$ is greater than unity ... (47)

and,

$G(jW_2)\ abExp(VB)$ is greater than unity (48)

which are simply found by noting that $I_0(bA)$ tends to unity as A tends to zero and

$$\lim_{A \to 0} \frac{2I_1(bA)}{A} = \lim_{A \to 0} \frac{2(1/2bA + b^3A^3/16+\ldots)}{A} = \lim_{A \to 0} (b + b^3A^2/16+\ldots) = b$$

and they are always satisfied if there are real solutions to the amplitude equations (30) and (31).

Two important points must be observed here: first of all, figure (13) shows that with this type of automatic bias and injection of the fixed bias, the loop gain is a maximum when the two amplitudes are zero; secondly, it also shows thatthe rate of change of gain to a small amplitude is greater than that to a large amplitude. One would intuitively expect, therefore, that if the two components are each capable of starting, as given by conditions (47) and (48), they will continue to increase together until the stable oscillating point is reached. This is, in fact, observed experimentally, but rigorous proof would require the solution of

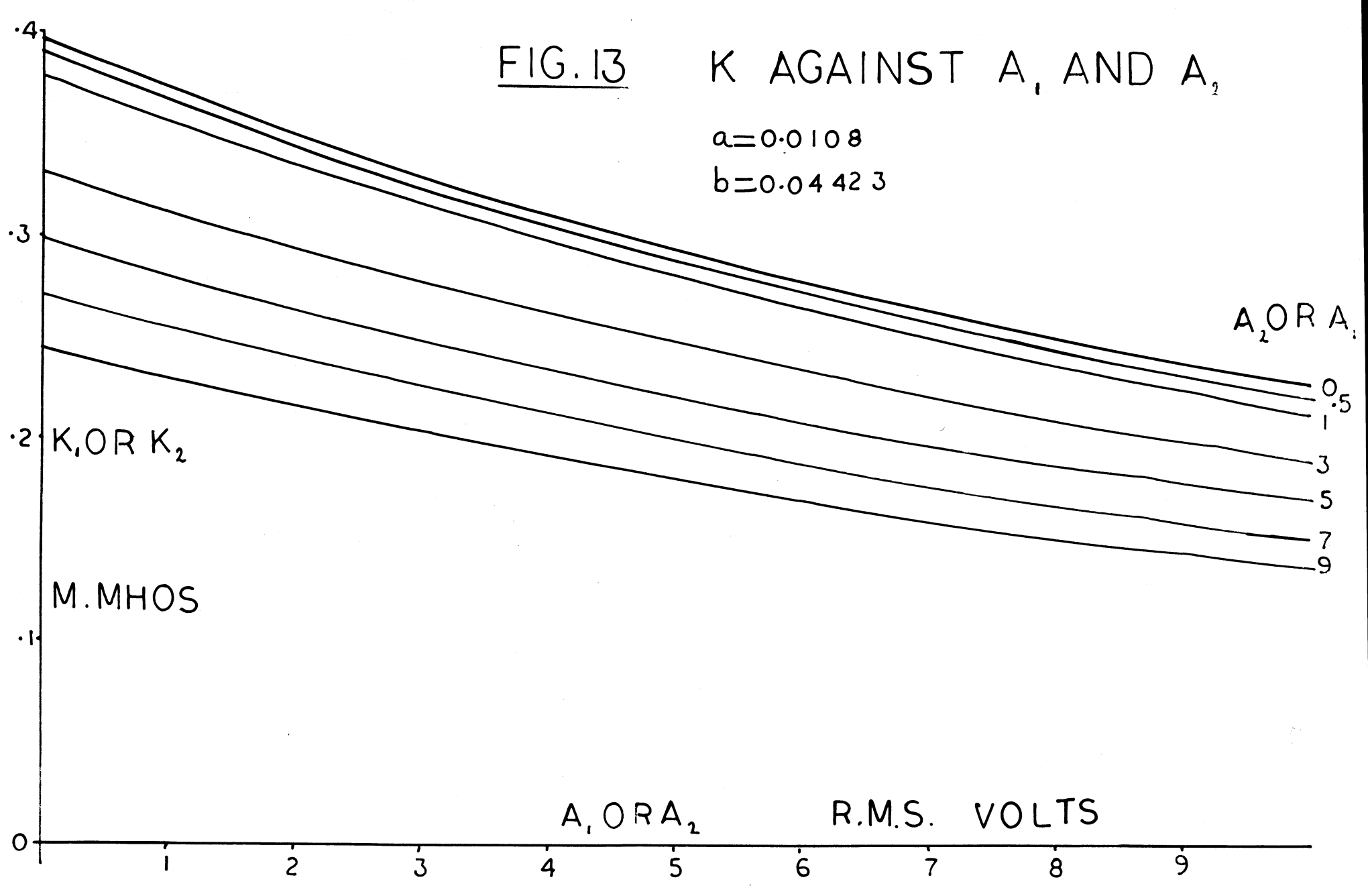
FIG. 13 K AGAINST A1 AND A2
a=0·0108
b=0·04423
A2 OR A1
0·5
1
3
5
7
9
K1 OR K2
M.MHOS
·4
·3
·2
·1
0
A1 OR A2 R.M.S. VOLTS
1
2
3
4
5
6
7
8
9

the non-linear differential equation governing the build-up.

Several alternative methods of injecting the fixed bias were tried, one of which was to feed the grid from a direct voltage source via a resistor. The external direct voltage was made equal to $-(A_1 + A_2 + VB)$ so that the grid would never become more positive than -VB. In this case, the system would have a minimum loop gain at the zero signal level, and it was observed that it would start in the single frequency mode and the second component would only appear after the loop gain had become sufficiently large.

(5.4) Single Frequency Mode

If we now consider the situation where only one of the conditions (47) or (48) is satisfied it can be seen that only the component corresponding to that condition can build up. As it does, the working point will move along the top curve in figure (13), and both the gain to this component, and to the other, which has not started, will decrease. There is therefore no reason to believe that the second component should start at all, and the system will behave like a normal single frequency oscillator which has a slightly distorted frequency response curve. The amplitude could be predicted by equating G(jw) to 1/K and solving it graphically. The stability can be examined by use of a similar technique to that used for the double frequency case, but it will, of course, result in a simpler equivalent gain k, and in only one set of conditions. The value of k needed for the stability criteria will be $abI_0(bA)Exp(-A + VB)b$

The value of K in this case would be $\frac{2aI_1(bA)Exp(-(A + VB)b)}{A}$ and for a given value of G(jw) the amplitude equation will require a greater

value of A for a solution than either of the amplitudes in the double frequency mode.

It is evident that a set of real circuit parameters can exist which complies with the stability conditions for this mode, since the system can easily be made to degenerate into a normal single frequency, Class C, oscillator, by reducing the Q of one of the tuned circuits.

(5.5) Modes Containing the Third Root of the Frequency Equation

The remaining part of this section will be concerned with the other solution of the frequency equation, namely the third root, which lies between W_1 and W_2.

This root could give rise to a component which, if it were stable, could produce four other modes of oscillation. The fact that none of these modes has occurred in practice would suggest that they are all unstable. However, to prove this would require that the oscillating conditions in each case should be evaluated and the conditions disturbed to see if the transients did, in fact, increase with time.

It should be observed that if the component did exist, along with the other two, the required value of $G(jW_3)$ in order that this component should have a non-zero amplitude would be:

$$\frac{A_3}{2AI_0(bA_1)I_0(bA_2)I_1(bA_3)\mathrm{Exp}(-(A_1 + A_2 + A_3 + VB)b)} \qquad (49)$$

which is greater than $1/(ab)$. But $1/(ab)$ is approximately equal to 2.10^3 ohms, whereas the value of $G(jW_3)$ is, at the most 200 ohms; hence, even if this component were stable, it could not exist under the present circumstances because the loop gain is too small.

The instability of one of these modes can be fairly simply established by observing that the polar locus of G(p) has a greater real part near $p=jW_3$, when $p=s+jw$ than when $p=jw$, for positive s (see appendix IV). The mode considered is that most likely to satisfy the loop gain condition, namely the one in which the other two components do not exist.

With reference to figure (14), it can be seen that even if the non-linear element or the feedback network were altered so that the amplitude equation did have a solution, the oscillation at W_3 could not possible be stable. This is due to the fact that the value of $1/K_3$ increases to the right along the positive real axis as the amplitude increases.

$$\left(\frac{1}{K_3} = \frac{A_3}{2aI_1(bA_3)\mathrm{Exp}(-(A_3 + VB)b)}\right)$$ The result of this is that any disturbance away from the working point at W_3 will either, cause a decrease in amplitude and a movement into the negative s region, or an increase in amplitude and a movement into the positive s region. In either case, the change in the oscillating conditions will be assisted, and the component will either die out, or quickly change, in amplitude and frequency, to stable oscillations at W_1 or W_2, or both.

(5.6) The Regions of the G Plane

In appendix (IV) the method of investigating the effect of putting $p = s + jw$ instead of jw, in the regions of W_1, W_2, and W_3 is shown, and the actual variations of G(p) with s in these regions are given in figures (34), (35), and (36) for values of s ranging from -12.10^3 (seconds)$^{-1}$ to

FIG.14 POLAR PLOT OF $G(jw)$

FREQUENCIES IN Kc./s

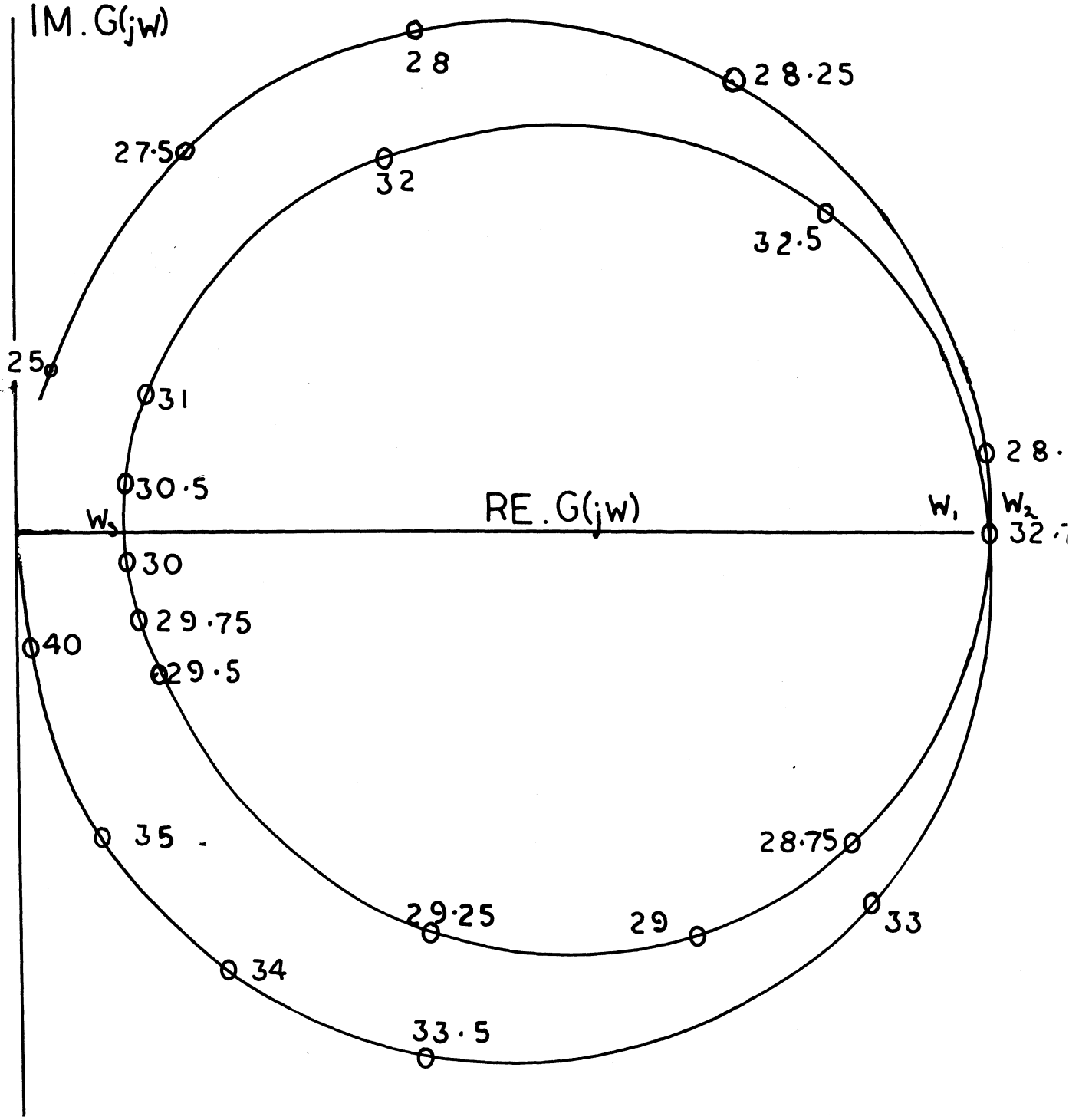

12.10^3 (seconds)$^{-1}$. These curves again represent the conditions of case (1). The first two of the figures indicate that oscillation frequencies W_1, and W_2 may be stable and the last one, figure (36) is the basis of the argument which has been used to show W_3 is an unstable oscillating frequency, at least when it exists alone.

(5.7) Squegging

Another form of instability exists, which is unaccounted for by the present theory. This is the amplitude instability known as "squegging". Instability of this form is not peculiar to double frequency oscillators, and in fact has been thoroughly investigated before (see reference (15)) in terms of the general single frequency oscillator.

One cause of this instability is that the gridis driven to cut off the tube by the accumulation of charge due to the grid time constant's being too long. Once the tube has cut off, the oscillations cease, and the grid loses its charge at the rate defined by the time constant C_gR_g, so at some point, the loop gain again returns to unity, and the oscillations can recommence. The result of this is a relaxation type of oscillation, which bursts of sinusoidal oscillations superimposed on it.

Any discussion of squegging applies equally well to the double frequency case, since if the time constant is too large, any type of oscillation could continuously tend to drive the grid negative, reduce the gain of the tube, and finally, suppress the oscillations. The important point for the present purposes is that, even if the stability conditions previously given are satisfied, then, in order to obtain the desired oscillations, it is also necessary to ensure that squegging does

not occur. If the stability conditions are satisfied, but the time constant of the detector is too long, then squegging will occur at double frequency. Such a phenomenon is demonstrated by figures (23) and (24) of section (7), in which the limitations imposed by the onset of squegging are discussed.

not occur. If the stability conditions are satisfied, but the time constant of the detector is too long, then squegging will occur at double frequency. Such a phenomenon is demonstrated by figures (23) and (24) of section (7), in which the limitations imposed by the onset of squegging are discussed.

SECTION 6

COMPARISON OF THEORY WITH PRACTICAL RESULTS

(6.1) The Practical Circuit

The final experimental arrangement, from which the measurements were taken is given in detail in figure (15), and as a block diagram in figure (16).

There are a few details left out of figure (15) for clarity, since they are unimportant for the present purposes. For the record, however, they are given here. The heaters of the two cathode followers are operated at an elevated D.C. level to avoid breakdown to the cathode; otherwise the heating system is normal. The other omissions are, loosely coupled secondaries on the coils L_1 and L_2 with various tapping points, and switching arrangements to select the various degrees of feedback and connect them to the grid, and at the same time to disconnect the second stage. Since the system would not oscillate in this configuration, due to insufficient gain, this selector switch was not used and the secondaries were left open-circuited. It may be noted in passing that the system can be made to oscillate in the double frequency mode, by amplifying the signals picked up on the secondaries and then applying them to the grid.

(6.2) Obtaining the Results

From the arrangement given in figures (15) and (16), the practical results were obtained by observing the amplitudes of the main

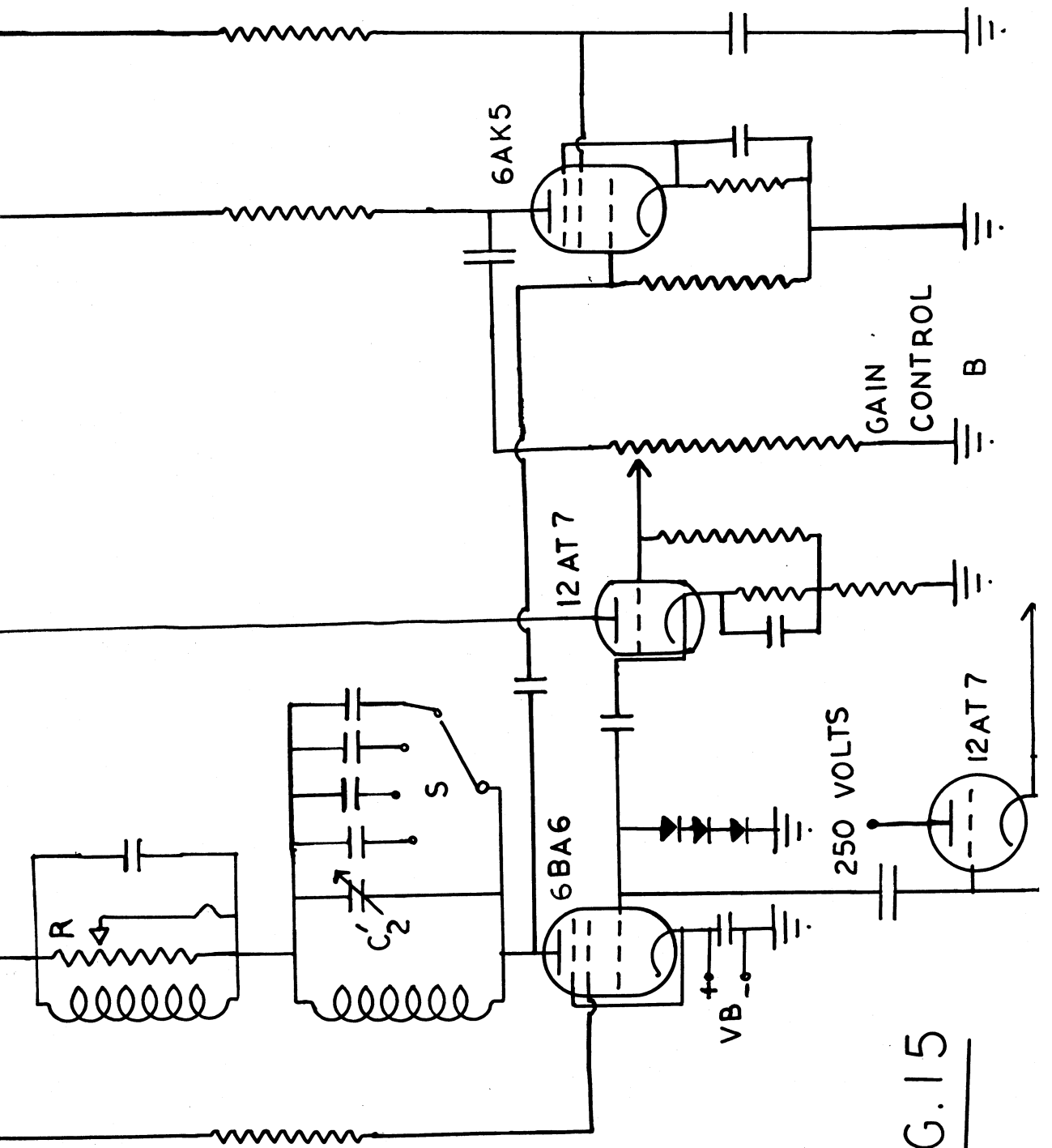

FIG. 15

FIG. 16

BLOCK DIAGRAM

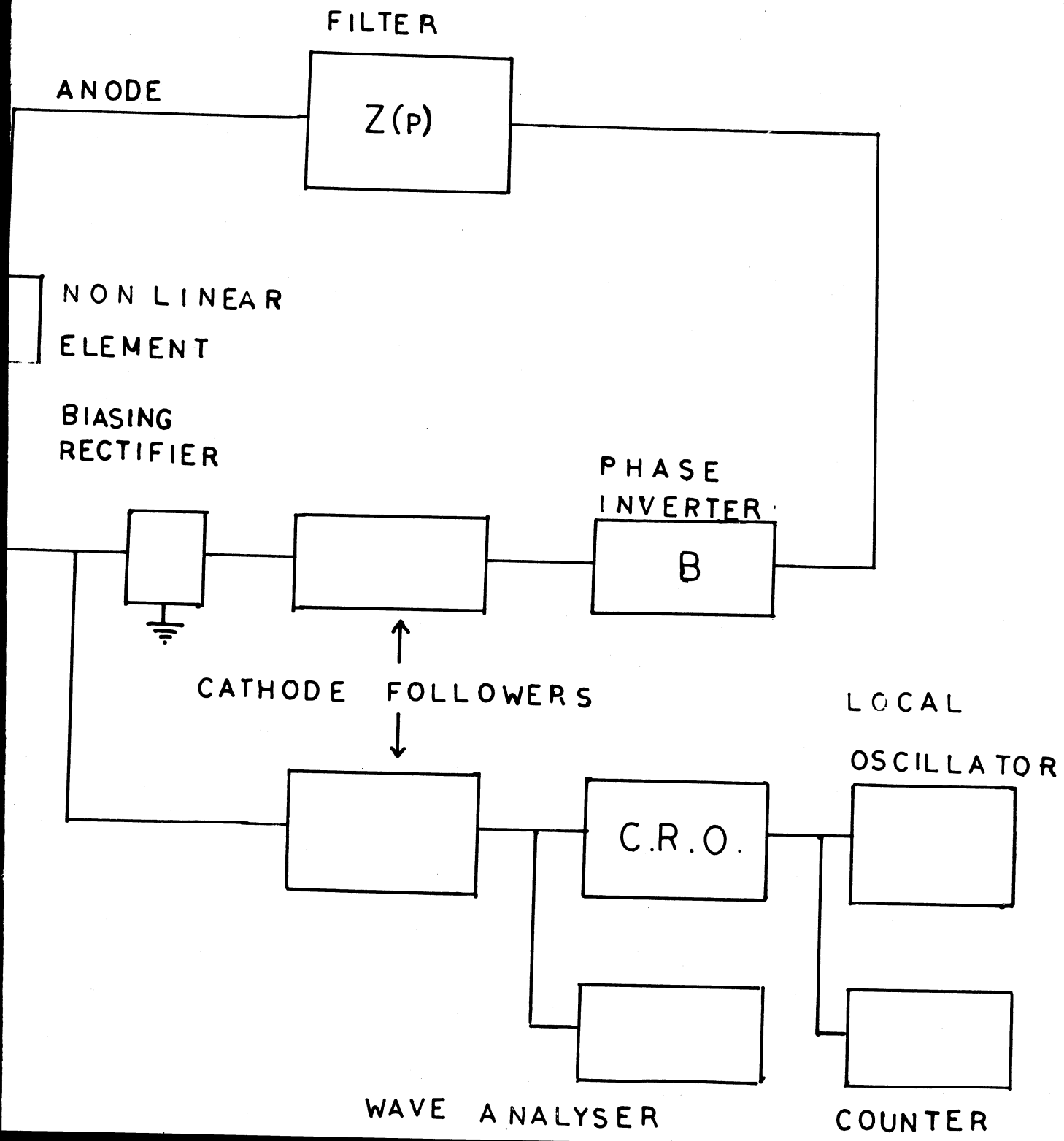

components by means of the wave analyser, after having selected the approximate oscillating frequencies on the switch S and using the fine adjustment variable condenser C_2' to ensure that the frequencies are incommesurable, in accordance with the method described in appendix (III).

To obtain the equal amplitude condition, the wave analyser was tuned alternately to f_1 and f_2, and each time half the amplitude difference was added to the smaller amplitude, or subtracted from the larger by adjustment of R, until finally A_1 was equal to A_2. The values of A_1 and A_2 in R.M.S. volts were found by dividing the wave analyser readings by the gain of the cathode follower.

The measurement of the frequencies was effected by applying the grid signal to the y-plates of an oscilloscope via a cathode follower. The frequency of the component being observed was then found by reading a counter driven by a local oscillator which was also used to supply the voltage on the x-plates of the oscilloscope. Hence, the required frequency could be read directly by adjusting the local oscillator until the corresponding Lissajous pattern was made stationary on the oscilloscope screen. This system of frequency analysis is discussed in more detail in appendix (III).

(6.3) Comparison with the Theoretical Values

The theoretical values for the amplitudes and frequencies were calculated using the direct method discussed in section (4). The required circuit parameters were obtained from the individual frequency response curves and the value of B. The gain of the phase inverter and cathode follower together was measured directly. The frequency response

FIG.17

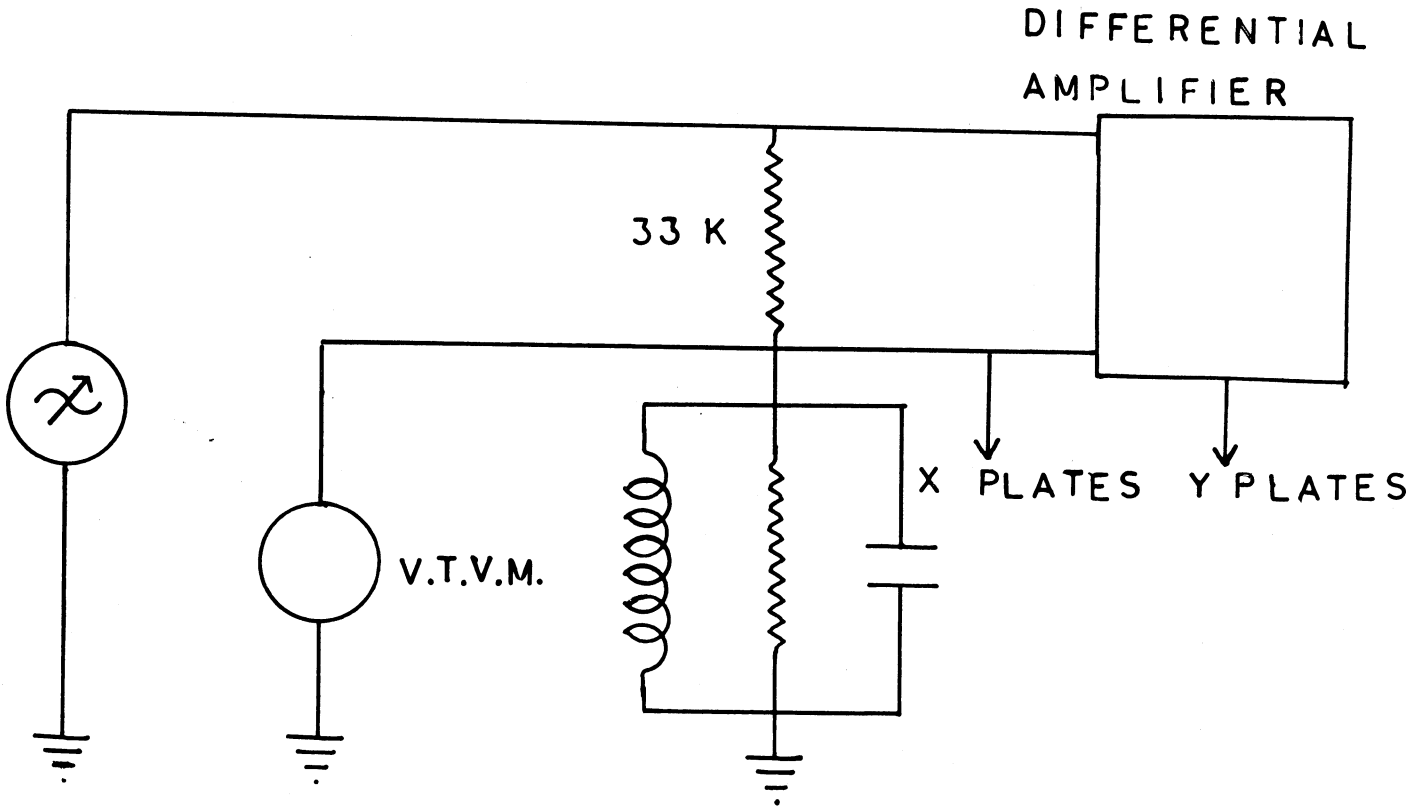

METHOD OF OBTAINING RESPONSE CURVES.

curves were obtained by isolating a tuned circuit, grounding one end, and forcing a current into the other end. The arrangement for reading the current is shown in figure (17), and it is to read the voltage drop across a resistance placed in series with the circuit by using the differential amplifier available in the Tetronix 502 oscilloscope. The zero phase shift frequencies could be read simply by observing the peak deflection on the V.T.V.M., or else by observing the Lissajous figure formed by applying a signal proportional to the current, to the y-plates, and one proportional to the voltage to the x-plates. The elliptical figure degenerated into a straight line when the two were in phase, and gave the same result as the peak deflection method, when corrections had been made for internal phase shift in the oscilloscope. The peak voltage was proportional to the equivalent shunt resistance. The effect of changes of load on the oscillator as the circuit impedence changed, was controlled by altering the oscillator output voltage so as to keep the current constant.

In some cases the frequency response was observed throughout a range near the zero phase shift frequency, but usually only this frequency and those two which produced an impedence equal to $R/(2)^{1/2}$ were taken.

With the circuit parameters calculated from these readings the zero phase shift frequencies were evaluated and then the value of $|G(jw)|$ at the highest and lowest of these was found. Using the average of these two values of $|G(jw)|$, the oscillating amplitudes were obtained from the graph of 1/K.

Some of these calculated results are now given, along with the actual oscillating conditions.

Case (1),

R_1 = 4.983 K.ohms.

R_2 = 4.761 K.ohms.

f_{10} = 31.16 Kc/s.

f_{20} = 22.62 Kc/s.

Df_{10} = 1.16 Kc/s.

Df_{20} = 0.71 Kc/s.

B = - 1.115

from which the two oscillating frequencies are calculated.

The frequencies are given here in Kc/s.

OSCILLATING FREQUENCIES

	Calculated Calues	Actual Values
f_1	31.133	31.077
f_2	22.641	22.671

The frequency errors, in this case, are of the order of 6/3000 .100%, i.e. .2%.

From these calculated values of f_1 and f_2, the values of $Re.G(jW_1)$ and $Re.G(jW_2)$ were found to be 5.557 K.ohms. and 5.308 K.ohms., whose average value is 5.433 K.ohms. By comparing this with the curve given in figure (10) for 1/K against A, the oscillating amplitudes can be calculated.

These amplitudes are given in R.M.S. volts;

OSCILLATION AMPLITUDES

Calculated Value	Actual Value
6.75	7.6

It can be seen that the error is about 12%.

Several other sets of results will now be tabulated;

	Case 2	Case 3	Case 4	Case 5
R_1 (K.ohms)	4.900	4.651	1.927	5.400
R_2 (K.ohms)	4.790	4.402	1.905	5.261
Df_{10} (Kc/s)	1.3210	1.3573	3.2890	1.2239
Df_{20} (Kc/s)	0.7130	0.8598	0.5730	1.6910
f_{10} (Kc/s)	31.1390	31.1917	31.2470	31.1509
f_{20} (Kc/s)	22.6340	24.3683	13.1330	22.6000
B	-1.137	-1.135	-0.940	-0.615

These yield the following results, besides which the corresponding practical results are given together with the approximate percentage error, E%.

SOLUTIONS OF THE FREQUENCY AND AMPLITUDE EQUATIONS AND THE CORRESPONDING PRACTICAL RESULTS

(E% is the approximate percentage error).

	f_1(Kc/s.)			f_2(Kc/s.)		
	Calculated	Practical	E%	Calculated	Practical	E%
1	31.133	31.077	0.2	22.641	22.671	0.1
2	31.108	31.064	0.1	22.648	22.645	0.1
3	31.146	31.073	0.1	24.408	24.455	0.1
4	31.122	31.041	0.1	22.620	22.599	0.1
5	31.210	30.910	0.1	13.148	13.136	0.1

	Re.G(jW_1) (K.ohms)			Amplitudes (R.M.S.Volts)		
	Re.G(jW_1)	Re.G(jW_2)	Average	Calculated	Practical	E%
1	5.557	5.308	5.433	6.75	7.60	12
2	5.572	5.445	5.508	6.85	7.03	2.5
3	5.280	4.994	5.137	5.11	4.30	16
4	3.321	3.235	3.278	3.00	2.60	13
5	1.811	1.790	1.301	1.06	.97	3.0

Approximations to the non-linear characteristic;

I $i_a = 0.0108\text{Exp}(0.04423v_g)$

2 $i_a = 0.0108\text{Exp}(0.04423v_g)$

3 $i_a = 0.00939\text{Exp}(0.05116v_g)$

4 $i_a = 0.00939\text{Exp}(0.05116v_g)$

5 $i_a = 0.01243\text{Exp}(0.11455v_g)$

It can be seen from these results that the errors in the oscillation frequencies are quite negligible in comparison with the errors involved in calculating the amplitude, and this is simply because the frequencies do not depend on the non-linear element.

The values of a and b chosen for the equivalent linear gain of the non-linear element have such a profound effect on the calculated values of the amplitudes that the non-linear characteristic should be plotted fairly often so as to account for any changes due to ageing. A new value of a and b should be selected for each new region of operation on the characteristic, for the same reason. The values of a and b for cases (1) and (2) are a = .01080, b = 0.04423 (figure (6)), for case (3) and (4) a = .0093933 amperes, b = .05116 (figure (18)), for case (5) a = .0124286 amperes, b = .11455 (figure (18)). The corresponding equivalent gain curves are given in figures (10), (19), and (20).

(6.4) Stability

At this point it is possible to verify the stability criteria given in section (5). The stability of the double frequency mode is dependent on the restriction that neither of the roots of equation (45) should contain positive real parts.

The conditions are now examined for the circuit parameters pertaining to case (1).

In this case,

$$k_1 = abExp(-b(2A_1 + VB))\ I_0^2(bA)$$

$$= .0108\ .04475\ \ .3198\ I.07$$

$$= 16.5378\ 10^{-5}$$

THE NON-LINEAR ELEMENT

FIG. 18

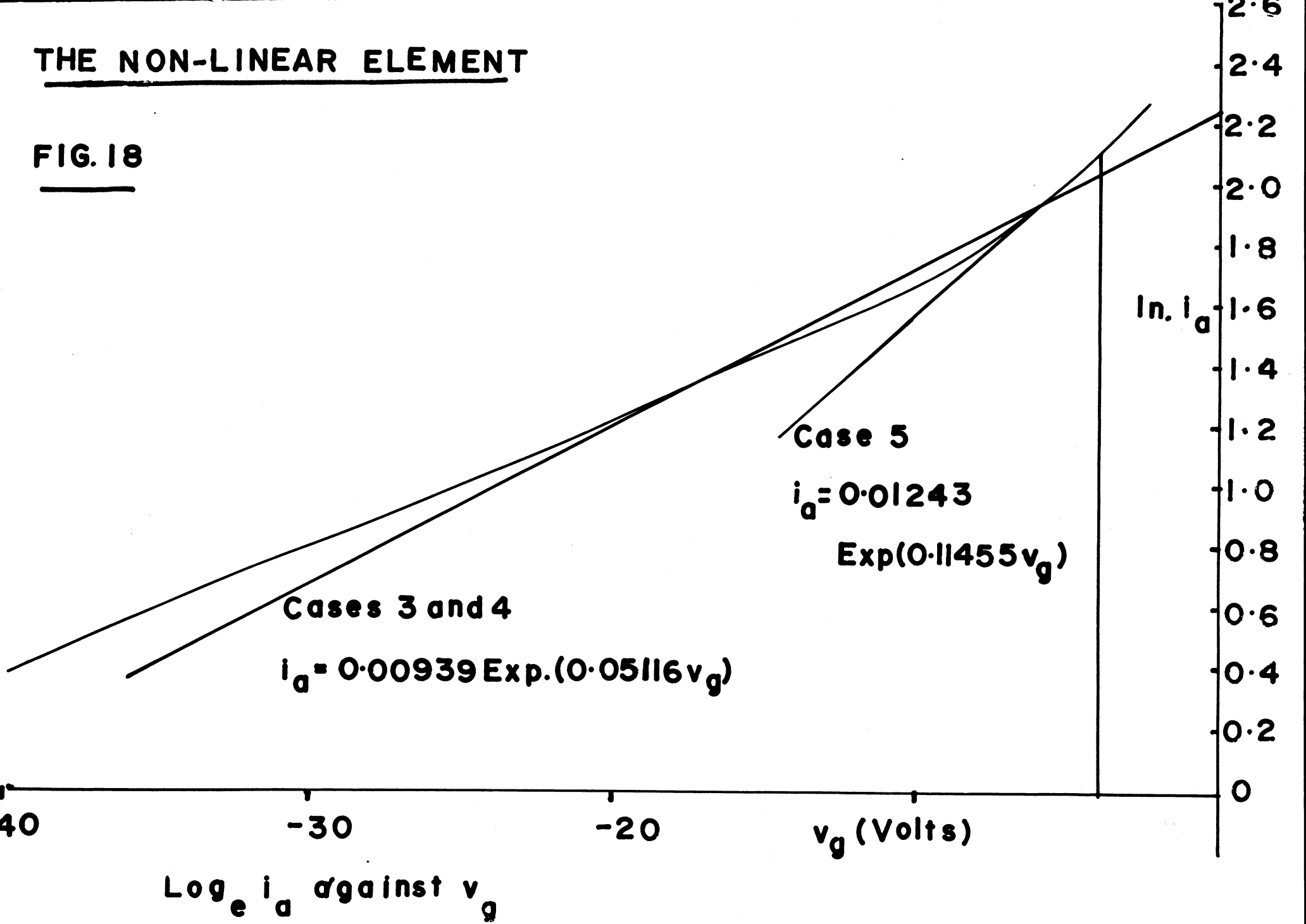

$\text{Log}_e\, i_a$ against v_g

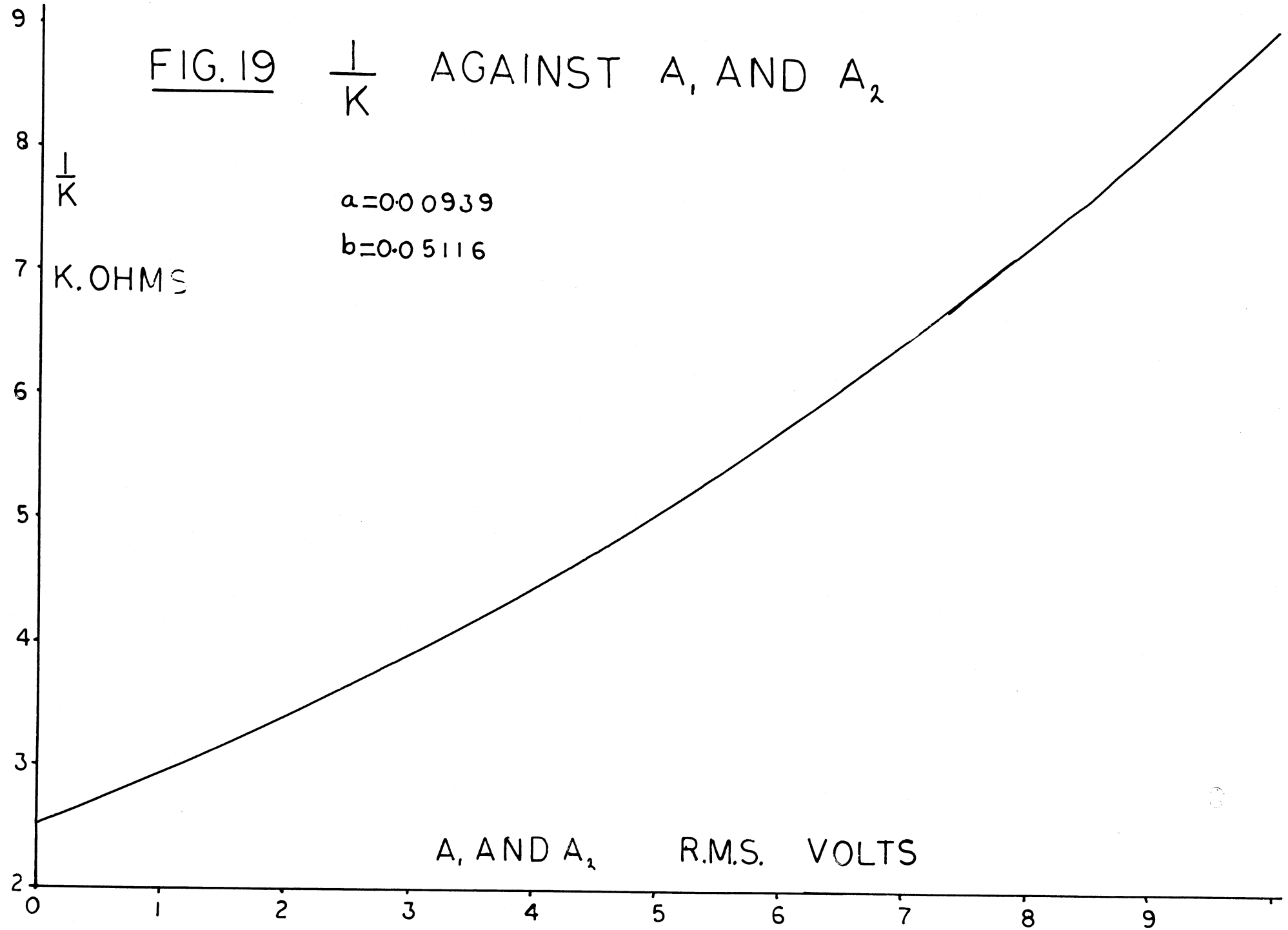
FIG. 19 1/K AGAINST A, AND A2
1/K
K. OHMS
a=0·00939
b=0·05116
A, AND A2 R.M.S. VOLTS
9
8
7
6
5
4
3
2
0
1
2
3
4
5
6
7
8
9

FIG. 20 VARIATION OF $\frac{1}{K}$ WITH A_1 AND A_2

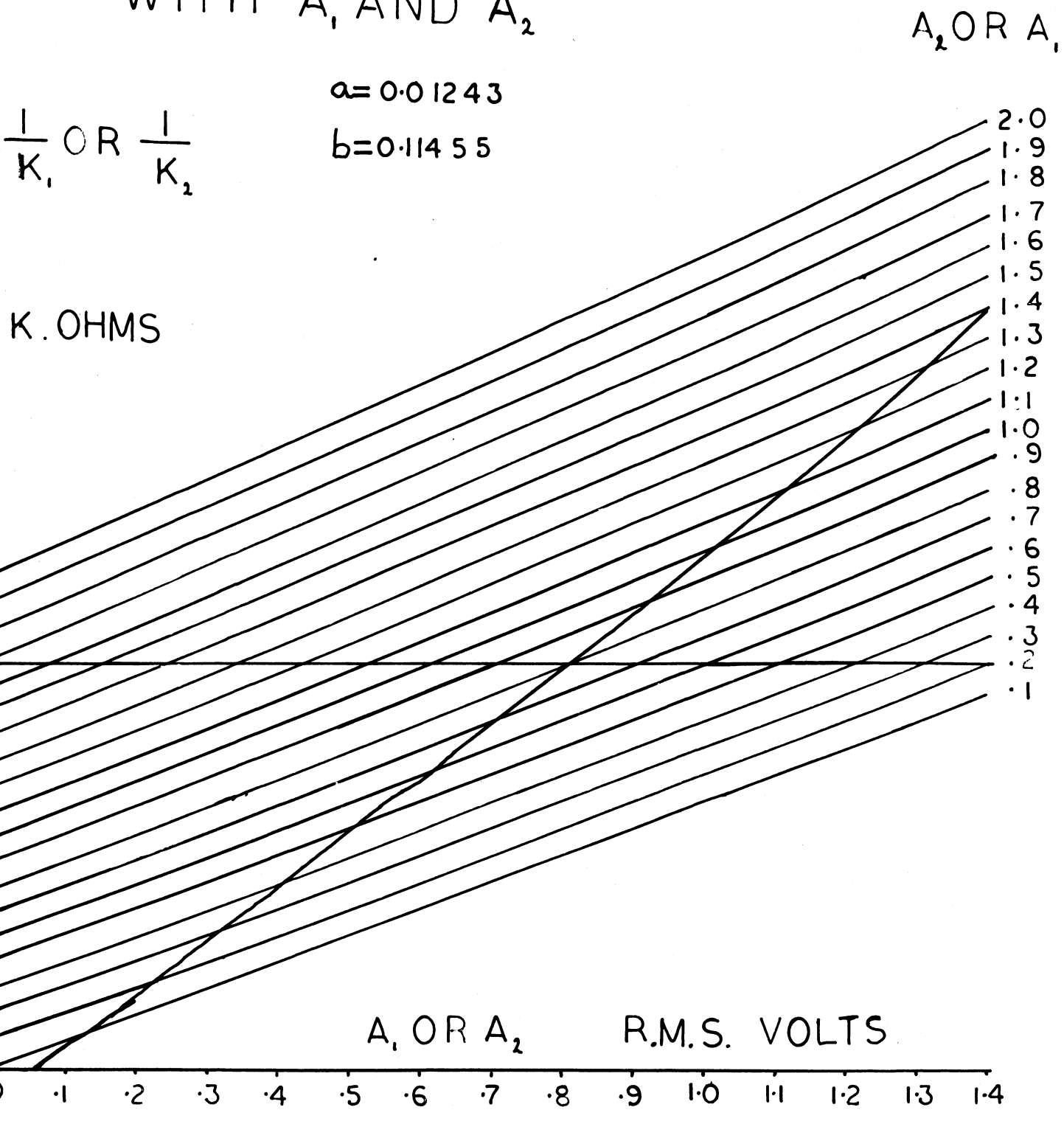

$$B = -1.115$$

therefore $Bk_1 = -18.43965\ 10^{-5}$

$= -1.844\ 10^{-4}$ approximately

The requirement for stability reduces to, $2a_1'\ W_{10}'\ C_1'$ must be greater than $-Bk_1$. But $2a_1'\ W_{10}'\ C_1' = \frac{1}{R_1'}$, and

$R_1' = \frac{31.32.3.2.(2)^{1/2}}{50}$ K.Ohms since when the input to G(p) was 50 volts peak to peak across a resistance of 31.32 K ohms, the output had peaks of 3 volts R.M.S. at resonance. Hence, $\frac{1}{R_1'} = 1.8814.10^{-4}$ mhos which is greater than $-Bk_1$ and so any transients about the assumed conditions will decay exponentially with time.

(6.5) Summary

This means that the theory presented has, in this typical case, predicted the oscillating frequencies to within .1% of the actual values, the amplitudes to within 12% of the actual values, and has shown that the assumed mode is stable, as it is in practice.

SECTION 7

ERRORS

(7.1) Errors in the Assumed Feedback Loop

Once the frequencies have been assumed incommensurable, the accuracy to which they can be predicted is limited by how closely the equivalent circuit of the linear portion of figure (15) corresponds to the actual facts. It is obvious, for instance, that there will be some stray capacitance unaccounted for, and also that the tuned circuits have been idealised. The last section shows, however, that the effect of these approximations on the frequencies is very small.

The effects of these approximations on the amplitudes, while still small, is more important, because an approximation in the equivalent circuit which produces an error of .1% in the oscillating frequency may well produce a larger error in Re(G(jw)). Any error in Re.(G(jw) has more than double the effect on the amplitudes because of the small gradient of the 1/K curves.

(7.2) Errors in the Assumed Non-Linearity

The errors in the assumed linear circuit are overshadowed by the errors resulting from the choice of straight line to represent the $\log_e i_a - V_g$ curve of the non-linearity. The 3% error, which is the minimum unavoidable deviation from the straight line, could produce an error of up to 8% in the predicted amplitudes when they are equal,

and up to three times as much when they are not equal. Errors in reading VB and in the observation of a and b can have similarly magnified effects on the result.

It is for these reasons that it is of such importance to define carefully the non-linear characteristic. The addition of the constant bias VB and the knowledge of the largest grid voltage excursion serves greatly to reduce the uncertainty as to which is the best approximation to the curve. The use of a sharp cut-off pentode would very much increase the difficulties involved in making such approximations on the basis of a continuous exponential characteristic unless the working range was severely restricted.

(7.3) The Neglected Components

The other important source of error in this analysis is the effect of the neglected harmonics and cross modulation products. The largest of these neglected components is at the difference frequency and represents at least 5% of the main component amplitudes (see figure (3)). This component is considerable because, not only is the attenuation due to G(p) not infinite at this frequency but also because there are two other mechanisms which give rise to its generation at the input of the non-linearity. Firstly, the rectification of the input to provide the grid bias must necessarily produce some difference frequency at the grid in the practical case. Secondly, the phase inventing amplifier, even with the cathode follower output stage, does not present zero impedence to the input of the non-linearity. Some effects of the presence of the cathode follower are considered in section (7.4).

It can be shown that the equivalent linear gain to the component at frequency f_1, in the presence of a difference frequency component of amplitude A_d can be expressed as,

$$K_1' = (a_1 b_0 c_0 + \frac{a_0 b_1 c_1}{2} + \frac{9}{8} a_0 b_1 c_3 + \frac{75}{8} a_0 b_1 c_5 + ...)\ a\ Exp(bD)$$

where $c_0 = I_0(bA_d)$

$c_1 = 2I_1(bA_d)$

$c_3 = 2I_3(bA_d)$ etc.

But $bA_d = .01$ approximately, and so $c_0 = 1$ approximately, c_1, c_3, c_5, all equal approximately zero.

Therefore $K_1' = \frac{a_1 b_0 a Exp(bD)}{A_1}$

D is the average value of the grid voltage, and since the grid time constant is assumed to be long compared with $\frac{1}{(W_1 - W_2)}$, D is approximately equal to $-(VB + A_1 + A_2 + A_d)$

Therefore $K_1 - K_1'$ is approximately equal to $K_1(I - Exp(-bA_d))$.

Therefore the percentage error in the calculated value of K, due to the neglected difference frequency component alone is $(I - Exp(-bA_d))100\%$.

Note that the error is a non-linear function of the amplitude. At about 6 volts R.M.S. A_d is approximately equal to $(2)^{1/2}6/20$, which is about .4 volts, and $Exp(-bA_d)$ equals .98 so this error in K is about 2%. Therefore this error in the amplitudes would amount to about 4%.

Several experiments were conducted to observe the effect on the main components of changing the magnitude of the difference frequency component. The conclusions drawn from these experiments are, that as the amplitudes of the difference frequency is increased one of the main

amplitudes decreases as the other increases, and that when A_d is about 20% of the smaller amplitude then this component disappears. The other main component suddenly increases its amplitudes at this point, as would be expected. The mechanism used for increasing A_d was to reduce the grid time constant. The results are summarised in figure (21). It is of interest to note that the point at which one component becomes unstable coincides with that value of A_d which causes every peak of the grid wave to be clipped by the diode.

(7.4) Extra Phase Shifts

At this point it is convenient to explain the presence of the cathode follower which is interposed between the phase inverting amplifier and the input to the non-linear element, as shown in figures (15) and (16).

First of all, it is useful in reducing the effect of changes in the output impedence of the phase inverter which results from the method of gain control. Its primary function is, however, to ensure that the outpput impedence of the phase inverting stage appears to be low to the circuit which is being used to provide the variable bias.

In order to understand the reason for this, it is necessary to appreciate that the difference frequency component, unlike the other neglected components, is largely introduced at the grid by the action of the rectifier. It can be seen from figure (1) that the proportion fed back through the linear circuit would be small. If the output impedence of the phase inverter were high then the wave form of the grid will not be very much different from that at a point between the grid capacitor and the phase inverter. This would mean that, in effect, the

FIG. 21

THE EFFECT OF CHANGING THE GRID TIME CONSTANT

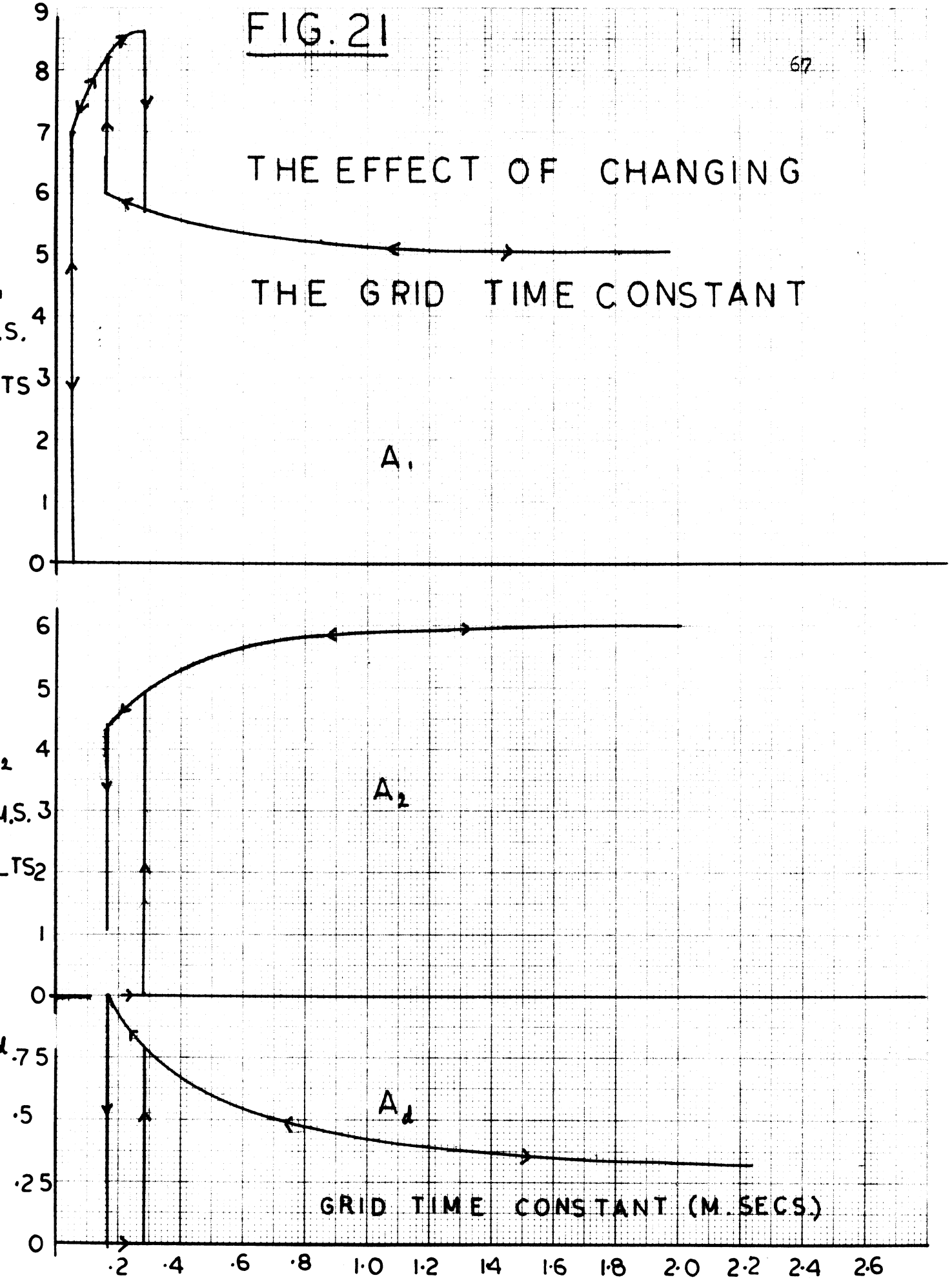

difference frequency component is appearing first on this side of the capacitor, and not on the grid. The result of this is to make possible a phase shift of the difference frequency through the grid $R_g C_g$ network, which is not the same as that of the main frequencies.

The equivalent linear gains of the non-linear element, when the difference frequency component is considered, are given by,

$$K_1 = \frac{aExp(bD)}{A_1}\left(a_1 b_0 c_0 + a_0 b_1\left(\frac{c_1}{2} + \frac{9c_3}{8} + \frac{75c_5}{8} + \ldots\right)\right)$$

and

$$K_2 = \frac{aExp(bD)}{A_2}\left(a_0 b_1 c_0 + a_1 b_0\left(\frac{c_1}{2} + \frac{9c_3}{8} + \frac{75c_5}{8} + \ldots\right)\right)$$

or writing $\frac{c_1}{2} + \frac{9c_3}{8} + \frac{75c_5}{8} + \ldots = c$

$K_1 = aExp(bD)(a_0 b_1 c_0 + a_0 b_1 c)/A_1$

and $K_2 = aExp(bD)(a_0 b_1 c_0 + a_0 b_1 c)/A_2$

But if there were a phase shift to the difference frequency the input to the non-linearity would be,

$$A_1 \cos W_1 t + A_2 \cos W_2 t + A_d \cos((W_1 - W_2)t + \theta) + D$$

where $\theta = \text{arc. tan } \frac{1}{(W_1 - W_2)C_g R_g}$ which would result in complex linear gains

$$K_1 = aExp(bD)(a_1 b_0 c_0 + a_0 b_1 c \cos\theta + j a_1 b_0 c \sin\theta)$$

$$K_2 = aExp(bD)(a_0 b_1 c_0 + a_1 b_0 c \cos\theta + j a_1 b_0 c \sin\theta)$$

The imaginary parts of these gains are dependent on the magnitude of $(W_1 - W_2)$ as well as on the pamlitude of the component.

Complex gains produced in this way would result in different oscillating frequencies due to the extra phase shift, as well as different amplitudes.

To avoid such difficulties the cathode follower is introduced, and so any difference frequency component produced by the rectifying action of the diode can be considered to exist only in the grid voltage and the anode current.

The effect can be further reduced by increasing $R_g C_g$ as much as possible, firstly to reduce the phase shift, and secondly to reduce the magnitude of A_d. Also, separation of the two main frequencies to make the difference frequency fairly large again reduces any possible different phase shifts. When all these precautions have been taken, it is possible to ignore the effect of the grid rectifier circuit on the value of G(p) since, although its transfer function is strictly $pT_g/(1+pT_g)$, T_g is so large that this transfer function can be approximated to unity.

There is an upper limit set on the size of the grid time constant, and hence on the amount by which the difference frequency component can be reduced. This limit is defined by the onset of the instability known as squegging. The value of T_g used was given by the grid capacitance .001 microfarads, and the back resistance of five IN96 point contact diodes in series, about three megohms. That is, T_g was approximately .003 seconds, as compared with $\frac{1}{(W_1 - W_2)}$ which was about .00006 seconds.

If the grid capacitance was increased much above this value, it was found that the system would commence squegging in the double frequency mode as illustrated in figure (22) and (23).

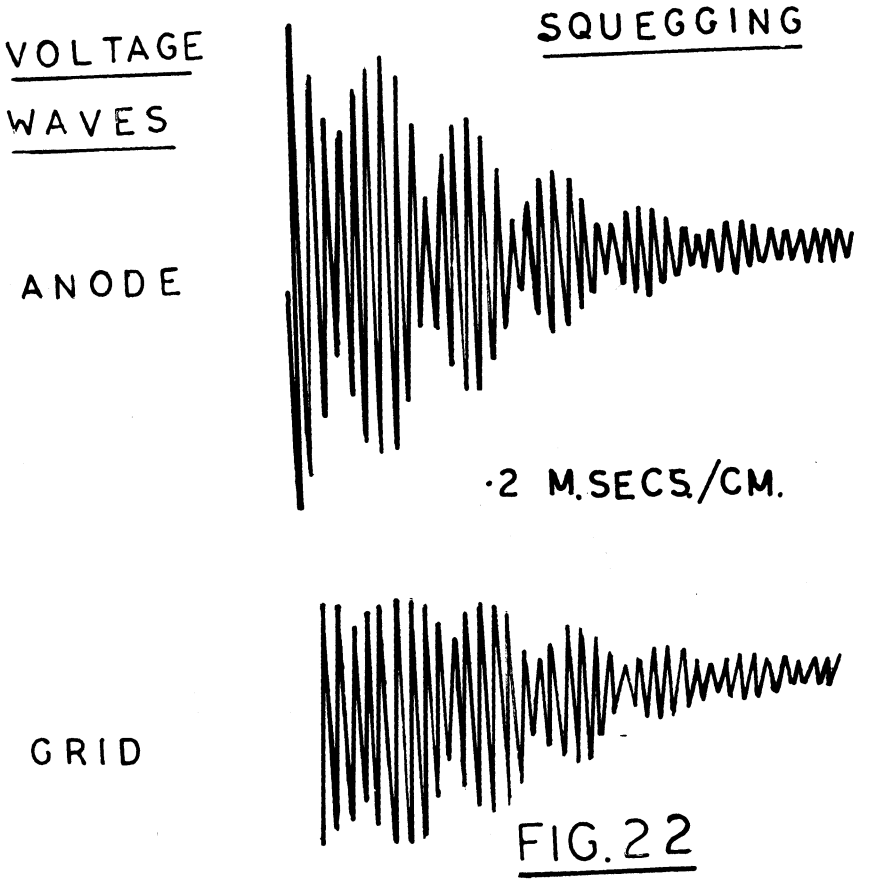
VOLTAGE
WAVES
SQUEGGING
ANODE
·2 M.SECS./CM.
GRID

FIG. 22

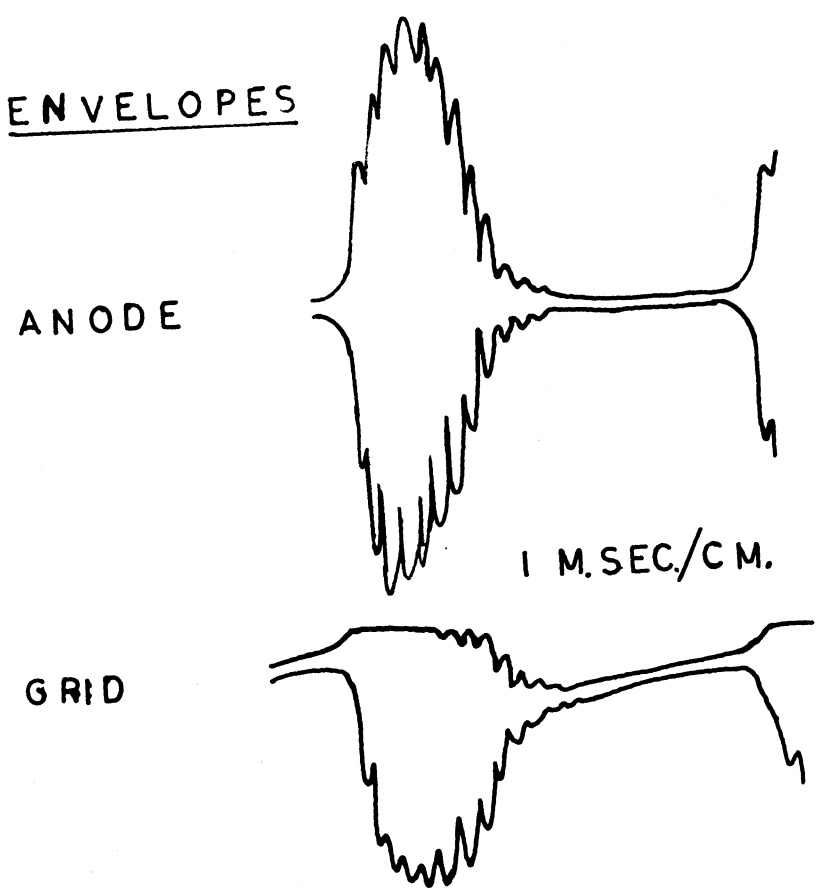
ENVELOPES
ANODE
1 M.SEC./CM.
GRID

FIG. 23

SECTION 8

COMPARISON WITH PREVIOUS WORK

(8.1) Grid Circuit Tuned to the Difference Frequency

One of the early investigators to produce double frequency oscillations was Edwin H. Armstrong in 1915 (Reference (5)). He found that a phenomenon similar to the squegging action mentioned in section (5) could be utilised to amplify incoming oscillations. The incoming signal consisted of bursts of radio frequency oscillations which drive the grid negative, and cut off the tube. The system then relaxed when each burst had passed. The tuning of the grid circuit time constant to the audio frequency was found to produce an amplifying effect. This led Armstrong and later, L. Hazeltine (Reference (4)) to produce systems in which self-sustaining double frequency oscillations could be produced by tuning the grid circuit to the beat frequency of the two main components. Neither of these two papers were primarily concerned with self-starting, unrelated double frequency oscillations, and no attempt was made to predict any values of amplitudes that might be expected. The theory presented was basically linear and the possibility of the continued existence of the two frequencies together was only discussed qualitatively.

(8.2) External Limiting Devices

One other method of obtaining multi-frequency oscillations of any

frequency relationship which can be self-starting is to limit each component separately. Two of the many examples of this type of system are given in references (2) and (3), and they can all, in theory, be ultimately reduced to several separate oscillators.

(8.3) Power Series Representation of the Non-Linear Element

Fontana (Reference (16)) has shown that with the simplest power series representation, namely a cubic, self-starting double frequency oscillations can be obtained in the case where the two components have related frequencies. In his paper, he also established the limitation on the number of frequency relationships which can result in this effect. H. J. Reich, J. G. Skalnick, and J. D. Crone (Reference (1)) have conversely shown that a cubic characteristic cannot support general double frequency oscillations and that separate limitation of the two components is required if they are to adjust stably together.

J. S. Shaftner (Reference (11)) has agreed with the conclusion reached by L. Skinner (Reference (12)) that a fifth order power series can support two unrelated frequencies, but he has also shown that the system will not be self-starting under these circumstances. Hence, at least a seventh power term must be included to ensure stable and self-starting double frequency oscillations of this type.

In reference (17) it is shown that double frequency oscillations of either the synchronous or asynchronous types can exist together in an oscillating circuit in which the active element is a triode. The non-linearity is again represented by a power series, but this time without any limit on the number of terms. It is concluded by this investigator

that with a triode the unrelated frequency condition is difficult to obtain because the system is not self-starting in this mode.

(8.4) Other Approximations for the Non-Linear Element

The alternatives to the equivalent linearisation used in this paper which has been referred to in section (2), is "Piecewise linear approximations". This technique has been used by G. M. Utkin in his paper (Reference (18)) in which he shows that two frequency oscillations can exist stably together. In this case, the asynchronous condition is obtained by detuning a circuit when a synchronous condition exists. It is not stated in this paper whether the author found it possible to start the unrelated oscillations from zero. Presumably this was not the case, since it is implied that he used a triode valve which has been shown by Mostofa (Reference (12)) not to give the system this self-starting property.

The use of a finite functional type of approximation to the non-linearity has, it is believed, only previously been used by Disman and Edson (Reference (6)). These investigators also used an exponential function as an approximation to the actual non-linear element. The element they used in practice was a 6AK5 sharp cut-off pentode, which will be shown in Appendix 1 to have a transfer characteristic which does not very closely resemble an exponential. There is also no mention in their paper of any limitation of the working range. The authors resolve the problem of the stability and starting ability by drawing a map of isoclines and the trajectories of the build up.

In the section of reference (6) on experimental results, the

authors state that the elements were adjusted so that the loop gains to each component were approximately equal. This would suggest that difficulties were experienced in correlating the actual amplitudes with those predicted when the loop gains were not equal. It is significant that no results are quoted for the amplitudes even when they are equal, since as it has been shown here the predicted amplitudes are extremely sensitive to the approximation to the non-linearity used. The two sets of frequencies quoted in this reference have relationships 12:11 and 51:61 and so would probably not have contributed very much energy to each other. The system discussed in appendix III could have been used to recognize immediately any relationship of these orders of magnitude.

(8.5) Single Frequency Modes

Several of the authors referred to in this section have found that if the conditions of the system were such that the two components would not start together, then the component which did start and build up to a steady state was the one which corresponded to the tuned circuit with the higher Q. If the Q's were made equal the component which finally existed was unpredictable. These results were observed with this experimental arrangement also. The system could be made to support only one component by reducing the grid time constant, and the frequency of this component depended upon which circuit had the higher Q.

APPENDIX I

CURVE FITTING

I.1 Introduction

This section will be used to show three of the commonly available non-linear negative resistances, namely, the transfer characteristics of a sharp cut-off pentode, a remote cut-off pentode, and a semi-remote cut-off pentode. Some fairly simple mathematical equations will be used as an approximation to these, and it will be shown that the curve of a remote cut-off pentode with variable screen voltage, obtained as described in section (3), can be closely approximated by an exponential characteristic. The next section, appendix II, shows that this is also easy to treat mathematically.

Finally a method will be discussed for quickly obtaining a good fit for a curve approximated by the sum of two exponentials.

The approximation of the curves using a power series is not discussed here, since all that is necessary is to take one more point of the curve than the order of the highest power to be used, and solve the simultaneous equations for the coefficients. This gives a fit in the region of the points. It has been decided, because of the experience of previous investigators, to use a functional approximation rather than a power series.

I.2 Sharp Cut-off Pentode

Figure (24) shows the transfer characteristic of a 6AK5 sharp

FIG. 24

6 A K 5 SHARP CUT-OFF PENTODE

SCREEN VOLTAGE = 60

ANODE VOLTAGE = 180

I_a AGAINST V_g

x GIVES POINTS CALCULATED FROM

$i_a = 1{\cdot}864(2{\cdot}75 + V_g)^{3/2}$

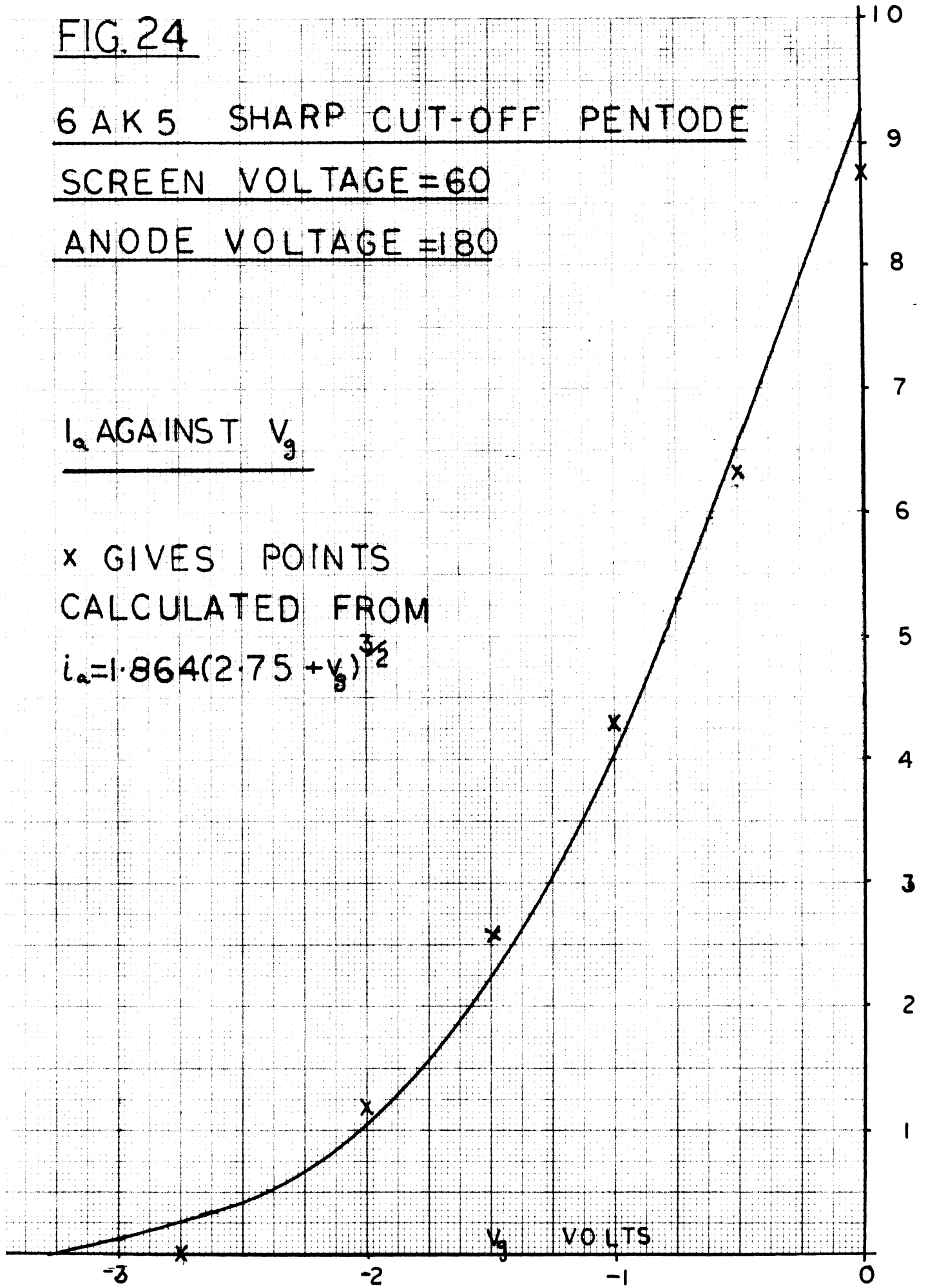

FIG. 25 SHARP CUT-OFF PENTODE

$LOG_E i_a$ AGAINST V_g.

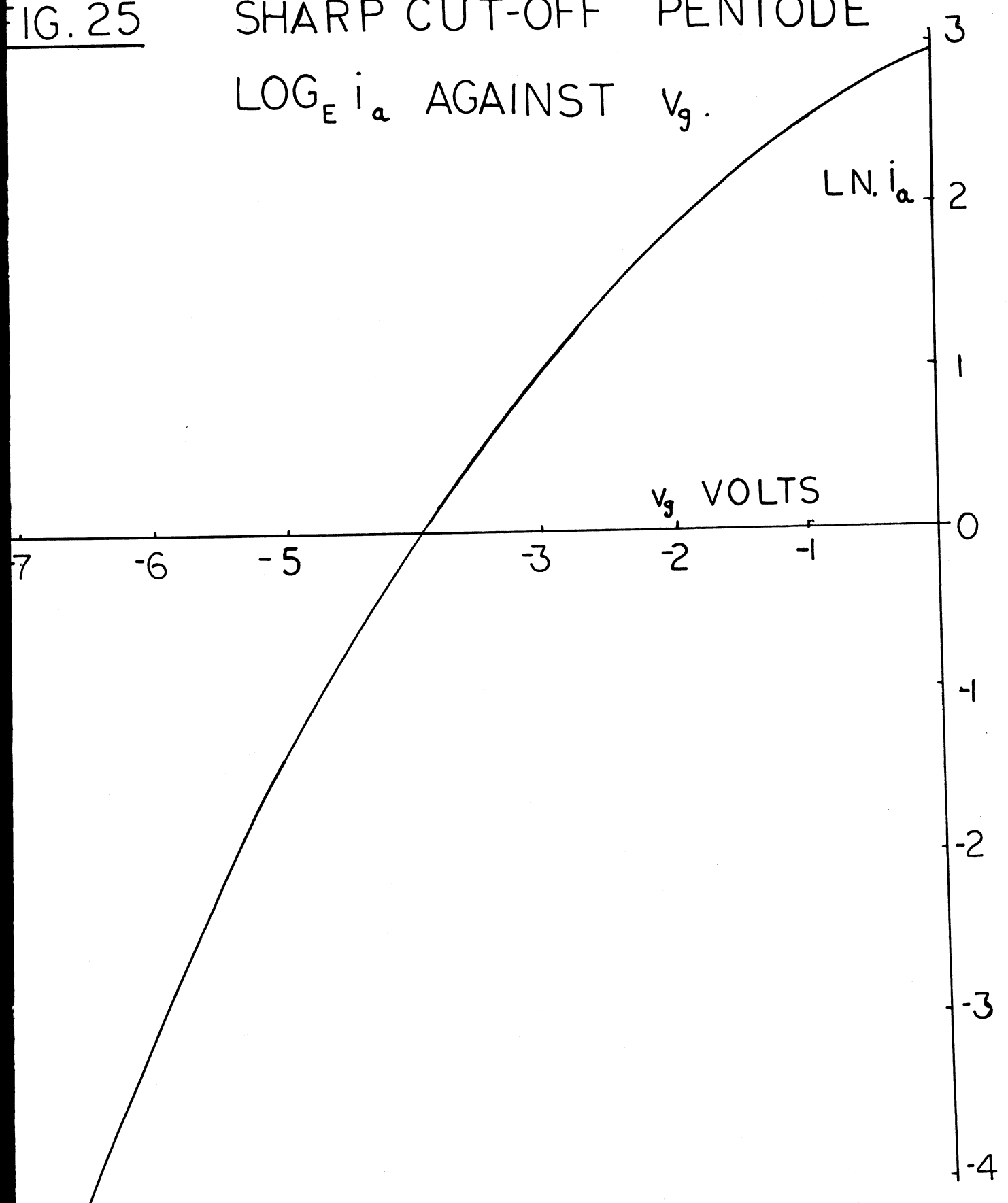

cut-off pentode. This can be very accurately represented by a discontinuous curve, one which is zero beyond cut-off and is $i_a = 1.864 (2.75 + V_g)^{3/2}$ between cut-off and zero grid volts. The constants in this formula are easily found by using the points at which the curve intersects the two axes. This equation has been found to present great difficulties in the analysis of the problem, and so some other approximation was sought. The possibility of an exponential can easily be investigated by observing how close the $\log_e i_a = V_g$ curve is to a straight line. Figure (25) shows that this condition is far from satisfied unless the working range is severely limited. The curve becomes asymptotic to the line $V_g = -3.5$ volts (the cut-off voltage), since the logarithm of zero is minus infinity.

I.3 Remote Cut-off Pentode

Because the use of an exponential characteristic is attractive from the mathematical point of view, the possibility of using some other means of obtaining it was considered. As shown in figure (4), section (3), the 6BA6 characteristic does in fact follow an exponential curve over a much wider range of grid voltages than does the sharp cut-off pentode. This situation can be much improved by the arrangements discussed in that section to provide some negative feedback by automatic reduction of the screen voltage at the high current values. The selection of the screen dropping resistance to provide the correct amount of negative feedback produced the curve of figure (6), which can be approximated by a straight line to within 3% over a range of about 35 volts of grid swing.

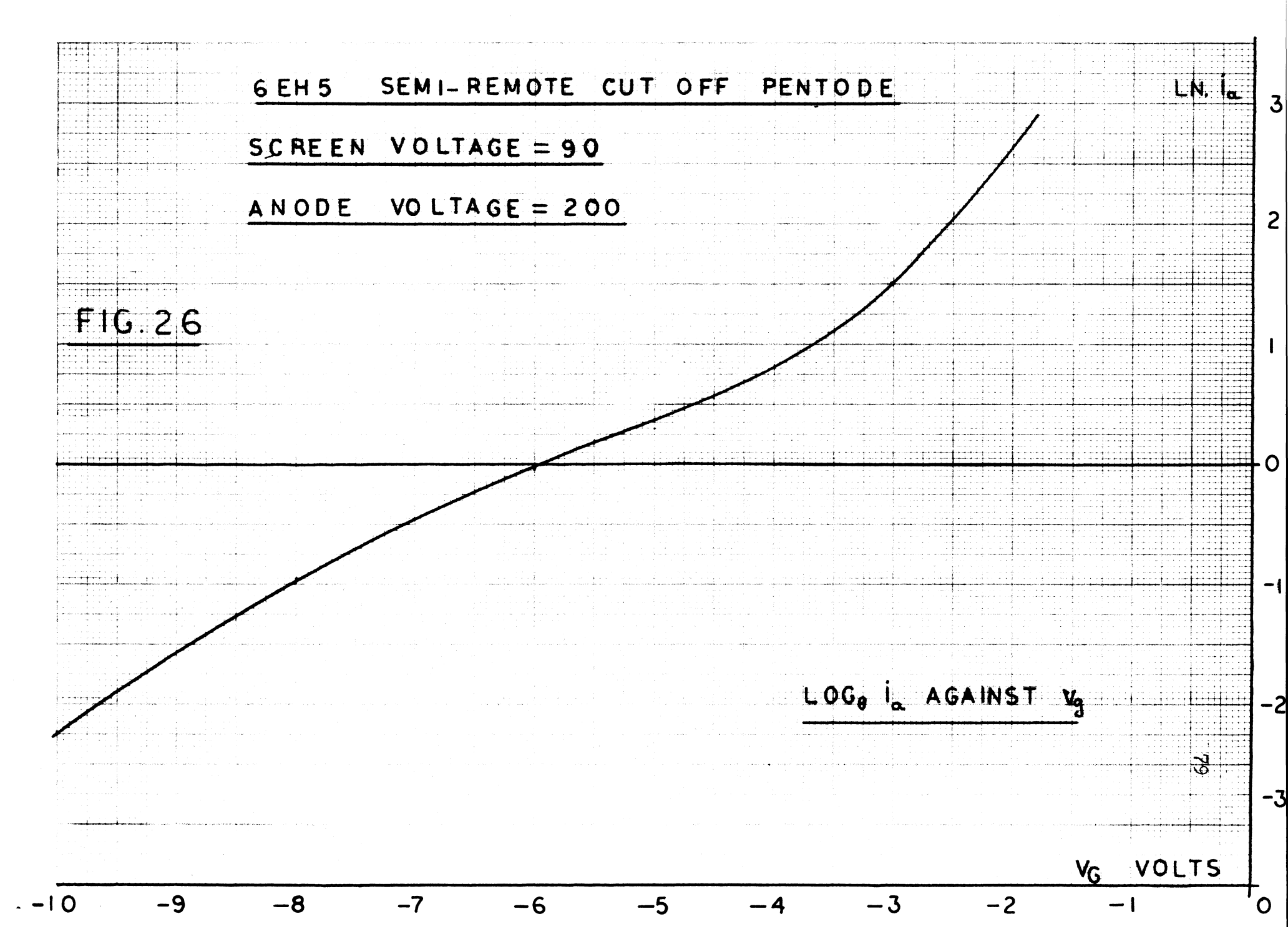
6EH5 SEMI-REMOTE CUT OFF PENTODE
SCREEN VOLTAGE = 90
ANODE VOLTAGE = 200
LN. i_a
3
2
1
0
-1
-2
-3
$LOG_e\ i_a$ AGAINST V_g
V_G VOLTS
-10
-9
-8
-7
-6
-5
-4
-3
-2
-1
0

FIG. 26

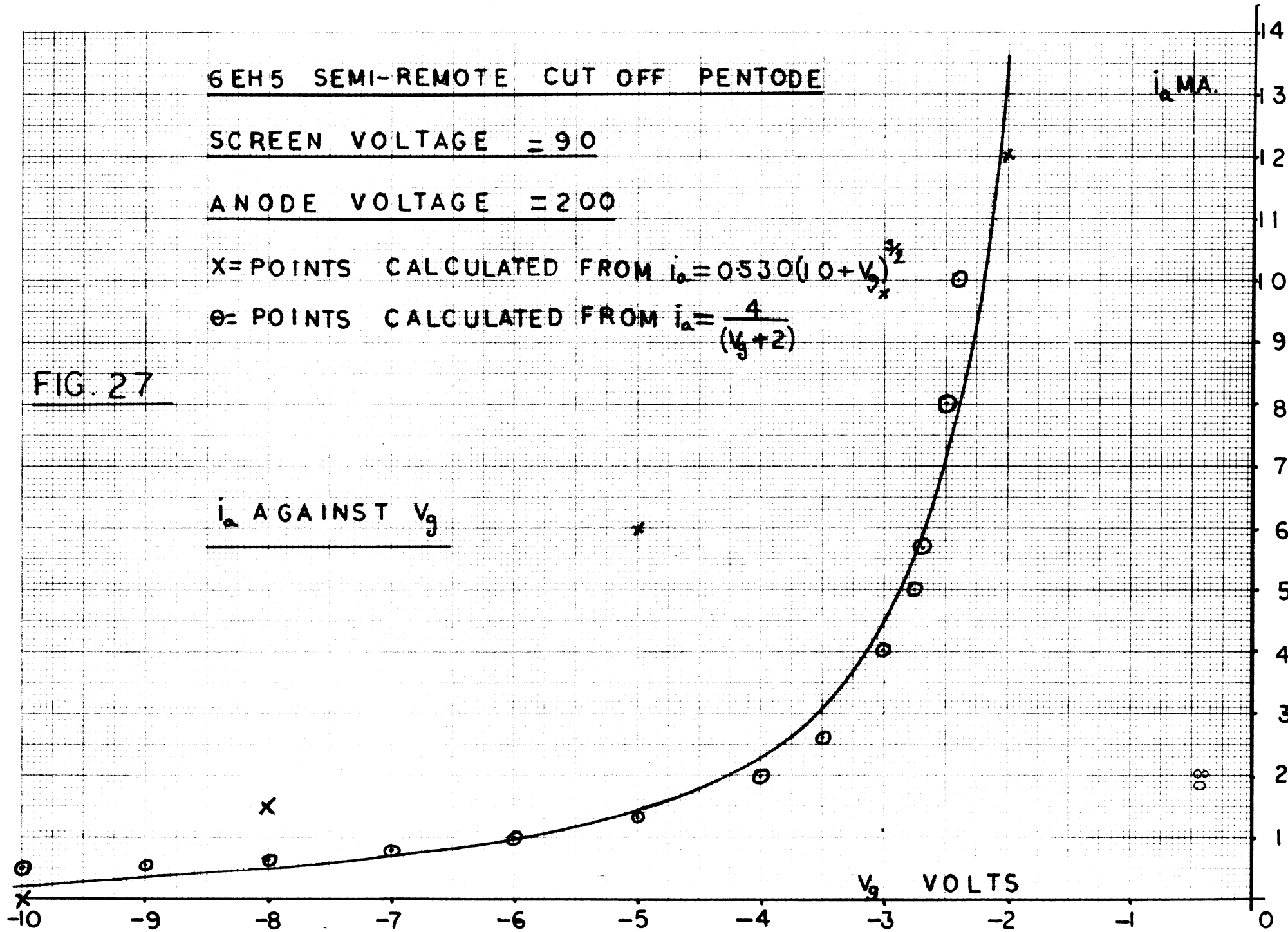
6EH5 SEMI-REMOTE CUT OFF PENTODE
SCREEN VOLTAGE = 90
ANODE VOLTAGE = 200
X= POINTS CALCULATED FROM $i_a = 0530(10+V_g)^{3/2}$
⊙= POINTS CALCULATED FROM $i_a = \frac{4}{(V_g+2)}$
FIG. 27
i_a AGAINST V_g
i_a MA.
V_g VOLTS
-10
-9
-8
-7
-6
-5
-4
-3
-2
-1
0
1
2
3
4
5
6
7
8
9
10
11
12
13
14

I.4 Semi Remote Cut-off Pentode

It can be seen by comparison of figures (4) and (6) with figure (24) that, at low grid voltages, the characteristic of a remote cut-off pentode deviates to one side of the best exponential approximation, while that of the sharp cut-off tube deviates to the other. It was natural, therefore, to consider the possibility of using a semi-remote cut-off pentode to try for a closer approximation. Figure (26) shows the transfer characteristic of a tube of this type (6EH5) expressed in the log. i_a against v_g form. It can be seen from this that the curve possesses a shape similar to that of the remote cut-off tube with negative feedback, but deviates considerably more from being a straight line. One factor contributing to this is that the tendency for the curve of figure (26) to approach minus infinity begins to set in at lower grid voltages. It is evident from the nature of the curve that any reduction of screen voltage at low grid voltages would not improve the approximation because the cut-off voltage is too low.

Figure (27) shows that the $i_a - v_g$ curve of the 6EH5 does not correspond closely to a three-halves power law either. This curve is not as good a fit as it was for the sharp cut-off tube. The curve does bear some resemblance to a rectangular hyperbola but this again has errors at cut-off.

I.5 Double Exponential Approximations to a Remote Cut-off Pentode Characteristic

As it was pointed out in section (7), the main source of error in this investigation has been the approximation of the non-linear

element. In the present section, it has been shown that, apart from a discontinuous curve containing a three-halves power law portion, for a sharp cut-off tube, the best simple combination is an exponential curve for a remote cut-off tube. The possibility of using a more complicated expression for the characteristic has been considered as a means of improving the approximation. Although it was decided that the improvement in accuracy obtained by using the sum of two exponentials, was not enough to warrant using this for the analysis, a quick method of obtaining this approximation was devised. This method will now be briefly set down and the corresponding equivalent linear gains are derived in appendix II.

Let the curve be approximated by the equation

$$a_1 \mathrm{Exp}(b_1 v_g) + a_2 \mathrm{Exp}(b_2 v_g) = i_a$$

This equation contains four arbitrary constants and so four points are required on the curve to find them. The method of choosing the position of these points is usually to space them evenly along the curve within the range of interest, although more complicated systems exist to reduce the mean square error to a minimum. The system given here is designed for easy calculation but it is found that it is in this case close to the minimum mean square error approximation.

The first step is to decide upon the grid swing which is to be used. The range of v_g should then be divided into seven equal parts, in order to distribute the error throughout the range. The points used are given by the grid voltages at the second, fourth, and sixth division. Let these be (v_1, i_1) (v_2, i_2) and (v_3, i_3) respectively. The fourth point is $(0, i_0)$. A better distribution of the error is obtained by

dividing into eight parts and using the first, third, fifth and seventh to calculate the arbitrary constants; but this detracts from the simplicity of the method.

Using the points stated, therefore, the simultaneous equations required for the constants a_1, a_2, b_1 and b_2 are,

$$a_1 + a_2 = i_0 \tag{I.1}$$

$$a_1 \text{Exp}(b_1 v_1) + a_2 \text{Exp}(b_2 v_1) = i_1 \tag{I.2}$$

$$a_1 \text{Exp}(b_1^2 v_1) + a_2 \text{Exp}(b_2^2 v_1) = i_2 \tag{I.3}$$

$$a_1 \text{Exp}(b_1^3 v_1) + a_2 \text{Exp}(b_2^3 v_1) = i_3 \tag{I.4}$$

since $v_2 = 2v_1$ and $v_3 = 3v_1$. Hence if we let $\text{Exp}(b_1 v_1) = x_1$ and $\text{Exp}(b_2 v_1) = x_2$ the above four equations reduce to,

$$a_1 + a_2 = i_0 \tag{I.5}$$

$$a_1 x_1 + a_2 x_2 = i_1 \tag{I.6}$$

$$a_1 x_1^2 + a_2 x_2^2 = i_2 \tag{I.7}$$

$$a_1 x_1^3 + a_2 x_2^3 = i_3 \tag{I.8}$$

From (I.5) $a_2 = i_0 - a_1$

therfore $(i_0 - a_1)x_2^2 + a_1 x_1^2 = i_2$

and $(i_0 - a_1)x_2^3 + a_1 x_1^3 = i_3$

Hence $a_1(x_1^2 - x_2^2) = (i_2 - x_2^2 i_0)$ (I.9)

and $a_1(x_1^3 - x_2^3) = (i_3 - x_2^2 i_0)$ (I.10)

Also $(i_0 - a_1)x_2 + a_1 x_1 = i_1$

therefore $a_1(x_1 - x_2) = (i_1 - x_2 i_0)$ (I.11)

Dividing (I.9) and (I.10) by (I.11) gives,

$$x_1 + x_2 = (i_2 - x_2^2 i_0)/(i_1 - x_2 i_0)$$

and $$x_1^2 + x_1 x_2 + x_2^2 = (i_3 x_2^3 i_0)/(i_1 - x_2 i_0)$$

therefore $x_1 = (i_2 - x_2^2 i_0)/(i_1 x_2 i_0) - x_2$

therefore $(i_2 - x_2^2 i_0)^2/(i_1 - x_2 i_0)^2 + x_2^2 - 2x_2(i_2 - x_2^2 i_0)/(i_1 - x_2 i_0)$
$+ (i_2 - x_2^2 i_0)\, x_2/(i_1 - x_2 i_0) - x_2^2 + x_3^2 = (i_3 - x_2^3 i_0)/(i_1 - x_2 i_0)$
(I.12)

The expansion of (I.12) reveals the useful property that the cubes and fourth powers of x_2 have zero coefficients. Equation (I.12) can simply be shown to be equal to,

$$x_2^2(i_1^2 - i_0 i_2) - x_2(i_1 i_2 - i_0 i_3) + i_2^2 - i_1 i_3 = 0 \qquad (I.13)$$

This is a quadratic which has as solutions x_1 and x_2.

But, $\mathrm{Exp}(bv_1) = x_1$

therefore $b_1 = \dfrac{\log_e I/x_1}{-v_1}$ (I.14)

and $b_2 = \dfrac{\log_e I/x_2}{-v_2}$ (I.15)

From (I.14) and I.15) the other two parameters a_1 and a_2 can be calculated using the facts that

$$a_1 = (i_1 - x_2 i_0)/(x_1 - x_2) \qquad (I.16)$$

and $a_2 = (i_1 - x_1 i_0)/(x_2 - x_1)$ (I.17)

An example showing the use of this system to obtain a fit is now given.

Using four points from figure (28) and taking $v_1 = -5$ volts one would expect a reasonable fit up to about 17.5 volts. With this value of v_1 the currents are, $i_0 = 15\text{mA}$, $i_1 = 5.85\text{mA}$, $i_2 = 3.3\text{mA}$ and $i_3 = 2.1\text{mA}$. Hence equation (I.13) for x is,

$$x^2(5.85^2 - 15\ 3.3) - x(5.85\ 3.3 - 2.1\ 15) + (3.3^2 - 2.1\ 5.85) = 0$$

That is $x^2 15.25 - 12.2x + 14 = 0$

FIG.28

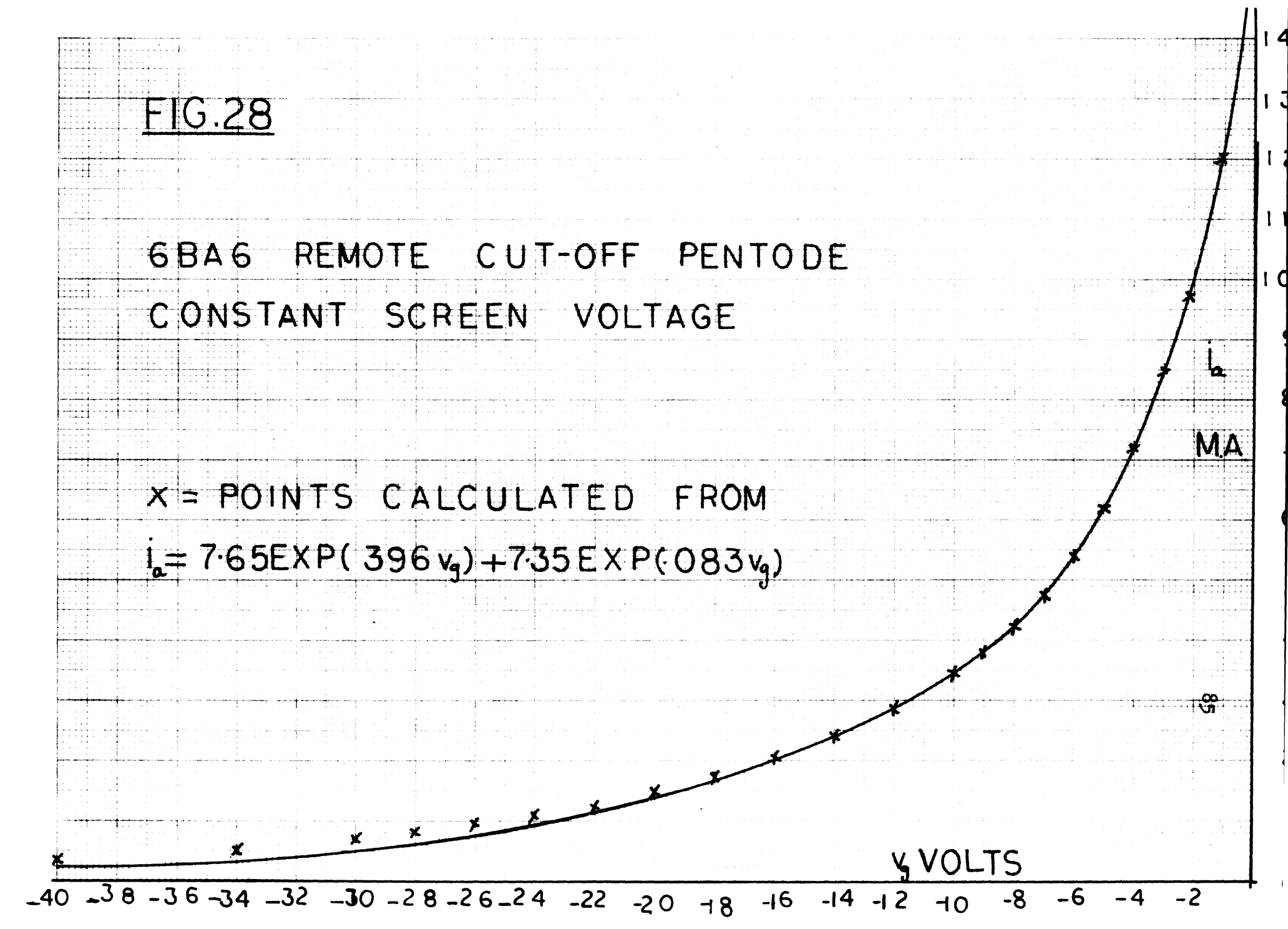
6BA6 REMOTE CUT-OFF PENTODE
CONSTANT SCREEN VOLTAGE
x = POINTS CALCULATED FROM
$i_a = 7{\cdot}65EXP(396v_g) + 7{\cdot}35EXP(083v_g)$
i_a
MA
v_g VOLTS
-40 -38 -36 -34 -32 -30 -28 -26 -24 -22 -20 -18 -16 -14 -12 -10 -8 -6 -4 -2

This gives x = .66 or .138, from which equations (I.16) and (I.17) can be used to give

$$a_1 = -(5.85 - .66\ 15)/.522 = 7.7$$

and

$$a_2 = (5.85 - .138\ .15\ )/.522 = 7.4$$

As a check, we note that $a_1 + a_2 = 15.1$ which is within rounding errors of the true value. Equations (1.14) and (1.15) now give

$$b_1 = (\log_e 7.25)/5 = .396$$

and

$$b_2 = (\log_e 1.515)/5 = .083$$

Hence the equation is $i_a = 7.65\mathrm{Exp}(.396v_g) + 7.35\mathrm{Exp}(.083v_g)$, (where a_1 and a_2 have both been adjusted slightly to give an exact fit at $v_g = 0$, in order to minimize rounding errors.)

Some points calculated from this equation are shown in figure (28), and it can be seen that the fit is almost perfect from $v_g = 0$ to $v_g = -18$ volts.

APPENDIX II

EQUIVALENT LINEAR GAINS

II.1 Exponential Characteristics With Two Inputs

a) Double input equivalent linear gains can be calculated in several ways, as mentioned in section 2.2. Definitions (2) and (3) given in that section are equivalent, and it has been shown (Rf. 10) that the equivalent linear gains so defined can be obtained by a two step method, in which a modified non-linear element is calculated from the probability density distribution of one of the inputs together with the non-linear function, and any direct input. This modified characteristic is then used to calculate the overall gain to the other component. This procedure is only valid if the two inputs are statistically independent which is the case here since the frequencies are unrelated.

If one input is x(t) and the other is y(t) the modified non-linearity is given by

$$g(z) = \int_{-\infty}^{\infty} f(z + D + y)p(y)dy \qquad (II.1)$$

where p(y) is the amplitude probability density distribution of y(t). From this the equivalent linear gain to x can be calculated using,

$$K_x = \frac{1}{\bar{x^2}} \int_{-\infty}^{\infty} xg(x)q(x)dx \qquad (II.2)$$

where $\bar{x^2}$ = mean square value of x(t) and q(x) is the amplitude

probability density distribution of x(t).

In this case $x(t) = A_1 \cos W_1 t$

$$y(t) = A_2 \cos W_2 t$$

$$p(y) = \frac{1}{\pi(A_2^2 - y^2)^{1/2}}$$

$$q(x) = \frac{1}{\pi(A_1^2 - x^2)^{1/2}}$$

$i_a = f(v_g)$ is the non-linearity therefore $f(v_g) = a\mathrm{Exp}(bv_g)$ (.13)

Therefore $$g(z) = \int_{-A_2}^{A_2} \frac{a\mathrm{Exp}(b(z + D + y))dy}{\pi(A_2^2 - y^2)^{1/2}}$$

By changing the variable from y to $y = A_2\cos\theta$, we obtain

$$g(z) = \frac{a}{\pi} \mathrm{Exp}(b(z + D)) \int_o^{\pi} \mathrm{Exp}(bA_2\cos\theta)\,d\theta$$

Therefore $$K_x = K_1 = \frac{2}{A_1^2} \int_{-A_1}^{A_1} xa\mathrm{Exp}(b(x + D)) \int_o^{\pi} \frac{\mathrm{Exp}(bA_2\cos\theta)\,d\theta dx}{\pi(A_1^2 - x^2)^{1/2}}$$

And again, the variable can be changed from x to $A_1\cos\phi$, which gives,

$$K_1 = \frac{2a\mathrm{Exp}(bD)}{A_1\pi^2} \int_o^{\pi} \mathrm{Exp}(bA_2\cos\theta)d\theta \int_o^{\pi} \cos\phi\ \mathrm{Exp}(bA_1\cos\phi)d\phi$$

b) The alternative approach is to use method I which is simply to express each part of the output of the non-linear element as a Fourier series, and to find the coefficients of those components at the

fundamental frequencies.

The input to the non-linear element is $A_1\cos W_1t + A_2\cos W_2t + D$ where in this case $D = -(A_1 + A_2 + VB)$. Therefore the output will be

$$aExp(bA_1\cos W_1t)Exp(bA_2\cos W_2t)Exp(bD)$$

Let $Exp(bA_1\cos W_1t) = e_0 + e_1\cos W_1t + e_2\cos W_1t + e_2\cos 2W_1t + e_3\cos 3W_1t + \ldots$ (II.4)

This is the Fourier expansion of $Exp(bA_1\cos W_1t)$ which is periodic.

$$e_0 = \frac{1}{2\pi}\int_{-\pi}^{\pi} Exp(bA_1\cos W_1t)d(W_1t) \qquad (II.5)$$

and

$$e_1 = \frac{1}{\pi}\int_{-\pi}^{\pi} Exp(bA_1\cos W_1t)\cos W_1t\,d(W_1t) \qquad (II.6)$$

etc.

Similarly if $Exp(bA_2\cos W_2t) = b_0 + b_1\cos W_2t + b_2\cos 2W_2t + \ldots$ (II.7)

$$\text{then } b_0 = \frac{1}{2\pi}\int_{-\pi}^{\pi} Exp(bA_2\cos W_2t)d(W_2t) \qquad (II.8)$$

$$\text{and } b_1 = \frac{1}{\pi}\int_{-\pi}^{\pi} Exp(bA_2\cos W_2t)\cos W_2t\,d(W_2t) \qquad (II.9)$$

But K_1 as defined in section (2.2) is

$$K_1 = \frac{\text{output component at frequency } W_1}{\text{input component of frequency } W_1} \qquad (II.10)$$

$$\text{therefore } K_1 = \frac{aExp(bD)}{2A_1\pi^2}\int_{-\pi}^{\pi} Exp(bA_2\cos\phi)d\phi\int_{-\pi}^{\pi} Exp(bA_1\cos\theta)\cos\theta\,d\theta$$

$$= \frac{2aExp(bD)}{A_1\pi^2}\int_{o}^{\pi} Exp(bA_2\cos\phi)d\phi\int_{o}^{\pi} Exp(bA_1\cos\theta)\cos\theta\,d\theta \qquad (II.11)$$

as before.

Hence, the equivalence of the two definitions has been verified.

c) It is known that

$$J_n(z) = (j)^{-n} \int_o^{\pi} \text{Exp}(jz\cos\theta)\cos n\,\theta d\theta$$

and $I_n(z) = (j)^{-n} J_n(jz)$ (Reference (19)), from which it can be established that

$$I_n(z) = \frac{(-I)^{-n}}{\pi} \int_o^{\pi} \text{Exp}(-z\cos\theta)\cos\theta d\theta.$$

And so the equivalent linear gains can be expressed in terms of modified Bessel functions, since

$$\frac{I}{\pi} \int_o^{\pi} \text{Exp}(bA_1\cos\theta)d\theta = I_0(-bA_1)$$

and $$\frac{I}{\pi} \int_o^{\pi} \text{Exp}(bA_2\cos\theta)\cos\theta d\theta = I_1(-bA_1)$$

But $I_0(-bA_1) = I_0(bA_1)$ and $-I_1(-bA_1) = I_1(bA_1)$

therefore the equivalent linear gains are given by

$$K_1 = \frac{2a\text{Exp}(bD)}{A_1} I_0(bA_2)I_1(bA_1) \qquad \text{(II.12)}$$

and $$K_2 = \frac{2a\text{Exp}(bD)}{A_2} I_0(bA_1)I_1(bA_2) \qquad \text{(II.13)}$$

II.2 The Three Input Equivalent Linear Gains.

If the component of the input at the difference frequency is

considered to be of such a size that it cannot be neglected, then the equivalent linear gain to each of the main components must be calculated as follows.

The input to the non-linear element is now $A_1\cos W_1 t + A_2\cos W_2 t +$

$$A_d\cos(W_2 - W_1)t + D$$

and so the output is

$$a\mathrm{Exp}(bA_1\cos W_1 t)\mathrm{Exp}(bA_2\cos W_2 t)\mathrm{Exp}(bA_d\cos(W_1 - W_2))\mathrm{Exp}(bD)$$

$$= a\mathrm{Exp}(bD)(e_0 + e_1\cos W_1 t + e_2\cos 2W_1 t + \ldots)$$

$$(b_0 + b_1\cos W_2 t + b_2\cos 2W_2 t + \ldots)$$

$$(c_0 + c_1\cos(W_1 - W_2)t + c_2\cos 2(W_1 - W_2)t + \ldots) \qquad \text{(II.14)}$$

By multiplying the last three factors of the output function together, it can be shown that,

$$K_1 = \frac{a\mathrm{Exp}(bD)}{A_1}\left(e_1 b_0 c_0 + e_0 b_1\left(\frac{c_1}{2} + \frac{9c_3}{8} + \frac{75c_5}{8} + \ldots\right)\right)$$

$$K_2 = \frac{a\mathrm{Exp}(bD)}{A_2}\left(e_0 b_1 c_0 + e_1 b_0\left(\frac{c_1}{2} + \frac{9c_3}{8} + \frac{75c_5}{8} + \ldots\right)\right)$$

The derivation of these series is rather tedious, but only involves the manipulation of certain trigonometrical formulae.

The coefficients in the expansion II.14 are again obtained using Fourier's theorem, so as before $e_0 = I_0(bA_1)$, $e_1 = 2I_1(bA_1)$ and $b_0 = I_0(bA_2)$, $b_1 = 2I_1(bA_2)$. In a similar manner it can be shown that,

$$c_0 = \frac{I}{2\pi}\int_{-\pi}^{\pi} \mathrm{Exp}(bA_d\cos(W_1 - W_2)t)\,d(W_1 - W_2)t = I_0(bA_d) \text{ and that}$$

$$c_1 = 2I_1(bA_d),\ c_3 = 2I_3(bA_d),\ c_5 = 2I_5(bA_d) \text{ etc.}$$

These higher order Bessel functions become progressively smaller, and

for normal values of A_d terms beyond c_3 can be neglected.

The problem remaining in this case is to express A_d and D in terms of A_1 and A_2 in order that solutions can be found for the amplitude equations.

To obtain a solution to this problem, some assumption must be made with regard to the effect of the input components on the average value of the grid bias, D. If it assumed that $A_d = 0$, the situation is as before, and $D = -(A_1 + A_2 + VB)$. The other extreme is to assume that the grid bias follows the envelope of the incoming wave, which is the same as assuming $A_d = \frac{2(A_1A_2)^{1/2}}{(A_1 + A_2)}$. The actual condition will be somewhere between these.

In this latter case, the value of D can be calculated as follows. It is simply shown (Reference (20)) that

$$A_1\cos W_1t + A_2\cos W_2t = (A_1^2 + 2A_1A_2\cos(W_1 - W_2)t + A_2^2)^{1/2}\cos(W_1t + \text{arc. } \tan(\frac{A_2\sin(W_2 - W_1)t)}{A_1 + A_2\cos(W_1 - W_2)t}$$

therefore D in this case is the average value of

$$(A_1^2 + 2A_1A_2\cos(W_1 - W_2) + A_2^2)^{1/2}$$ plus any fixed bias, VB.

that is

$$D = VB + \frac{1}{2\pi}\int_{-\pi}^{\pi} A_1^2 + 2A_1A_2\cos(W_1 - W_2)t + A_2^2)^{1/2} d(W_1 - W_2)t$$

$$= VB + \frac{1}{\pi}\int_{0}^{\pi} (A_1^2 + A_2^2 + 2A_1A_2(I - 2\sin^2 1/2\theta)d\theta$$

therefore

$$D = VB + \frac{2}{\pi}\int_{o}^{\pi/2} (A_1^2 + A_2^2 + 2A_1A_2 - 4A_1A_2\sin^2 x)^{1/2} dx$$

$$= VB + \frac{2(A_1 + A_2}{\pi} \int_0^{\pi/2} \frac{(I - 4A_1A_2\sin^2 x)}{(A_1 + A_2)^2}\, dx$$

But $(A_1 + A_2)^2 = A_1^2 + A_1^2 + 2A_1A_2$ and $A_1^2 + A_2^2 - 2A_1A_2 = (A_1 - A_2)^2$ which is not negative. Hence $(A_1 + A_2)^2$ is greater than $4A_1A_2$. Therefore D can be expressed as an elliptic integral of the second kind, namely $D = VB + \frac{2}{\pi}(A_1 + A_2)E\left(2\frac{(A_1A_2)^{1/2}}{A_1 + A_2}, 1/2\pi\right)$ with the usual notation.

APPENDIX III

METHOD OF FREQUENCY COMPARISON

The most obvious method of reading the two main oscillating frequencies is to filter out each component separately and to measure their frequencies on counters. This method does, however, prove to be both inconvenient and inefficient in this case, for several reasons, the most important of which is that the relationship between the frequencies is difficult to observe.

One of the requirements of the present problem is that the two main frequencies should be unrelated or, at the most, the relationship $mf_1 = nf_2$ should only be satisfied for very large values of m and n. The only way that this condition could be tested by means of the method mentioned above is to read the frequencies, calculate the first thirty or so harmonic frequencies, and compare each one with every one of the harmonics of the other components. Should it prove that a certain harmonic of one has a frequency which is very close to a harmonic of the other, the decision must then be made as to whether the frequencies are within experimental error of being equal, and if so, whether the values of m and n are acceptably large. If the values of m and n are not large enough, then one of the frequencies must be altered, and the process repeated. The other alternative is that the frequencies are not equal, in which case it must be decided whether or not they are close enough together to give rise to the possibility of pulling in and out of synchronism.

Because of these difficulties, it was decided to try some more direct method of comparing the frequencies. There was the possibility, for instance, of observing the wave on the screen of an oscilloscope by applying all the alternating part to the y-plates while the x-plates were driven by the built-in time base. This did give some indication of the relationship between the various components in the wave but it was not used, because the time base in the synchronising mode could not be relied upon to stay exactly constant, and in the free-running mode, the picture was in continually rapid motion.

The method finally adopted was that shown diagramatically in figure (16). In this, an oscilloscope has its x-plates driven by a voltage sine-wave from a local oscillator which has a continuously variable frequency, measured by a six decade counter. The alternating part of the grid voltage was fed to the y-plates via a cathode follower.

By sweeping the local oscillator frequency slowly through the range of interest, stationary patterns could be formed on the screen momentarily each time the local oscillator frequency became equal to a harmonic or cross modulation frequency. The nature of these patterns could be used to indicate which component is causing it and, more importantly, whether any other component has a related frequency.

Since, in this case, there are only two basic frequencies, it is only essential to observe two patterns to obtain all the information. Any two can be used, but the most obvious are those belonging to the basic frequencies themselves. From one pattern, and the corresponding counter reading, one frequency can be found, and any relationship between this and the second frequency can be observed at once. The

local oscillator can then be tuned to make the pattern of the other main component stationary, and so its frequency can be read.

This method depends on the concept that a complicated wave of this type can be assumed to consist of the sum of sine waves. If the frequency of the signal on the x-plates is made equal to that of one of these sine waves then the component of the y deflection resulting from this wave repeats itself with a period which is related to that of the deflection in the x direction. The deflections in the y direction arising from the sum of all the other waves are added to this with the result that the average value of these other deflections follows the stationary Lissajous figure formed by the first component, and the signal on the x-plates. The proposition here is that, if the other deflections do not form a stationary pattern around the original pattern, then their sum is either not periodic, or else has a period which is unrelated to that of the wave on the x-plates. In the present case, only two frequencies are involved, so that, if the pattern on the screen can be made entirely stationary, then both frequencies are related to each other. If the pattern can be made to be continually moving within a stationary envelope, then one frequency is related to that of the x deflection, but the other is not, that is, the two frequencies contained in the y deflection are unrelated as required.

To prove this, consider first the pattern formed by two sine waves of equal frequency, one on each axis. It is well known, that if there is some phase difference between the two, the resulting figure will be a stationary ellipse (figure (29). If now a second sine wave of voltage is added to that already on the y-plates, the y deflection

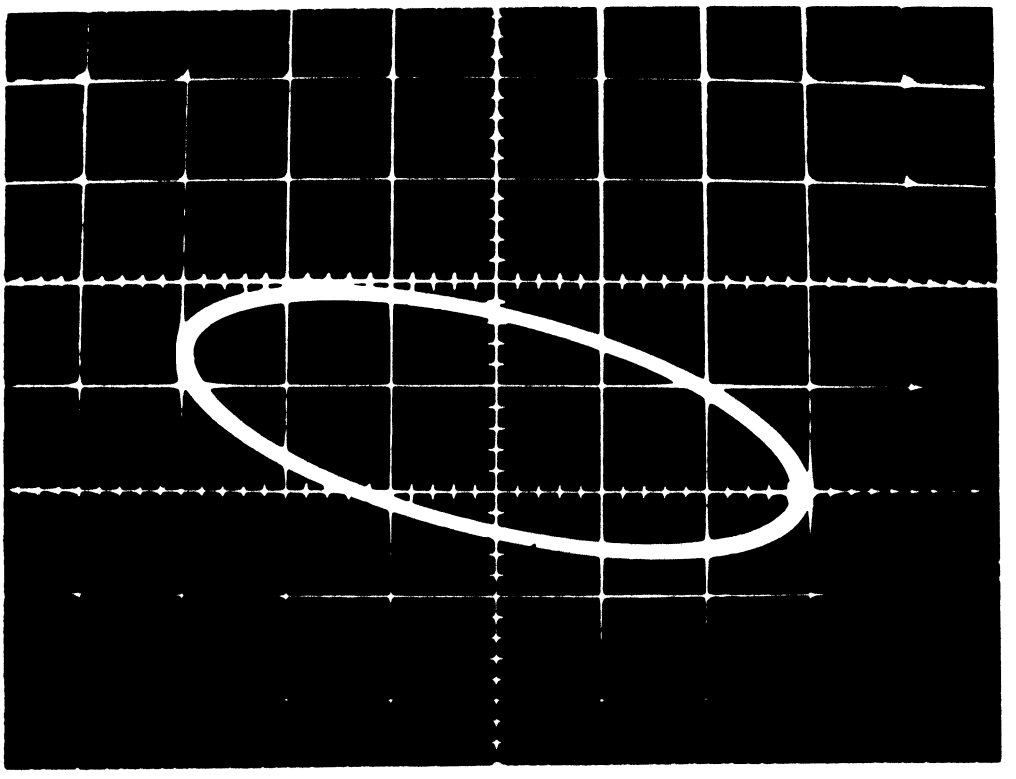

FIG 29

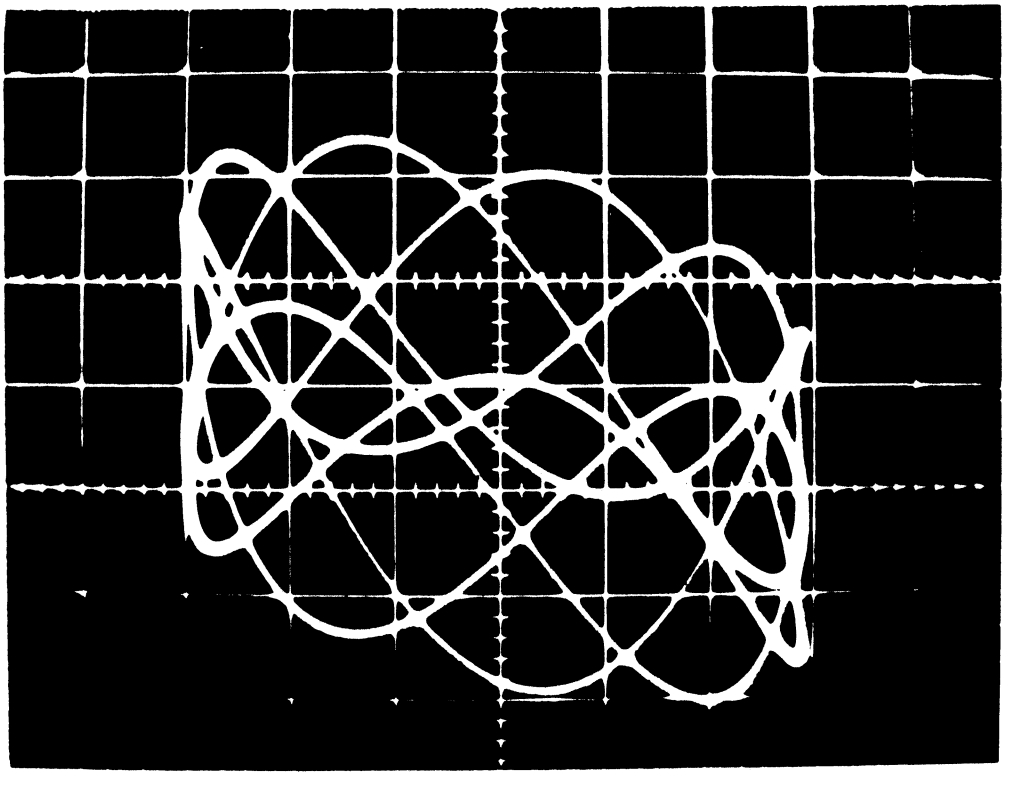

FIG.30

at any time will simply be the sum of the two. If, in addition, it is arranged that in m cycles of the x deflection, the second sine wave executes n cycles, then it is evident that at every m complete cycles of the x deflection the total change in the y displacement of the spot will be zero. Hence at normal frequencies, the persistance of the screen will cause the appearance of a single stationary pattern because every pair of coordinates on the pattern repeats itself with exactly the same frequency (figure (30)).

If, on the other hand, the frequency of the second sine wave is adjusted so that it does not quite execute n cycles each time the first sine wave and the wave on the x axis execute m cycles, then the pattern will appear to regress slowly about the original ellipse. These two statements can be best appreciated by the following argument. If the signal on the x-plates gives a deflection of $x=X\cos W_1 t$ and those on the y-plates $y_1 = Y_1\cos(W_1 t + \phi_1)$ and $y_2 = Y_2\cos(W_2 t + \phi_2)$ then the total y deflection at time t is $y = Y_1\cos(W_1 t + \phi_1) + Y_2\cos(W_2 t + \phi_2)$ when $x = X\cos W_1 t$. In the time taken for the x deflection to go through m complete cycles, the total y deflection will be

$$y = Y_1\cos\left(W_1\left(t + \frac{2\pi m}{W_1}\right) + \phi_1\right) + Y_2\cos\left(W_2\left(t + \frac{2\pi m}{W_1}\right) + \phi_2\right)$$

$$= Y_1\cos(W_1 t + \phi_1) + Y_2\cos\left(W_2 t + \phi_2 + \frac{2\pi m W_2}{W_1}\right)$$

where again $x = X\cos W_1 t$.

From this it can be seen immediately that a pair of coordinates can only repeat regularly if $\frac{2\pi m W_2}{W_1} = n2\pi$ that is, $mW_2 = nW_1$ where m and n are integers.

To fix a point on the pattern, like a peak for example, we can consider the changes of the x and y displacements of the spot in time separated by the interval $\frac{2n\pi}{W_2}$, since y_2 will be in the same point of its cycle at such intervals.

Hence, a point fixed on the pattern will move through total displacements of $X\cos W_1 t - X\cos(W_1 t + \frac{2n\pi W_1}{W_2})$ in the x direction and $Y_1\cos(W_1 t + \phi_1) - Y_1\cos(W_1 t + \phi_1 + \frac{2n\pi W_1}{W_2})$ in the y direction in the time $\frac{2\pi n}{W_2}$. Note that these displacements have a periodic dependence on the time origin t.

It can be seen that the x and y displacements of any part of the pattern change by these amounts every time the spot completes n cycles of its x displacement, and they are only zero when $\frac{nW_1}{W_2}$ = some integer.

The rate at which the pattern regresses depends on how far $nW_1 - mW_2$ is away from zero. It is difficult to establish an expression for the rate of regression, but the following facts are known. Firstly, the higher the numbers n and m, the more complex is the pattern. (There will be a total of m peaks and the pattern will overlap itself n times). Secondly, if the pattern is initially completely stationary, it can be made to regress by changing W_2. If W_2 is continually changed in the same sense then the pattern will accelerate until all resolution is lost. It will then slow down, stop momentarily when $nW_1 = mW_2$ is satisfied by some other pair of values for m and n, and will then commence moving in the opposite direction, and so on. All this time it moves within the envelope defined by the stationary patterns.

From this evidence it is concluded that when all the resolutions of the pattern is lost, and it appears simply as an ellipse with its boundary extended in the y direction to a width of $2Y_2$ (figure (31)), then either the oscillations are related in such a manner that n and m are both extremely large (greater than 1000), or else they are not related at all, and in fact the value of $nW_1 - mW_2$ is near its maximum in that region. In either case, the situation is conducive to concluding that, for all practical purposes, the two frequencies are incommesurable.

It should be noted that several pairs of frequencies were measured and compared in this way and shown to be unrelated, at least up to the thirtieth harmonic, by direct calculation.

This system of frequency comparison also proved to be useful in several other ways. For instance it could be used to detect even weak pulling between the two components. If the two frequencies, on the average, were almost related by $mW_1 = nW_2$, then they often became weakly coupled, and pulled in and out of synchronism. The direct method of observation of the frequencies could only detect this by a change in the scatter of the counter readings from about two or three parts in a million to between five and ten parts in a million. This exchange of energy could be observed directly from the Lissajous figures, since the movement of the ellipse became jerky and fine background patterns, such as shown in figure (32) periodically pulled into view.

In reference (21) there is a discussion of mechanically obtained Lissajous figures, and a proof of the fact that if the two frequencies of the wave forming the pattern are incommesurable, the point in the plane will traverse all areas of the envelope. This amounts to saying

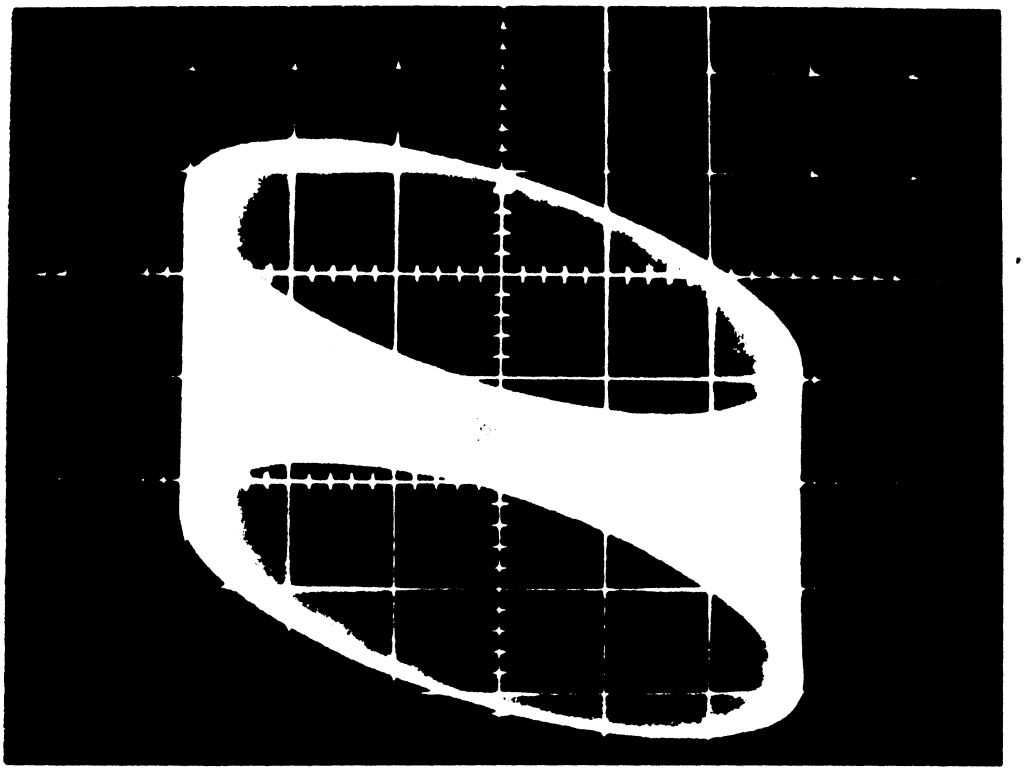

FIG. 31

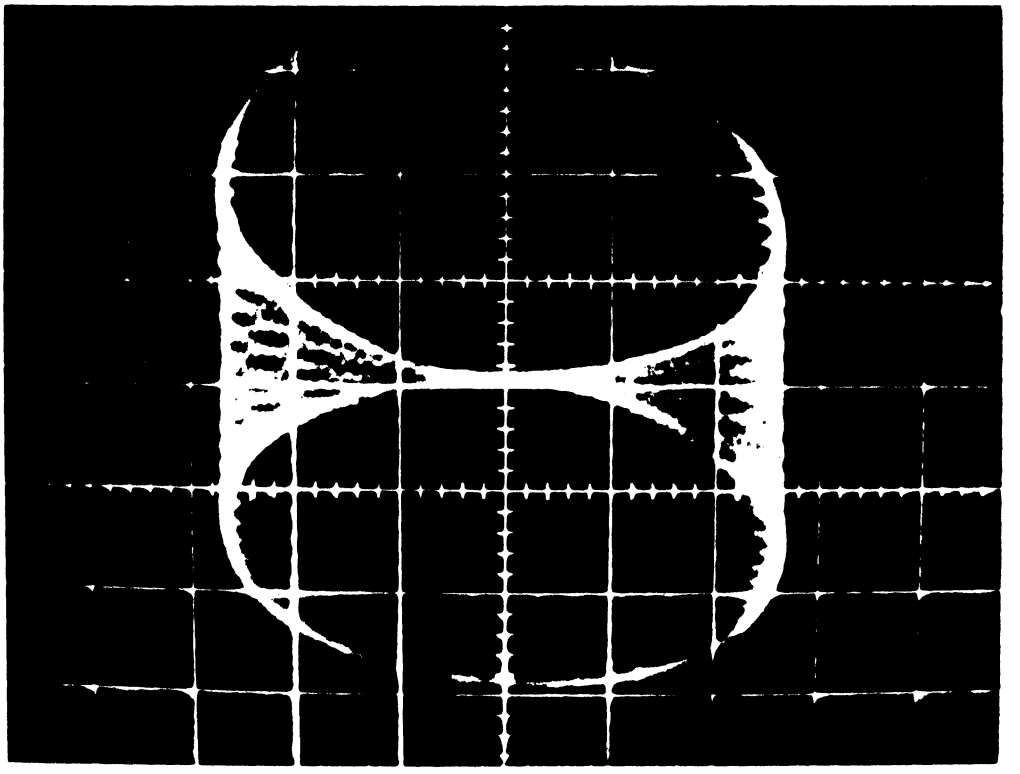

FIG. 32

that, at higher frequencies, the pattern is irresolvable, which is as contended here.

APPENDIX IV

VARIATION OF RE. G(p) WITH S.

In section (5) it was shown that any oscillation at W_3 alone would be unstable. This depended on the fact that any disturbance of the oscillating conditions away from the equilibrium would increase with time. This can be shown to be true by plotting the variation of G(p) with the real part of p in the region of W_3 and observing that, if the disturbance was such as to increase the amplitude , then the working point moves into a region of positive s and the amplitude will continue to increase.

Any single input equivalent linear gain from a single value non-linearity will be entirely real, and with the present exponential characteristic its reciprocal will always increase with amplitude. The oscillating conditions are defined by observing the intersection of the reciprocal of the equivalent linear gain function with the curve representing G(jW) in the complex plane. Hence, an oscillation will be stable if the value of G(p) for positive s is less than the value for s = 0, and for negative s is greater than the value for s = 0.

The value of G(p) in the region of the three zero phase shift frequencies can be calculated by assuming that the addition of a small real part to p does not alter the phase shift.

Any expression of the form $p^2 + 2aW_0 + W_0^2$ becomes approximately $-w^2 + 2jw(s+W_0a) + (W_0^2 + s^2)$ when p is made equal to s + jw, (since as is much less than W_0a and s). Hence, the value of G(p) in regions

close to $p = jW_1$, jW_2, and jW_3 can be calculated from equation (18) by first adding s^2 to W_{10}^2, W_{20}^2, and W_0^2, replacing a by $\frac{(s + W_0 a)W_0}{(W_0^2 + s^2)^{1/2}}$

$$a_1 \text{ by } \frac{(s + W_{10}a_1)W_{10}}{(W_{10}^2 + s^2)^{1/2}}$$

$$a_2 \text{ by } \frac{(s + W_{20}a_2)W_{20}}{(W_{20}^2 + s^2)^{1/2}}$$

and finally by multiplying by $(W_3^2 + s^2)^{1/2}/W_3$, $(W_1^2 + s^2)^{1/2}/W_1$ or $(W_2^2 + s^2)^{1/2}/W_2$ depending on which oscillating point is being considered.

The results of these calculations are shown in figures (33), (34) and (35), from which it can be seen that near $p = jW_3$ the larger values of G(p) correspond to positive s, whilst in the other two cases this is not so.

It should be noted that the first two of these graphs can only be used to prove that a single oscillation is stable, since there is no provision for showing the effect of one component on the other. They are included, however, to show that stable single frequency modes might be expected if the other component was suppressed in some way, and also as a check on the calculations. The values of $G(jW_1)$ and $G(jW_2)$ have been calculated directly in section (6.3).

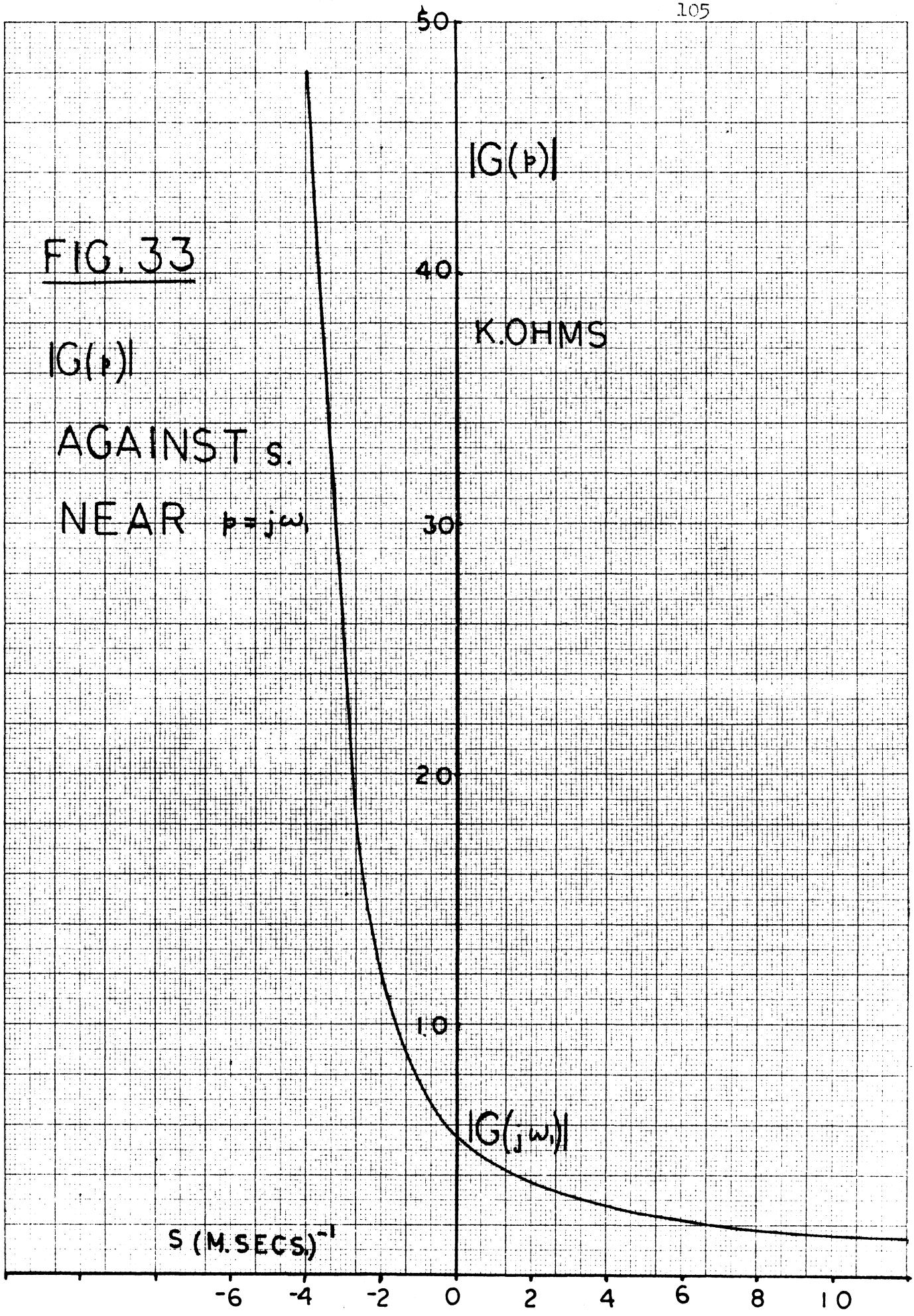

FIG. 33

$|G(p)|$ AGAINST s. NEAR $p = j\omega_1$

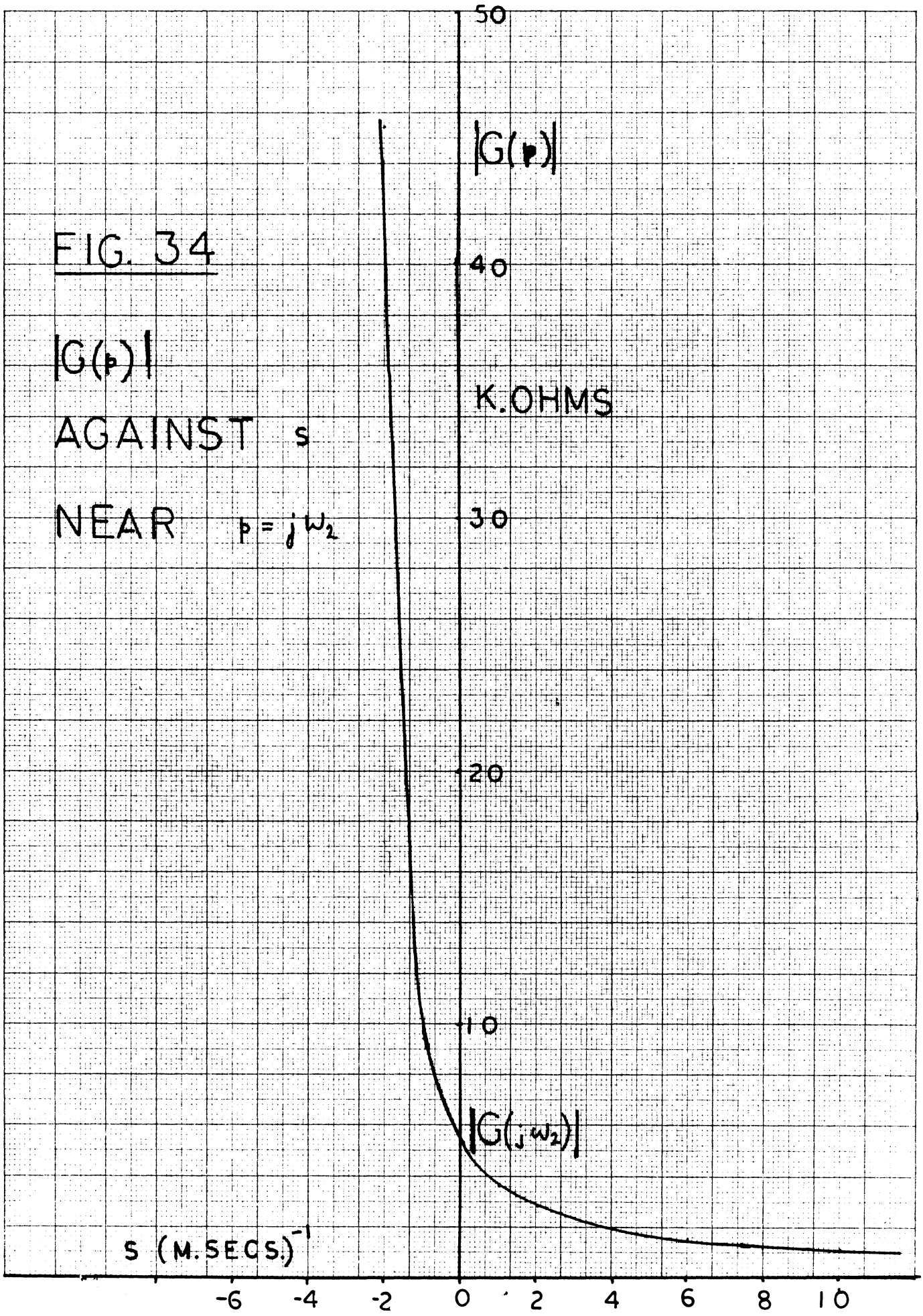

FIG. 34

$|G(p)|$ AGAINST s NEAR $p = j\omega_2$

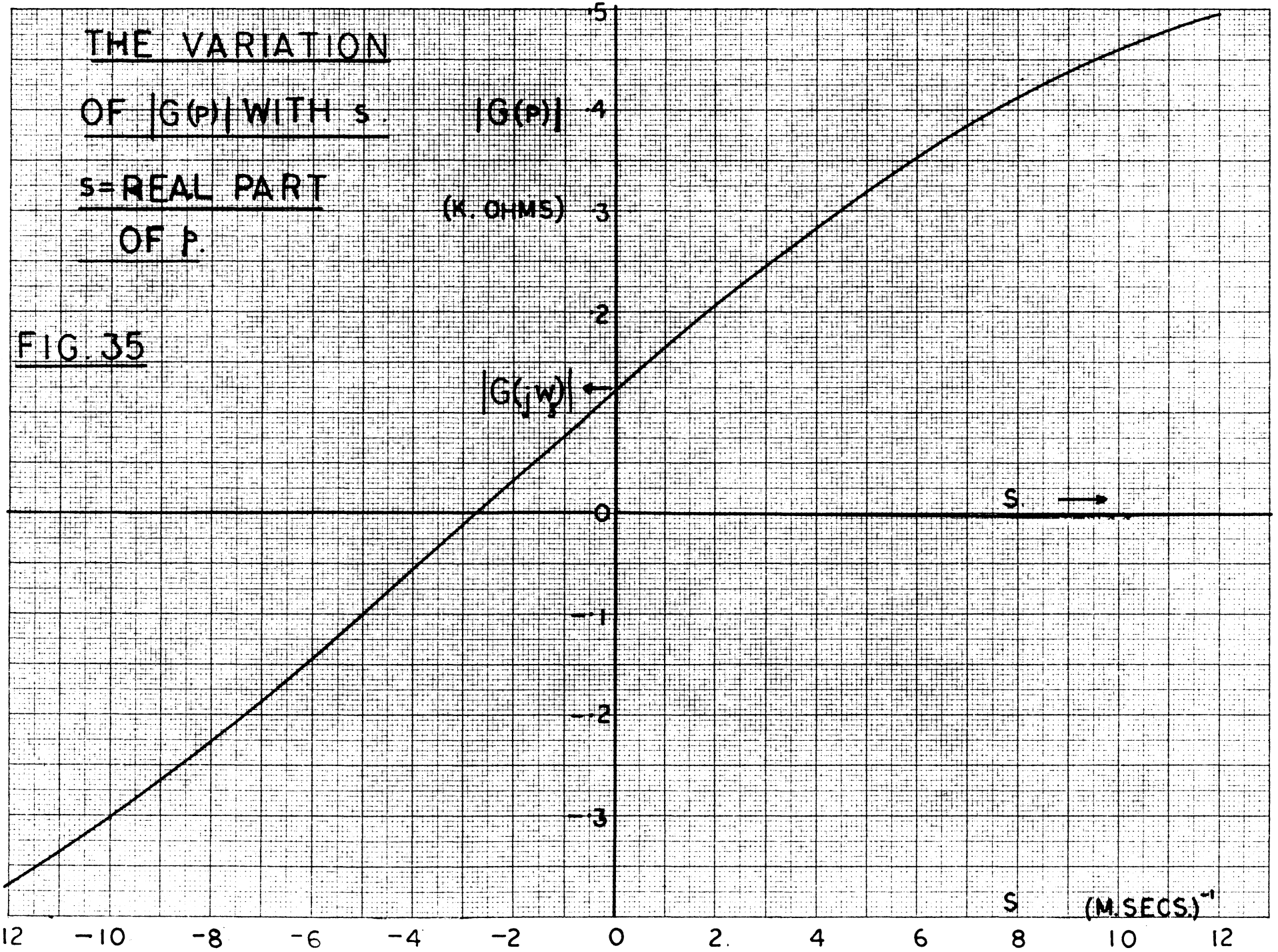
THE VARIATION OF |G(P)| WITH s.
s = REAL PART OF P.
FIG. 35
|G(P)|
(K. OHMS)
|G(jw)|
S
S (M.SECS.)⁻¹
5
4
3
2
0
−1
−2
−3
−12
−10
−8
−6
−4
−2
0
2
4
6
8
10
12

REFERENCES

1. H. J. Reich, J. D. Skalnik and J. D. Crone "Simultaneous oscillations at two or more frequencies." Proc. I.E.E.E. vol. 51 p. 1051 July 1963.

2. R Stapelfeldt "Multitone oscillators - new source of simultaneous frequency". Electronics vol. 36 p.86 Jan 1963.

3. S. Lubkin "Bimodal oscillator" ibid. vol. 19 p.242 Feb. 1946.

4. L. Hazeltine "Oscillating audion circuits" Proc. I.R.E vol. 6 pp63-98. April 1918.

5. E. H. Armstrong "Some recent developments in the audion receiver" ibid. vol.3 p. 215 1915.

6. M I. Disman and W. A. Edson "Asynchronous oscillations in class C oscillators" ibid. vol 46 pp.895-899. May 1958.

7. N. Kryloff and N. Bogoliuboff "Introduction to non-linear mechani s" Princeton University Press, Princeton, N.J. 1943.

8. L. C. Goldfard "On some non-linear phenomena in regulatory systems" Automatica i Telemektronica" vol.8 no.5. pp349-383, 1947.

9. J. C. West "Analytical Techniques for non-linear control systems" English Universities Press pp. 119-159 1960.

10. Somerville and Atherton "Multigain representation for a single valued non-linearity with several inputs." Proc. I.E.E. monograph no. 309M, vol. 105C p.537 July 1958.

11. J. S. Shaftner "Simultaneous oscillations in oscillators" Trans. I.R.E. Professional group on circuit theory, vol. CTI p.2 June 1954.

12. L. Skinner "Criteria for stability in circuits containing non-linear resistance". Ph.D. dissertation, University of Illinois 1948.

13. Mathematical tables from the "Handbook of chemistry and physics" The Chemical Rubber Publishing Co., p.320. 1963.

14. E. J. Routh "Advanced rigid dynamics" chapter 6. MacMillan Co. London, 1892.

15. A. S. Gladwin "Stability of oscillations in valve generators" Wireless Engineer, p.272, Oct. 1955.

16. R.Fontana "Internal resonance in circuits containing non-linear resistence" Proc. I.R.E., vol. 39, pp.945-951 Aug. 1951.

17. Abd El-Somie Mostofa "Simultaneous pulled oscillations in a triode oscillator incorporating two oscillating circuits." Communications and Electronics, no. 30, pp. 120-127, May 1957.

18. G M. Utkin "Simultaneous oscillations at two frequencies in a self-oscillating system with automatic bias." Radio Engineering (Radio Teknika) vol. 12, p. 76, April 1958.

19. Whitaker and Watson "Modern analysis" Fourth Edition, Cambridge University Press. Chapter 17, 1963.

20. Stanford Goldman "Frequency analysis, Modulation and noise" McGraw Hill Book Company, New York p.160 1948.

21. W. F. Osgood "Mechanics" MacMillan. New York p. 186 1957.